

Wilfrid Laurier University

Scholars Commons @ Laurier

---

Theses and Dissertations (Comprehensive)

---

2002

## Radiation budget, ground thermal regime and hydrological balance of a low arctic tundra basin, Coppermine River, Northwest Territories

David S. Turcotte  
*Wilfrid Laurier University*

Follow this and additional works at: <https://scholars.wlu.ca/etd>



Part of the [Physical and Environmental Geography Commons](#)

---

### Recommended Citation

Turcotte, David S., "Radiation budget, ground thermal regime and hydrological balance of a low arctic tundra basin, Coppermine River, Northwest Territories" (2002). *Theses and Dissertations (Comprehensive)*. 438.

<https://scholars.wlu.ca/etd/438>

This Thesis is brought to you for free and open access by Scholars Commons @ Laurier. It has been accepted for inclusion in Theses and Dissertations (Comprehensive) by an authorized administrator of Scholars Commons @ Laurier. For more information, please contact [scholarscommons@wlu.ca](mailto:scholarscommons@wlu.ca).

## **INFORMATION TO USERS**

This manuscript has been reproduced from the microfilm master. UMI films the text directly from the original or copy submitted. Thus, some thesis and dissertation copies are in typewriter face, while others may be from any type of computer printer.

**The quality of this reproduction is dependent upon the quality of the copy submitted.** Broken or indistinct print, colored or poor quality illustrations and photographs, print bleedthrough, substandard margins, and improper alignment can adversely affect reproduction.

In the unlikely event that the author did not send UMI a complete manuscript and there are missing pages, these will be noted. Also, if unauthorized copyright material had to be removed, a note will indicate the deletion.

Oversize materials (e.g., maps, drawings, charts) are reproduced by sectioning the original, beginning at the upper left-hand corner and continuing from left to right in equal sections with small overlaps.

ProQuest Information and Learning  
300 North Zeeb Road, Ann Arbor, MI 48106-1346 USA  
800-521-0600

**UMI<sup>®</sup>**





**National Library  
of Canada**

**Acquisitions and  
Bibliographic Services**

**385 Wellington Street  
Ottawa ON K1A 0N4  
Canada**

**Bibliothèque nationale  
du Canada**

**Acquisitions et  
services bibliographiques**

**385, rue Wellington  
Ottawa ON K1A 0N4  
Canada**

*Your file Votre référence*

*Our file Notre référence*

**The author has granted a non-exclusive licence allowing the National Library of Canada to reproduce, loan, distribute or sell copies of this thesis in microform, paper or electronic formats.**

**The author retains ownership of the copyright in this thesis. Neither the thesis nor substantial extracts from it may be printed or otherwise reproduced without the author's permission.**

**L'auteur a accordé une licence non exclusive permettant à la Bibliothèque nationale du Canada de reproduire, prêter, distribuer ou vendre des copies de cette thèse sous la forme de microfiche/film, de reproduction sur papier ou sur format électronique.**

**L'auteur conserve la propriété du droit d'auteur qui protège cette thèse. Ni la thèse ni des extraits substantiels de celle-ci ne doivent être imprimés ou autrement reproduits sans son autorisation.**

0-612-72639-8

**Canada**

**RADIATION BUDGET, GROUND THERMAL REGIME AND  
HYDROLOGICAL BALANCE OF A LOW ARCTIC  
TUNDRA BASIN, COPPERMINE RIVER, N.W.T.**

By

David S. Turcotte  
B.Sc., Trent University, 1998

THESIS

Submitted to the Department of Geography and Environmental Studies  
in partial fulfilment of the requirements for the  
Master of Environmental Studies Degree  
Wilfrid Laurier University  
2002

© David S. Turcotte 2002

---

---

## ABSTRACT

---

---

The effects of slope, aspect and vegetation cover on the radiation balance and active layer thermal regime of arctic tundra were investigated during the summer of 1999 and the spring of 2000. The study site is located at Daring Lake, N.W.T (64°52'N, 111°35'W) in the Slave Geological Province of the Coppermine River Basin. A sub-basin 14 ha in area and with approximately 30 meters of relief was intensely monitored for hydrological, radiation and energy balance components.

Initiation of active layer development and subsequent thawing was earlier and more pronounced on predominantly west facing slopes due to increased receipt of incoming solar radiation. Late summer active layer depths were the greatest on west-facing slopes as compared to north- and east-facing slopes (>170 cm, 84.0 ±21.7 cm, 49.2 ±0.8 cm respectively). Incoming shortwave radiation values were extrapolated from the met site to various basin sites taking slope and aspect into account. Spatial and diurnal variations in albedo were minimal within the Kakawi Lake Basin. As well, surface temperature measurements varied little from site to site causing the long wave radiation balance to remain relatively constant. Incoming shortwave radiation was determined to control diurnal fluctuations in the net radiation balance on a daily and seasonal basis but represented less than one half (41%) of the radiative supply to the surface.

Ground heat flux increased downslope on west- and north-facing hillslopes corresponding with an increase in active layer development during the summer season. Conversely, basal flux out of the active layer to the underlying permafrost decreased downslope. The sensible heat flux varied least with depth between the study sites but accounted for a significant proportion of the ground flux at sites with deeper active layers. Active layer depths at peat dominated, east-facing hillslope sites were only 59% of the average depth on west- and north-facing slopes primarily due to the high water content and reduced thermal conductivity of peat soils. Latent heat is largest at the beginning of the thaw season when there is rapid active layer development but is later reduced as ground thaw slackens.

Kakawi Lake Basin precipitation input, outflow and lake water level were recorded daily throughout the 36 day study period while evaporation was estimated based on a study conducted in a nearby basin. Lateral inflow from catchment hillslopes was determined to be the dominant component of the Kakawi Lake Basin hydrological balance for the 1999 study period. Peat dominated areas were disconnected throughout much of the study period but drained as a single source during rainfall events.

---

## ACKNOWLEDGEMENTS

---

Conducting research in Canada's Arctic is a difficult undertaking, but the rewards associated with this experience have proven to extend far beyond the completion of a Master's degree. Such an opportunity would not have been possible without the assistance and support of numerous people who helped me in various ways to achieve this goal.

First, I would like to thank my thesis committee, Dr. Mike English, Dr. Mike Stone, and Dr. Jon Price as well as my outside readers Dr. Eric Mattson and Dr. Bill Quinton for their valuable comments and discussion at my thesis defence.

Next, I would like to acknowledge several people who assisted me here in Waterloo. Thanks to Dave Keirstead, Pam Schauss, Aaron Holmes and Sarah Kennedy for lending me their cartographic expertise in creating the GIS projects and maps that are included in this thesis. Special thanks to Alex Maclean for his numerous hours of guidance with the construction of field instrumentation and preparation for excursions to Kakawi Lake. I would also like to acknowledge Richard Petrone for his valuable assistance with radiation and energy balance methodologies and calculations.

During my visits to the Northwest Territories I have had the pleasure to meet several people who have kindly assisted me with my research efforts. Thanks to Dave Milburn and Bob Reid from the Department of Indian Affairs and Northern Development (DIAND) for their financial, scientific and logistical assistance with this research project. As well, I would like to thank Steve Matthews and Karin Clark from Resources Wildlife and Economic Development (RWED) for providing us with accommodations at the Tundra Ecosystem Research Station (TERS). I would also like to acknowledge John Witteman from the BHP Ekati Camp for donating helicopter time and for transporting our research team to and from Daring Lake.

I could not have completed this research project nor maintained a reasonable degree of sanity without great company during visits to Daring Lake. Thanks to Steve Matthews, Karin Clarke, Liisa Peramaki, Bob Reid, Dave Olesen, the Waterloo crew, and a host of other "neighbours" in the area for providing countless laughs and for making my arctic adventure a truly enjoyable and rewarding experience. Special thanks to Aaron Holmes for tackling the black flies, long days, and sometimes difficult conditions with me in the field. His assistance and company were an integral part of my thesis work.

Most importantly, I would like to thank my advisor Dr. Mike English for his guidance, support and encouragement throughout the duration of my graduate studies. In working with Mike I have gained a more thorough understanding of hydrological concepts, valuable experience with the planning and implementation of a field study, and

a much deeper appreciation of the north. As well as being an exceptional advisor, Mike has been a mentor and a friend who I am grateful to have worked with and look forward to collaborating with again.

I would like to reserve special thanks to individuals who have supported me on an important personal level during the past few years. Thanks to my parents and family for their constant words of encouragement and for taking interest in every aspect of my research efforts in Waterloo and during my time away at Daring Lake. Thanks to Sarah for her continuing friendship and support and for her motivation when the thesis battle seemed uphill. Finally, I would like to thank my family, colleagues and many friends, both new and old, for helping me to achieve my goals and to view the future as an open door.

---

---

# TABLE OF CONTENTS

---

---

	<u>Page</u>
<b>Abstract</b> .....	i
<b>Acknowledgements</b> .....	ii
<b>List of Tables</b> .....	vi
<b>List of Figures</b> .....	vii
<b>CHAPTER 1 - INTRODUCTION</b> .....	<b>1</b>
1.1 - Introduction .....	1
1.2 - Research Objectives .....	3
1.3 - Literature Review .....	3
1.3.1 - Active Layer Thermal Regime .....	3
1.3.2 - Radiation Balance .....	7
1.3.3 - Ground Heat Flux and Active Layer Development .....	11
1.3.4 - Energy Balance .....	18
1.4 - Relevance of Research Objectives .....	21
<b>CHAPTER 2 - STUDY SITE</b> .....	<b>23</b>
2.1 - Selection of Kakawi Lake Study Basin .....	23
2.2 - Landscape .....	25
2.3 - Geology .....	26
2.4 - Till Deposits .....	26
2.5 - Eskers .....	29
2.6 - General Vegetation and Climate .....	30
<b>CHAPTER 3 - METHODOLOGY</b> .....	<b>32</b>
3.1 - Kakawi Lake Vegetation Characterization .....	32
3.2 - Meteorological Stations .....	35
3.3 - Hillslope and Site Selection .....	40
3.4 - Survey and GIS Analysis .....	40
3.5 - Soil Sampling and Analysis .....	45
3.6 - Soil Temperature .....	48
3.7 - Soil Moisture .....	50
3.8 - Measurement of Active Layer/Permafrost Table .....	52
3.9 - Radiation Balance .....	53
3.10 - Ground Heat Flux .....	57
3.11 - Surface Energy Budget .....	59
3.12 - Irrigation Experiments .....	60

3.13 - Basin Hydrology .....	61
<b>CHAPTER 4 - METEOROLOGICAL TRENDS .....</b>	<b>64</b>
<b>CHAPTER 5 - RADIATION BALANCE .....</b>	<b>69</b>
5.1 - Incoming Short-Wave Radiation .....	69
5.2 - Radiation Balance .....	74
5.3 - Potential Sources of Error .....	84
<b>CHAPTER 6 - SOIL MICROCLIMATE .....</b>	<b>87</b>
6.1 - Soil Analyses .....	87
6.2 - Active Layer Development .....	91
6.3 - Soil Temperature .....	96
6.4 - Soil Moisture .....	102
6.5 - Irrigation Experiment .....	106
6.6 - Subsurface Latent Heat ( $Q_L$ ) .....	110
6.7 - Subsurface Sensible Heat ( $Q_s$ ) .....	114
6.8 - Ground Heat Flux ( $Q_G$ ) .....	119
6.9 - Potential Sources of Error in Determination of $Q_G$ .....	126
<b>CHAPTER 7 - SURFACE ENERGY BUDGET .....</b>	<b>128</b>
<b>CHAPTER 8 - HYDROLOGY .....</b>	<b>131</b>
8.1 - Hydrological Parameters .....	131
8.2 - Hillslope Contribution .....	135
<b>CHAPTER 9 - CONCLUSIONS .....</b>	<b>144</b>
9.1 - Conclusions .....	144
9.2 - Future Research .....	148
<b>APPENDICES .....</b>	<b>150</b>
Appendix A - Soil temperature regression equations (1999 and 2000) .....	150
Appendix B - Soil temperature figures (1999 and 2000) .....	152
Appendix C - Active layer development regression equations (1999 and 2000) .....	159
<b>REFERENCES .....</b>	<b>161</b>

## LIST OF TABLES

	<u>Page</u>
Table 3.1 - Kakawi Lake Basin Vegetation .....	33
Table 3.2 - Kakawi Lake Basin Peat Species .....	33
Table 3.3 - Kakawi Lake Lichen Species .....	34
Table 3.4 - Daring Lake Met Station .....	38
Table 3.5 - Laurier Met Station .....	39
Table 3.6 - Kakawi Lake Level Station .....	39
Table 5.1 - Slope and aspect values for each study site .....	71
Table 5.2 - Albedo values for each study site .....	75
Table 5.3 - Albedo measurements as cited for studies in arctic and alpine environments .....	76
Table 5.4 - Total incoming and outgoing radiation balance components and net shortwave, longwave and total radiation values for 1999 study period at each site. ....	83
Table 5.5 - Total incoming and outgoing radiation balance components and net shortwave, longwave and total radiation values for 1999 study period at each site. ....	83
Table 5.6 - Average surface temperature for each study site .....	85
Table 6.1 - Heat capacity values for different materials .....	91
Table 6.2 - Descriptive Statistics for 1999 Soil Temperature .....	97
Table 6.3 - Descriptive Statistics for 2000 Soil Temperature .....	98
Table 6.4 - Average temperature gradients at polar desert site and fen site in continuous permafrost area of Arctic Canada (Woo and Xia 1996) .....	101
Table 6.5 - Average soil moisture content (Julian Day 212 to 226) for 1999 field season .....	105
Table 6.6 - Soil temperature and water content differences from 1999 field season irrigation experiments. ....	107
Table 6.7 - Daily and seasonal total $Q_t$ for each site during 1999 and 2000 field seasons. ....	113
Table 6.8 - Sensible heat ( $Q_s$ ) stored in each soil layer for 1999 and 2000 study periods. ....	118
Table 6.9 - Site $Q_t$ for 1999 and 2000 study periods. ....	119
Table 8.1 - Ranges of values of Hydraulic Conductivity .....	137
Table 8.2 - Hillslope discharge calculated using varying groundwater table depths (GWT) .....	139
Table 8.3 - Hillslope discharge calculated using varying gradients .....	139

# LIST OF FIGURES

	<u>Page</u>
Figure 1.1 - The extent of the periglacial zone in the northern hemisphere .....	2
Figure 1.2 - Permafrost terminology .....	2
Figure 1.3 - Seasonal changes in the active layer .....	6
Figure 2.1 - Coppermine River Basin, Northwest Territories .....	24
Figure 2.2 - Bedrock types of Slave Geological Province .....	27
Figure 2.3 - Eskers and surficial sediment of Slave Geological Province .....	28
Figure 3.1 - Kakawi Lake study basin and greater Daring Lake area .....	36
Figure 3.2 - Kakawi Lake Basin instrumentation .....	37
Figure 3.3 - Kakawi Lake Basin survey point locations .....	42
Figure 3.4 - Kakawi Lake Basin vegetation polygon map .....	43
Figure 3.5 - Kakawi Lake Basin 3-D orthographic image with vegetation overlay .....	44
Figure 4.1 - Mean monthly air temperature recorded at the Daring Lake meteorological station from May to October for years 1996 to 2000. ....	64
Figure 4.2 - Mean monthly rainfall (mm) recorded at the Daring Lake meteorological station for years 1996 to 2000. ....	65
Figure 4.3 - Mean daily snow depths recorded at the Daring Lake meteorological station from 1996 to 2000. ....	66
Figure 4.4 - Average daily temperature and daily total precipitation at Kakawi Lake basin during 1999 study period. ....	67
Figure 4.5 - Average daily temperature and daily total precipitation at Kakawi Lake basin during 2000 study period. ....	68
Figure 5.1 - Diurnal variation of direct-beam solar radiation on surfaces with varying slope and aspect for YD 212 .....	70
Figure 5.2 - Diurnal variation of direct-beam solar radiation upon Hillslope #1 on YD 212 .....	72
Figure 5.3 - Diurnal variation of direct-beam solar radiation upon Hillslope #2 on YD 212 .....	73
Figure 5.4 - Diurnal variation of direct-beam solar radiation upon Hillslope #3 on YD 212. ....	74
Figure 5.5 - Diurnal radiation balance for met site on (a) cloudy	

# LIST OF FIGURES

	<u>Page</u>
Figure 1.1 - The extent of the periglacial zone in the northern hemisphere .....	2
Figure 1.2 - Permafrost terminology .....	2
Figure 1.3 - Seasonal changes in the active layer .....	6
Figure 2.1 - Coppermine River Basin, Northwest Territories .....	24
Figure 2.2 - Bedrock types of Slave Geological Province .....	27
Figure 2.3 - Eskers and surficial sediment of Slave Geological Province .....	28
Figure 3.1 - Kakawi Lake study basin and greater Daring Lake area .....	36
Figure 3.2 - Kakawi Lake Basin instrumentation .....	37
Figure 3.3 - Kakawi Lake Basin survey point locations .....	42
Figure 3.4 - Kakawi Lake Basin vegetation polygon map .....	43
Figure 3.5 - Kakawi Lake Basin 3-D orthographic image with vegetation overlay .....	44
Figure 4.1 - Mean monthly air temperature recorded at the Daring Lake meteorological station from May to October for years 1996 to 2000. ....	64
Figure 4.2 - Mean monthly rainfall (mm) recorded at the Daring Lake meteorological station for years 1996 to 2000. ....	65
Figure 4.3 - Mean daily snow depths recorded at the Daring Lake meteorological station from 1996 to 2000. ....	66
Figure 4.4 - Average daily temperature and daily total precipitation at Kakawi Lake basin during 1999 study period. ....	67
Figure 4.5 - Average daily temperature and daily total precipitation at Kakawi Lake basin during 2000 study period. ....	68
Figure 5.1 - Diurnal variation of direct-beam solar radiation on surfaces with varying slope and aspect for YD 212 .....	70
Figure 5.2 - Diurnal variation of direct-beam solar radiation upon Hillslope #1 on YD 212 .....	72
Figure 5.3 - Diurnal variation of direct-beam solar radiation upon Hillslope #2 on YD 212 .....	73
Figure 5.4 - Diurnal variation of direct-beam solar radiation upon Hillslope #3 on YD 212. ....	74
Figure 5.5 - Diurnal radiation balance for met site on (a) cloudy	

and (b) cloudless day. ....	78
Figure 5.6 - Daily incoming longwave, shortwave and net radiation values at met site for (a) 1999 and (b) 2000 field seasons .....	80
Figure 5.7 - Daily shortwave, longwave and net radiation balance values at met site for (a) 1999 and (b) 2000 field seasons. ....	81
Figure 6.1 - Soil bulk density measurements for each site .....	87
Figure 6.2 - Soil porosity measurements for hillslopes 1 and 2. ....	88
Figure 6.3 - Soil carbon measurements for met site and for hillslopes 1 and 2. ....	89
Figure 6.4 - Soil heat capacity for each study site .....	90
Figure 6.5 - Active layer development for (a) hillslope transect 1 and (b) hillslope transect 3 during the 1999 field season .....	92
Figure 6.6 - Active layer development for (a) hillslope transect 1 and (b) hillslope transect 2 during the 2000 field season. ....	93
Figure 6.7 - Daily soil moisture contents measured at depth at (a) Laurier met site (hillslope) and (b) Daring Lake met site (relatively flat ground) during 1999 field season. ....	102
Figure 6.8 - Daily soil moisture content measured at depth at the Daring Lake met site during 1999 field season. ....	104
Figure 6.9 - Irrigation experiment Site 3-A changes in (a) soil temperature and (b) soil water content .....	108
Figure 6.10 - Irrigation experiment Site 3-B changes in (a) soil temperature and (b) soil water content. ....	109
Figure 6.11 - Regressed active layer development for (a) hillslope transect 1 and (b) hillslope transect 3 during the 1999 field season .....	111
Figure 6.12 - Regressed active layer development for (a) hillslope transect 1 and (b) hillslope transect 2 during the 2000 field season .....	112
Figure 6.13 - Subsurface $Q_s$ on hillslope 1 for (a) 1999 and (b) 2000 study seasons .....	114
Figure 6.14 - $Q_s$ on hillslope 2 for (a) 1999 and (b) 2000 study periods. ....	115
Figure 6.15 - $Q_s$ on hillslope 3 for (a) 1999 and (b) 2000 study periods. ....	116
Figure 6.16 - Active layer heat balance components expressed as percentage of total $Q_G$ for the 1999 study period. ....	122
Figure 6.17 - Active layer heat balance components expressed as percentage of total $Q_G$ for the 2000 study period .....	122
Figure 6.18 - Total active layer development as compared to total study season $Q_i$ for 1999 and 2000 study periods. ....	125

<b>Figure 7.1 - Daily sensible and latent heat fluxes during 1999 study season .....</b>	<b>128</b>
<b>Figure 8.1 - Daily lake level fluctuation and precipitation total for the 1999 study period .....</b>	<b>131</b>
<b>Figure 8.2 - Kakawi Lake basin daily inflow and outflow during the 1999 study period. ....</b>	<b>132</b>
<b>Figure 8.3 - Water level depths at sites 3-A, 3-B and 3-C for 1999 study period .....</b>	<b>134</b>
<b>Figure 8.4 - Hillslope areas used in calculation of subsurface discharge .....</b>	<b>138</b>
<b>Figure 8.5 - Kakawi Lake discharge berm elevation profile .....</b>	<b>141</b>

---

---

# CHAPTER 1 - INTRODUCTION

---

---

## 1.1 - INTRODUCTION

The term 'permafrost' is used to describe the thermal condition of earth materials such as soil and rock. Permafrost includes ground that freezes in one winter and remains frozen through the following summer and into the next winter. This permafrost layer may be as little as a few centimetres thick (Brown, 1970). Permafrost can range in thickness from a few centimetres to hundreds of metres and take over one thousand years to form. The term 'periglacial' refers to environments in which frost-action and permafrost-related processes dominate (French, 1996). The extent of the periglacial zone in the northern hemisphere is illustrated in Figure 1.1. In total, a fifth of the world's land surface, including over half of Canada, is underlain by permafrost (Brown, 1970). Several different periglacial zones can be recognized occurring both in high latitude and tundra regions as well as below the treeline and in high altitude (alpine) regions of middle latitudes (French, 1996).

Above the permafrost is a surface layer of ground called the active layer (Figure 1.2). The active layer includes the uppermost part of the permafrost that thaws and refreezes annually, even though the material remains cryotic (i.e. below 0°C). Depending on the interaction of such factors as the ambient air temperature, degree and orientation of slope, vegetation, drainage, snow cover, soil and rock type and water content, the thickness of the active layer may vary from year to year (French, 1996). The biological and physical processes which characterize the arctic ecosystem are all affected by the

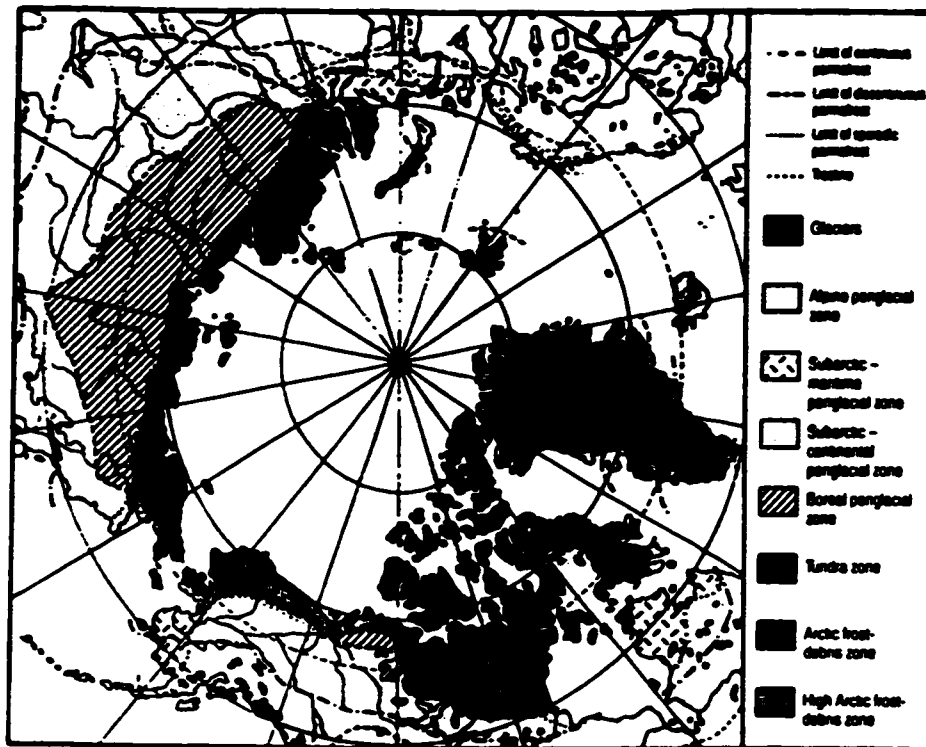


Figure 1.1 - Regional extent of different periglacial zones in the northern hemisphere (French, 1996)

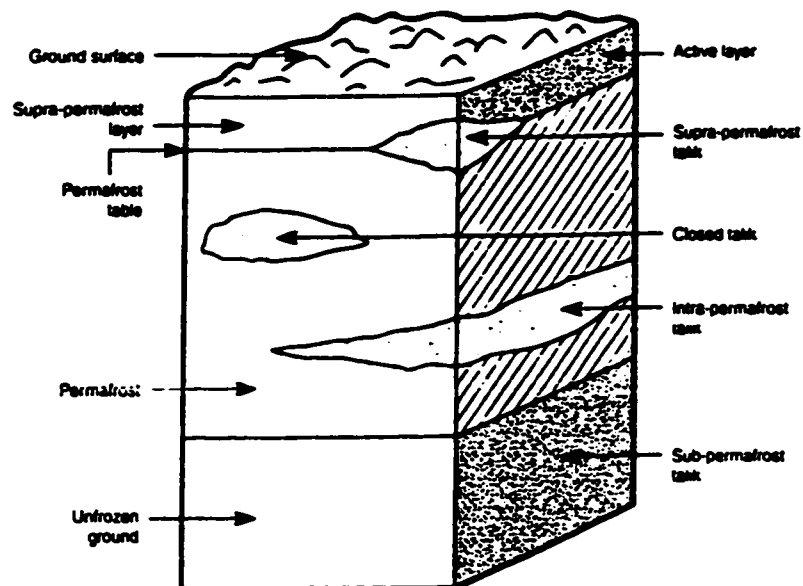


Figure 1.2 - Permafrost terminology (French, 1996)

thermal and hydrologic boundary conditions of the active layer (Hinzman *et al.*, 1991). Disturbances such as development and global climate change can upset the balance of the periglacial zone and cause dramatic change throughout the entire system. Therefore, in order to quantify the rate of change in this region resulting from natural and anthropogenic stress and reduce the risk of upsetting the delicate balance of the arctic system the hydrologic and thermal processes of the active layer must be better understood.

## **1.2 - RESEARCH OBJECTIVES**

The following study is a detailed investigation of active layer dynamics, hydrology and energy balance of a small esker basin in Canada's Arctic. Specifically, this paper will outline methods and results pertaining to the following research objectives:

- (1) To examine the effects of slope, aspect and vegetation cover on the radiation and energy balance of an arctic esker basin.
- (2) To describe the soil microclimate under varying vegetation cover and soil characteristics.
- (3) To determine spatial and temporal variability in active layer development within the study basin.
- (4) To quantify the hydrological budget of the study basin.

## **1.3 - LITERATURE REVIEW**

### **1.3.1 - Active Layer Thermal Regime**

Both the nature and the rate of the spring thaw and autumn freezeback are of interest with respect to the active layer. Spring thaw influences the nature of spring

runoff while the autumn freezeback controls the nature of frost heaving and ice segregation in the soil (French, 1996). Spring thaw initiates quickly when air temperatures are above 0°C and occurs in one direction from the surface downwards. Autumn freeze-back is a much more complex two-sided process where freezing of the active layer may proceed upward from the permafrost table as well as downward from the ground surface.

Ground thermal regimes are affected by a number of factors including soil particle size, ice content, snow thickness and density, and surface vegetation. As noted by Owens and Harper (1977), the active layer is normally thicker in sands and gravels than in fine-grained soils. However, the reverse has been reported where coarse material has permitted meltwater to penetrate rapidly to depth and refreeze, thereby building up an icy layer that delays thawing because of its latent heat of fusion (Washburn, 1980). Grain size influences the movement of water to the freezing front because the potential for drawing water to the freezing front increases with decreased depth.

Whether seasonally frozen or permafrost, the thermal regime of frozen ground is affected considerably by the amount and distribution of ice. Heat flow is influenced by the latent heat of fusion of ice. Ice lenses and massive ice beds are predominantly horizontal and delay the thawing of underlying ground compared with adjacent ground lacking such ice masses. Conversely, ice veins and ice wedges are vertical in their structure and promote vertical heat flow because of the greater thermal conductivity of ice than soil (Washburn 1980). With respect to snow thickness and density, heavy snowfall retards active layer thawing yet prevents extremes of ground freezing (French, 1996).

Increasing snow layer thickness and density insulates the active layer from the cold winter air keeps the subsurface temperatures much warmer than the air and reduces surface heat flux (Hinzman et al., 1991).

Finally, the atmosphere's influence on the active layer regime may be moderated by the buffering effect of processes in the vegetation layer. Riseborough and Burn (1988) note that the organic layer is significant primarily due to the effects of its moisture retention properties on throughflow, storage, and evaporation. When the organic material is moist, evaporation lowers the ground surface temperature and subsequently cools the active layer. Therefore, an increase in vegetation density directly above the active layer may be expected to increase cooling of the ground beneath.

The presence of moisture has a profound affect on the thermal and hydrologic dynamics of the active layer. Complicating active layer processes is the fact that not all water freezes at 0°C and, in certain frost-susceptible soils, as much as 40 per cent of the water content may remain unfrozen (French, 1996). Therefore, it is important to differentiate between the seasonally thawed layer that possess a temperature > 0°C (i.e. seasonally cryotic) and the upper layer of permafrost that thaws seasonally but remains below 0°C (i.e. seasonally active permafrost). As well, it is useful to differentiate between the freezing point which is the boundary between the frozen and unfrozen soil and the cryofront which is the 0°C boundary (French, 1996).

As illustrated in Figure 1.3, the seasonal dynamics of the active layer are significantly different between the spring thaw and summer freeze. For example, in the winter freezeback period, the ice content in the upper part of the active layer will increase

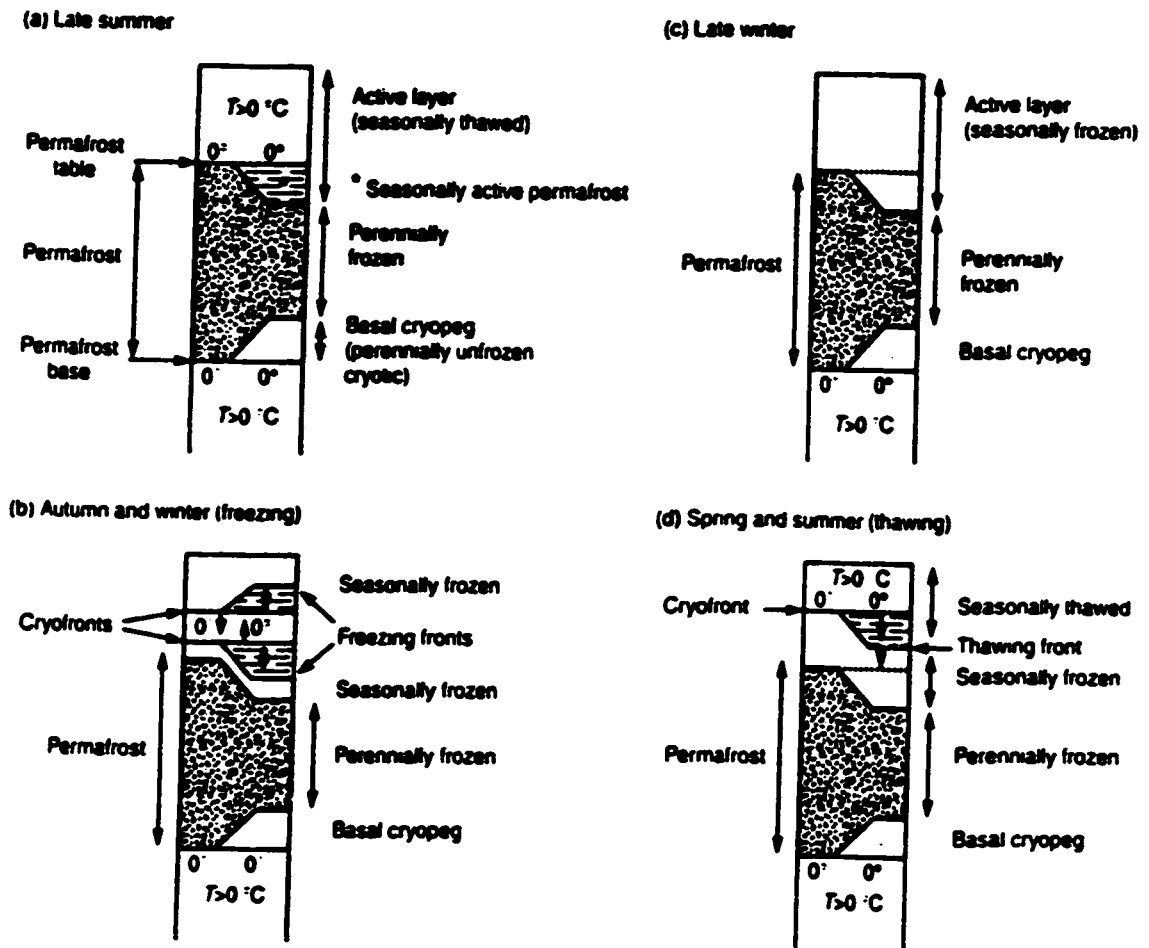


Figure 1.3 - Seasonal changes in the active layer. Temperature relative to  $0^{\circ}\text{C}$  and state of water are also indicated (French, 1996)

due to a positive ground temperature gradient. As noted by Hinzman et al. (1991), the movement of water upward and out of the surface soil causes subsequent desiccation of the organic layer. As well, freezing occurs in a two-sided manner both from the permafrost table upward and from the surface downward. In the summer however, a negative ground temperature gradient exists which causes unfrozen water to migrate downwards.

In any one year, the upward and downward movements of unfrozen water in the active layer are unequal. The upward migration of unfrozen pore water occurs in the winter when the unfrozen pore water content is low. By contrast, the amount of downward migration of unfrozen pore water in the summer via the negative ground temperature gradient is greater. Therefore, the result is that more water migrates downward to the permafrost in the thaw cycle than migrates upward in the freezing cycle (French, 1996).

### **1.3.2 - Radiation Balance**

Net radiation is the sum of the short-wave and long-wave radiation balances. The short-wave radiation balance is composed of the incoming global solar radiation and the reflected solar radiation. The long-wave radiation balance is the sum of the incoming long-wave radiation from the atmosphere and outgoing terrestrial long-wave radiation. To understand and explain regional climate and its variability, it is necessary to examine each component of the radiation balance, each of which is subject to unique controls specific to the particular environment in which they are being measured.

Controls on radiation balance for a given surface include the slope and aspect of the incident plane and the surface cover type. With respect to slope and aspect, the slope that most directly faces the Sun will receive the most radiation whereas if the Sun is grazing the surface minimal radiation is received (Dingman, 1984). The ratio of incoming versus reflected short-wave radiation is otherwise known as the albedo of a surface. Albedo is directly controlled by surface characteristics including vegetation cover and roughness. Average albedo values for tundra environments in the snow free season vary between 0.15 and 0.20 (Rouse, 1984; Lafleur et al., 1993). Despite changes in the development of the surface vegetation and the seasonal trend in surface soil moisture, daily albedo remains relatively constant throughout the summer months (Rouse, 1984; Bailey et al., 1989; Babrauckas and Schmidlin, 1997). On a diurnal basis however, it should be noted that albedo is slightly higher at sunrise and sunset compared to mid-day values (Bailey et al., 1989).

On average 81% of the global solar radiation occurs in the 6 months of March through August in Canada's Arctic (Rouse and Bello, 1983). Due to high albedo of snow, much of the incoming radiation is relatively ineffective as an energy source in arctic environments from March to May, when 39% of the yearly total occurs, because little is absorbed due to high albedos of snow (Rouse and Bello, 1983). As a result almost two-thirds of the yearly solar radiation that is absorbed at the surface occurs in the period June through August.

The first continuous measurement of global radiation in the Canadian Arctic was started at Aklavik, N.W.T in 1948. Maps of the monthly distribution of global radiation

for the whole of Canada were published by Mateer in 1955. Understanding of the regional distribution of global radiation in Canada was greatly improved throughout the 1960s and 1970s by Vowinckel and Orvig [1962], Barry [1964], and Dahlgren [1974] (Ohmura, 1982). During this time studies were conducted in different regions of the Canadian Arctic including Resolute by Vonwinckel [1966], Norman Wells by Brown [1965], northern Keewatin by Pugsley [1970] and Sachs Harbour by Vonwinckel and Orvig [1971] (Ohmura, 1982). By the mid 1970s, radiation and energy balance studies were being conducted in many parts of northern Canada, most notably by researchers including Ohmura, Muller and Rouse. Ohmura and Muller carried out extensive studies comparing regional differences in the climate of the Arctic by comparing net radiation over sea ice, the tundra and on glaciers. As well, Rouse and Stewart [1972] began a series of field experiments near the south-west shore of Hudson Bay, Manitoba in the summers of 1971 and 1972 examining energy balances between a ridge and sedge meadow (Ohmura, 1982). Work at this particular study site is ongoing and has expanded to the study of seasonal behaviour of components of the energy balance of subarctic tundra and open forest.

More recently, work has been published on studies examining components of the radiation balance components from a number of different cold regions environments within Canada including alpine tundra (Bailey et al., 1989), glaciers (Young, 1981; Munro, 1982), high arctic (Szidler et al., 1996) and arctic treeline (Rouse and Bello, 1983; Rouse, 1984; Lafleur, 1993; Duguay et al., 1999). As noted by Lynch et al. (1999) though, there has been much more emphasis on tropical and boreal environments as

compared to arctic sites with respect to energy balance and radiation component analysis. Concerns regarding the effects of global climate change in permafrost areas are prompting the need for a more thorough understanding of the effects of increases in near-surface temperatures.

Bailey et al. (1989) reported results from a study regarding the radiation balance of alpine tundra in the Rocky Mountains of southwestern Alberta. Their study focussed on the amount and duration of cloud cover and its effects on the radiation balance. The authors concluded that surface control on short-wave radiation through albedo was minimal, except for a brief period following snowfall. They also noted that there was no seasonal impact on albedo as a result of surface drying. Atmospheric haze resulting from distant forest fires had the most significant effect reducing all solar radiation balance components during the summer of 1985.

Rouse and Bello (1983) examined the behaviour of the summer radiation balance for a diversity of terrain type characteristics of the low Arctic. Terrain types in their study included upland tundra, upland open spruce forest, lowland peat and lowland swamp covered with sedge grass. On average for the summer, Rouse and Bello found that incoming solar radiation comprised 41 per cent of the total incoming flux with the remainder consisting of longwave radiation. Surface albedos in the non-snow period were generally small, being largest and the same for upland tundra and lowland peat at 0.15, less for the forest at 0.12, and least for the swamp, which ranged between 0.08 and 0.12. With respect to albedo, Rouse and Bello (1983) noted that under clear skies there was a strongly developed diurnal pattern of large albedos in morning and evening and

smaller values at midday. This pattern, however, was not evident on cloudy days. Differences in net radiation between surfaces were small and ranged from 59 and 65 percent of incoming solar radiation and 24 to 27 per cent of incoming all-wave radiation.

More recently, radiation balance studies have used remotely sensed data to upscale measurements of surface net radiation from point measurements, as previously mentioned, to estimating fluxes at the regional scale. Duguay et al. (1999) estimated surface albedo, and net radiation using Landsat Thematic Mapper (TM) data over a wetland tundra at northern treeline near Churchill, Manitoba. Mean absolute differences between remote sensing estimates and field measurements were 0.01 for albedo and 14.1  $W m^{-2}$  for net radiation. Furthermore, the authors examined within and between terrain type variations in surface net radiation during the growing season. Results of Duguay's work show that surface wetness and, to a lesser extent, phenology are the two main factors controlling the radiation balance during the summer period in this subarctic tundra-forest landscape.

### **1.3.3 - Ground Heat Flux and Active Layer Development**

The thermal regime in the ground is the pattern of temperature variation occurring over time and depth from the surface (Linell and Tedrow, 1981). Moisture and heat transfer processes of the active layer are complex, owing in part to the three phases of water which coexist and redistribute over time (Boike, 1997). Specifically, thermal and hydrological properties of the active layer such as volumetric heat capacity, thermal conductivity and liquid water content affect the development of the active layer during the

thaw season and subsequent freeze-back processes in the fall.

Volumetric heat capacity is defined as the quantity of heat required to change the temperature of a unit of volume by one degree (Linell and Tedrow, 1981). The volumetric heat capacity of a soil is dependent on the volume fraction of soil solids, water and ice. Typical values of heat capacity for a sandy soil, ice, and water are  $1.28 \text{ MJ m}^{-3} \text{ K}^{-1}$ ,  $1.93 \text{ MJ m}^{-3} \text{ K}^{-1}$ , and  $4.18 \text{ MJ}^{-3} \text{ K}^{-1}$ , respectively (Oke, 1987). The value for a given soil is strongly dependent on the soil moisture because adding water, which has a very high heat capacity, excludes a proportionate volume of soil air of low heat capacity (Oke 1987). An increase in soil water content of a soil causes a related increase in heat capacity. For example, a dry sandy soil has an approximate heat capacity of  $1.28 \text{ MJ}^{-3} \text{ K}^{-1}$  whereas a saturated sandy soil has heat capacity of  $2.96 \text{ MJ}^{-3} \text{ K}^{-1}$ . Peat soils, due to their higher storage potential can range from  $0.58 \text{ MJ m}^{-3} \text{ K}^{-1}$  to  $4.02 \text{ MJ m}^{-3} \text{ K}^{-1}$  for dry and saturated water contents, respectively.

The thermal conductivity of a soil is a property describing its ability to conduct heat by molecular motion (Oke, 1987). Similar to its affect on heat capacity water content also has a notable affect on the thermal conductivity of a soil (Onishchenko et al., 1999). For example, a dry sandy soil has a thermal conductivity of  $0.30 \text{ W m}^{-1} \text{ K}^{-1}$  whereas a saturated sandy soil has a thermal conductivity of  $2.20 \text{ W m}^{-1} \text{ K}^{-1}$ . Thermal conductivity has been found to be the main mechanism of heat transfer in frozen soils (Nixon, 1975). Woo and Xia (1996) noted that in permafrost soils, heat flux is highest soon after snowmelt, at a time in when both the thermal conductivity and the temperature of the near surface layer are large. In saturated soils, thawing causes a sharp switch in the

thermal properties (thermal conductivity and heat capacity). For soils which experience moisture fluctuations, the thermal parameters are also sensitive to drying and wetting events. Thus, the moisture dynamics of the active layer strongly influence heat conduction through the effects of the thermal properties (Woo and Xia, 1996).

Another thermal property of soils important in controlling heat transfer and the thermal climate is thermal diffusivity. The product of specific heat and thermal conductivity is thermal diffusivity which is an index of the facility with which a material will undergo a temperature change (Linell and Tedrow, 1981). It controls the speed at which temperature waves move and the depth of thermal influence of the active surface. Thermal diffusivity may be viewed as a measure of the time required for temperature changes to travel (Oke, 1987). Thermal diffusivity is affected by the same soil properties that influence thermal conductivity and heat capacity, especially soil moisture.

Soil heat flux is only a minor component of the surface energy balance comprising typically 10 per cent of the net radiation absorbed at the surface. However, in permafrost terrain the phase change between water and ice represents a major energy sink or source and the magnitude of the soil heat flux can increase appreciably (Halliwell and Rouse, 1987). Soil heat flux is a function of solar radiation, soil texture, soil moisture content and state, surface vegetation cover and weather conditions. In general, the soil heat flux can be treated as the sum of the storage of sensible heat and the storage of latent heat. Sensible heat refers to the addition or subtraction of energy within the soil measured through a temperature change. Latent heat is the heat energy released or absorbed in a given volume of soil by a change in phase of water and accounts for 82% to 90% of the

total ground heat flux depending on the surface and the season. According to Rouse (1984), of the remaining heat, 75% goes into heat exchange with the mineral soils and about 25% goes into soil water and ice components.

A number of studies examining heat transfer processes during soil cooling, freezing and thaw have been conducted in Central and Northern Alaska. McGaw et al. (1978) measured in-situ thermal conductivity and temperature and reported the influence of phase change of soil moisture on thermal diffusivity. The authors concluded in their study that permafrost within a meter of the surface at Barrow, although apparently passive, has dynamic thermal properties under the influence of varying temperatures. More recently, Hinzman et al. (1991) reported in their study in Imnavait watershed located in the Brooks Range of Alaska that the layer of organic soil tends to mollify thermal and hydrologic fluctuations below it. They noted that the thermal conductivity of the surface organic layer at average moisture contents is about one-third that of the silt and thus functions as a layer of insulation for the permafrost.

Hinkel and Outcalt (1994) compared two sites in central Alaska, one located within a ground water seepage zone and another over a body of permafrost. They concluded that warming of the active layer in spring occurs nearly instantaneously and results from infiltration of snow cover meltwater and downward migration at the permafrost site. In contrast, they found that water saturation of pore space at the seepage site inhibits vertical migration of vapour and water. On a larger scale, studies by Romanovsky and Osterkamp (1995) and Nelson et al. (1998) examined differences in active layer thermal regime between areas extending from the Arctic Coastal Plain to the

Arctic Foothills of Alaska. Romanovsky and Osterkamp (1995) reported that active layer thickness increased from the coast inland (0.21 m and 0.72 m, respectively) and showed systematic temporal variations. Nelson et al. (1998) reported that patterns of active layer thickness are governed closely by topographic detail which influences the near-surface hydrology. On the coastal plain, smaller variability in active layer thickness was reported as compared to sites within the foothills where high variability occurs over much smaller distances.

Romanovsky and Osterkamp (2000) combined precise field temperature and soil water content data with computer modelling to provide quantitative measures of the dynamics of unfrozen water in the active layer and permafrost at four Alaskan permafrost sites (Prudhoe Bay, Barrow, and two sites near Fairbanks). The authors noted that unfrozen water contents are negligible for living and dead moss layers, small in the peat layers, larger in the silts, and show significant site-to-site variation. The effect of unfrozen water on the ground thermal regime is reported to be largest after freeze-up and during cooling of the active layer and is less important during warming and thawing of the active layer. Romanovsky and Osterkamp (2000) concluded that unfrozen water in the freezing and frozen active layer and near-surface permafrost protects the ground from rapid cooling. This process creates a strong thermal gradient at the ground surface that increases the heat flux out of the ground.

Active layer thermal regime studies have also been conducted in other permafrost regions including the Yukon Territory (Leverington, 1995; Harris, 1998), Schefferville, Quebec (Nicholson, 1978), Canada' High Arctic (Szidler et al., 1996; Woo and Xia,

1996), and Greenland (Jahn and Walker, 1983; Osterkamp, 1987; Tatenhove, 1994; Humlum, 1998). With respect to computer modelling of the effects of vegetation cover spatial variation in active layer depth, Leverington (1995) stressed the importance of supporting such programs with field measurements made in all areas being mapped. In a similar study conducted in the Yukon Territory, Harris (1998) referred to the profound differences in heat flow between five different slopes with varying aspect. Further to comments made by Leverington (1995), Harris (1998) suggested that flat-topped landforms such as peat plateaus require fewer field measurements for modelling than do landforms on sloping surfaces.

In order to determine some of the effects of a warmer climate on active layer development, Nicholson (1978) modified a tundra plot by removing the vegetation and erecting snow fences near Schefferville, Quebec. After 5 years of monitoring, profound changes in the energy budget were reported. Ground temperature at 10 m depth increased by 1.8°C while the active layer deepened from 2.8 to 6.5 m. Modifications to the study plot were reported to have completely prevented upward heat loss from 5.5 m in depth and below and there was an average gain in energy equivalent to 2% of net radiation at 5.5 m in depth. This study highlights the profound effects that global climate change and open pit mining for example could have on sensitive arctic environments.

Many studies have examined the microclimate of arctic tree line near Churchill, Manitoba. Rouse (1984) reported that forest and tundra soil display distinctive microclimates. Forest soils were found to be substantially warmer in the active layer than those of the tundra. The thaw period in the tree rooting zone lasted for 6 months as

compared to 4 months at the same depth in tundra. Soil heat storage was calculated to be large at both the tundra and forest sites, comprising 18% and 16% of net radiation respectively during the thaw season. Furthermore, Rouse (1984) determined that between 80% and 90% of the total soil heat storage is involved in the latent heat exchange coinciding with thawing and freezing. Of importance to future work concerning measurement of ground heat flux, Rouse was the first to note that soil heat flux plates underestimate the ground heat exchange and are unreliable in permafrost terrain.

Follow up studies to Rouse (1984) have further examined the subarctic surface energy budgets across northern treeline at the Churchill study site. Halliwell and Rouse (1987) introduced the calorimetric method of soil heat flux determination as a means of quantifying error associated with using soil heat flux plates in permafrost regions. They determined that heat flux plates underestimate the surface heat flux in organic permafrost terrain by about 50 percent. Halliwell and Rouse (1987) concluded that the largest portion of the soil heat flux is stored as latent heat in the thawing of ground ice. The smallest component of the surface flux was determined to be the portion stored as sensible heat in the layer between the surface and the permafrost table. Overall, they reported that the soil heat flux represents a high fraction (from 16 to 18 per cent) of the net all-wave radiation available at the surface.

Lafleur et al. (1992) furthered Rouse's work by examining energy balance differences and hydrologic impacts across the northern treeline. With respect to ground heat flux, the authors noted that values averaged 9 and 12 per cent of net radiation for the forest and tundra respectively. The slightly larger ground heat flux at the tundra site was

attributed to a larger amount of energy consumed in melting permafrost. Petrone et al. (2000) compared a subarctic wetland site near Churchill with a western wetland and western dry site near Inuvik, N.W.T. With respect to the ground thermal regime, the western dry site produced the deepest active layer (0.8 m) compared to the other two sites. Warm temperature enhanced the latent and ground heat fluxes while suppressing the sensible heat flux at all sites. Cold temperatures were found to have the opposite effect.

### **1.3.4 - Energy Balance**

The surface energy balance is the sum of three parts: (1) the latent heat flux accompanying the evapotranspiration process, (2) the sensible heat exchange with the atmosphere, and (3) heat exchange with the subsurface. Daytime energy surplus of the surface is transported away from the ground/air interface by means of convection (Oke, 1987). The availability of water for evaporation governs the relative importance of sensible versus latent heat with the ratio of these two fluxes referred to as Bowen's ratio ( $\beta$ ). Numerous studies have been undertaken in permafrost environments to quantify the surface energy balance both spatially and temporally. Surface energy balance studies can range from site specific to regional scales of study, each with unique controls and relationships with respect to meteorological conditions.

Harazano et al. (1998) compared energy budget components between a coastal tundra site at Prudhoe Bay, Alaska, and a wet sedge, and dry tussock tundra site around Happy Valley, Alaska. Findings of this study highlighted the importance of air mass conditions on energy partitioning. Specifically, under cold and humid conditions

(onshore winds) the temperature gradient over the tundra ecosystem increased, which resulted in a higher level of sensible heat. Under warm, dry conditions (offshore winds), air and soil temperatures were found to increase along with the water vapour deficit which resulted in an increase in latent heat. Such findings are important with respect to forecasted increases of global temperature due to climate warming. Findings from Harazano et al. (1998) indicate that an increase in temperature will increase the latent heat flux of tundra, especially in flooded areas. Furthermore, expanding areas of dry tundra will increase the sensible heat flux rather than the latent flux which will further enhance the warming of the tundra ecosystem.

Rott and Obleitner (1992) studied energy fluxes over dry tundra from mid-May to mid-June 1988 in Western Greenland. Temporal variations of energy fluxes in this study were shown to be dominated by the incoming solar radiation and the availability of moisture at the soil surface. The authors noted that desiccation of the soil crust during the first two weeks of the observation period resulted in decreased evaporation. On average, it was found that the sensible heat flux clearly surpassed the latent heat flux.

Measurements taken over various surface types including dry tundra and a swamp both indicated that daily evapotranspiration was found to be closely related to net radiation and to the difference between air temperature and surface temperature. The authors noted that this observation offers the opportunity to apply satellite data for estimation of latent heat flux with confidence in future regional scale energy budget analyses.

Studies on energy balance component fluxes in Canada's high Arctic have quantified physical processes driving such fluxes and the factors which control them.

Szidler et al. (1996) used short-term measurements in combination with a new mathematical model formulated to diagnose the diurnal variation of the energy fluxes and temperature on the snow-free tundra surfaces at Princess Marie Bay, Nunavut. The authors predicted the partitioning of net, short- and long-wave radiation reaching the surface into convective heat exchanged with the atmosphere and heat conducted into the soil. Their model suggested that heat conduction into the upper layers of the soil is very important in predicting the diurnal variation of the tundra microclimate. They also noted that the convective heat exchanged with the atmosphere is a heat sink for the surface layer. Rouse et al. (2000) stated that while the physical processes driving energy fluxes in the high latitudes are universal, some of the controlling factors such as permafrost, temperature and vegetation play a special role in terms of site specific processes.

Energy balance differences across the northern treeline are also well documented for the Hudson Bay coast near Churchill, Manitoba. Similar to the observations of Harazano et al. (1998), Rouse (1984) and Petrone et al. (2000) concluded that energy balance component measurements indicate a strong regional advective effect. In the premelt period during cold onshore winds, net radiation was very small and the other energy balance components were negligible. Under offshore warmer winds, net radiation was found to be large, as were the other fluxes, especially the ground heat flux. During the postmelt period, the magnitude of net radiation and the latent heat flux were little affected by wind direction. In a comparison of a wet tundra site and a nearby open conifer forest, Lafleur et al. (1992) showed that the sensible and latent heat fluxes were very different. When surface moisture was not limiting, the latent heat flux was

determined to be largest for the tundra whereas at the forest site the sensible heat flux was largest.

#### **1.4 - RELEVANCE OF RESEARCH OBJECTIVES**

Eskers are a prominent geomorphological feature throughout the Northwest Territories. Hydrologically, eskers play a significant role in terms of trapping large quantities of snow in their downwind side and in any depressions within the feature. Therefore they are regarded as significant features of surface and most probably groundwater recharge. Eskers are also biologically significant to the arctic environment as they provide denning sites for animals including foxes, wolves and bears, are important migratory paths for caribou and are home to unique plant communities. Economically, eskers are geomorphological indicators of mineral deposits and are therefore the focus of intensive diamond mine exploration and development. Extraction of such minerals is a large scale operation that leads to road networks, mining camps, and processing units which lead to displacement of large amounts of water and alteration of the natural environment.

Due to concerns outlined above a more thorough understanding of eskers and associated basins is required in Canada's North. Expanding on the current body of literature regarding energy fluxes in permafrost environments, the present study will examine the effects of slope, aspect and vegetation cover on active layer dynamics in an arctic esker basin. Due to the steep nature of the Kakawi Lake study basin, differences in slope and aspect and the effects of surface cover type are expected to have a significant

effect on spatial and temporal variations in the radiation balance. Furthermore, differences in net radiation balance will affect subsurface thermal regimes and active layer development which will also be quantified using detailed field measurements. Finally, due to the self-contained nature of the study basin a hydrological balance including measurement of subsurface lateral flow from hillslope segments will be calculated.

---

## **CHAPTER 2 - STUDY SITE**

---

### **2.1 - SELECTION OF KAKAWI LAKE STUDY BASIN**

The 14 ha Kakawi Lake basin was selected for this study based on logistical considerations, suitability to field research and representativeness with respect to the surrounding Daring Lake and Coppermine River basin area. Specifically, the study site location was based on four requirements: (1) the site was representative of the till material and regolith of the surrounding area, (2) the site has vegetation cover which is typical of the region, (3) that the site was logistically practical in terms of carrying out intensive fieldwork on a daily basis, and (4) the basin is a self-contained hydrological unit thus allowing for computation of a water budget. The Department of Resources Wildlife and Economic Development's Tundra Ecosystem Research Station (TERS) established in 1994 provided a well-equipped base camp to conduct this study. Therefore, research partnerships with both BHP Diamonds Inc. and the Government of the Northwest Territories (GNWT) provided our research team with transportation to Daring Lake, a well-equipped research station and lodging, and an important communication and transportation link in case of an emergency.

Daring Lake, N.W.T. ( $64^{\circ} 52' N$ ,  $111^{\circ} 35' W$ ) is situated in the Coppermine River basin which extends approximately 520 km from the headwaters near Lac de Gras (approximately 460 metres above sea level) in a generally northwest direction to its mouth at Kugluktuk located on the shores of the Coronation Gulf (Figure 2.1). The Coppermine Basin encompasses two geological provinces; the southern Slave Geological



Figure 2.1 - Coppermine River Basin, Northwest Territories

Province and the northern Bear Geological Province with a gross drainage area of 50 800 km<sup>2</sup> (Wedel et al., 1988). Daring Lake is located in the Slave Geological Province which is characterized hydrologically by a very dense network of interconnected lakes and rivers. The Kakawi Lake study basin is located on the north shore of Daring Lake, east of the narrows joining Yamba Lake and Daring Lake and is at the base of a large sand and gravel esker that runs continuously in an east-west direction for 100 km (Matthews and Clark 1996).

## **2.2 - LANDSCAPE**

The Kakawi Lake basin is located 1 km northeast of the narrows joining Yamba Lake and Daring Lake. The topography surrounding this area is generally gently undulating to moderately rugged with relief on the order of 10-20 m (Dredge et al., 1999). Most relief on this glacial terrain was created by eskers, drumlins, and hummocky till. Raised beaches, deltas, marine blankets and incised river terraces create relief that is typically less than 10 m (Dredge et al., 1999). Some eskers in the area are more than 45 m high and rugged, rocky areas around Yamba Lake have about 50 m local relief. Numerous lakes occupy glacially scoured bedrock basins and drainage ways are shallow because streams have not cut into the bedrock or till plain (Geological Survey of Canada, Map 1870A)

Situated at the intersection of a trunk esker and a tributary esker, the Kakawi Lake study basin has moderate local relief of 30 m from the lake edge to the top of the basin divide. Slopes range from less than 10 degrees on portions of the west-facing slope up to

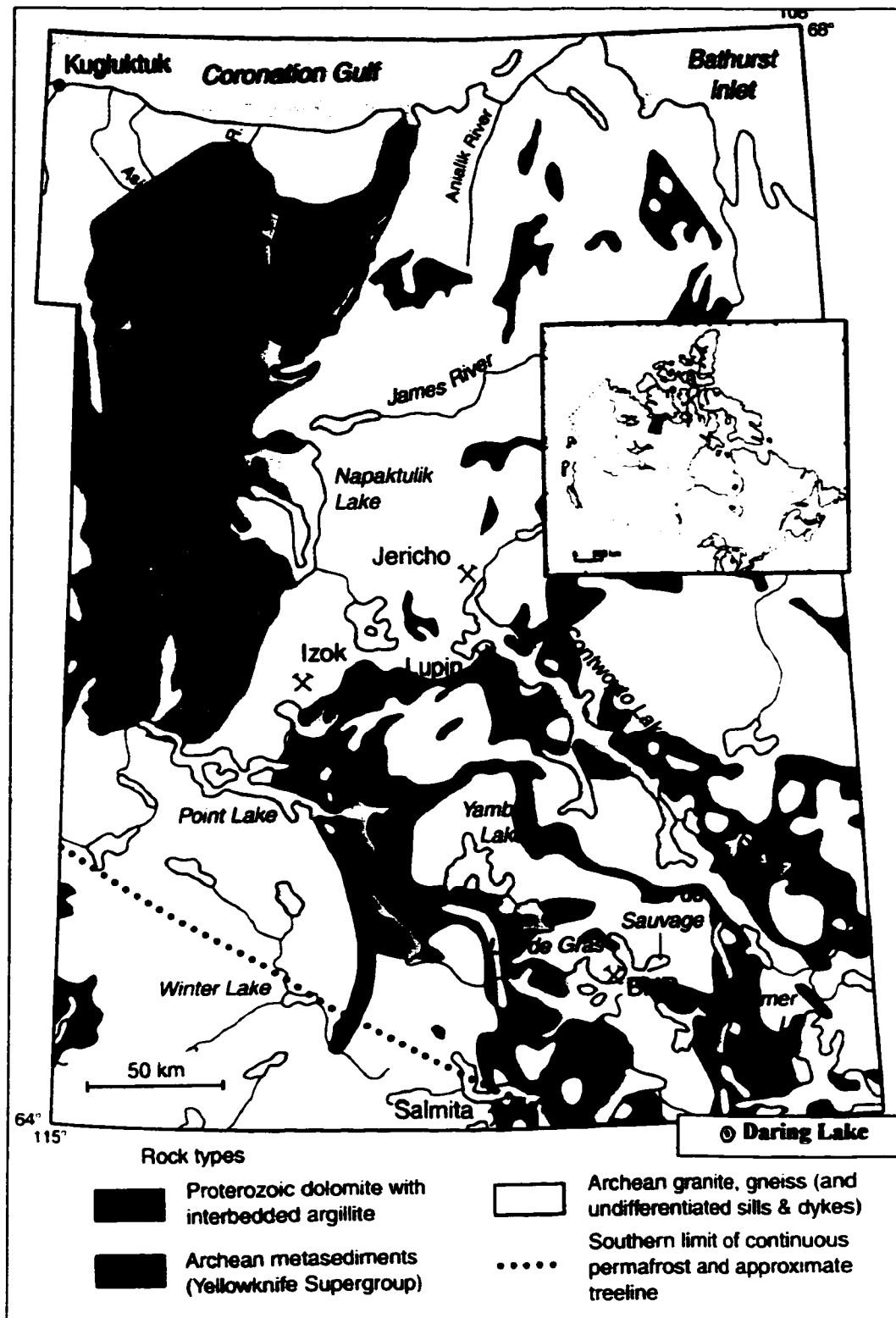
35 degrees on east-facing slopes. The contained lake drains north into Yamba Lake via groundwater flow through a series of interconnected ponds and wetland areas.

### **2.3 - GEOLOGY**

The Kakawi Lake basin lies in the central Slave Province of the Canadian Shield. Bedrock underlying the Slave Province consists primarily of Archaen sedimentary, volcanic, and plutonic rocks that have been variably metamorphosed (Geological Survey of Canada, Map 1870A). The Daring Lake basin encompassing the Kakawi Lake study basin is underlain by metasedimentary rocks belonging to the Yellowknife Supergroup (Figure 2.2). All rock types within this area have been subjected to intense frost shattering in the postglacial period, resulting in the frost heaving of large blocks commonly above the level of the surrounding bedrock surfaces (reference: geology map). Permafrost attains thickness between 160 m and more than 350 m but varies considerably depending on local site. Permafrost is, however, absent beneath most lakes within the Slave Province.

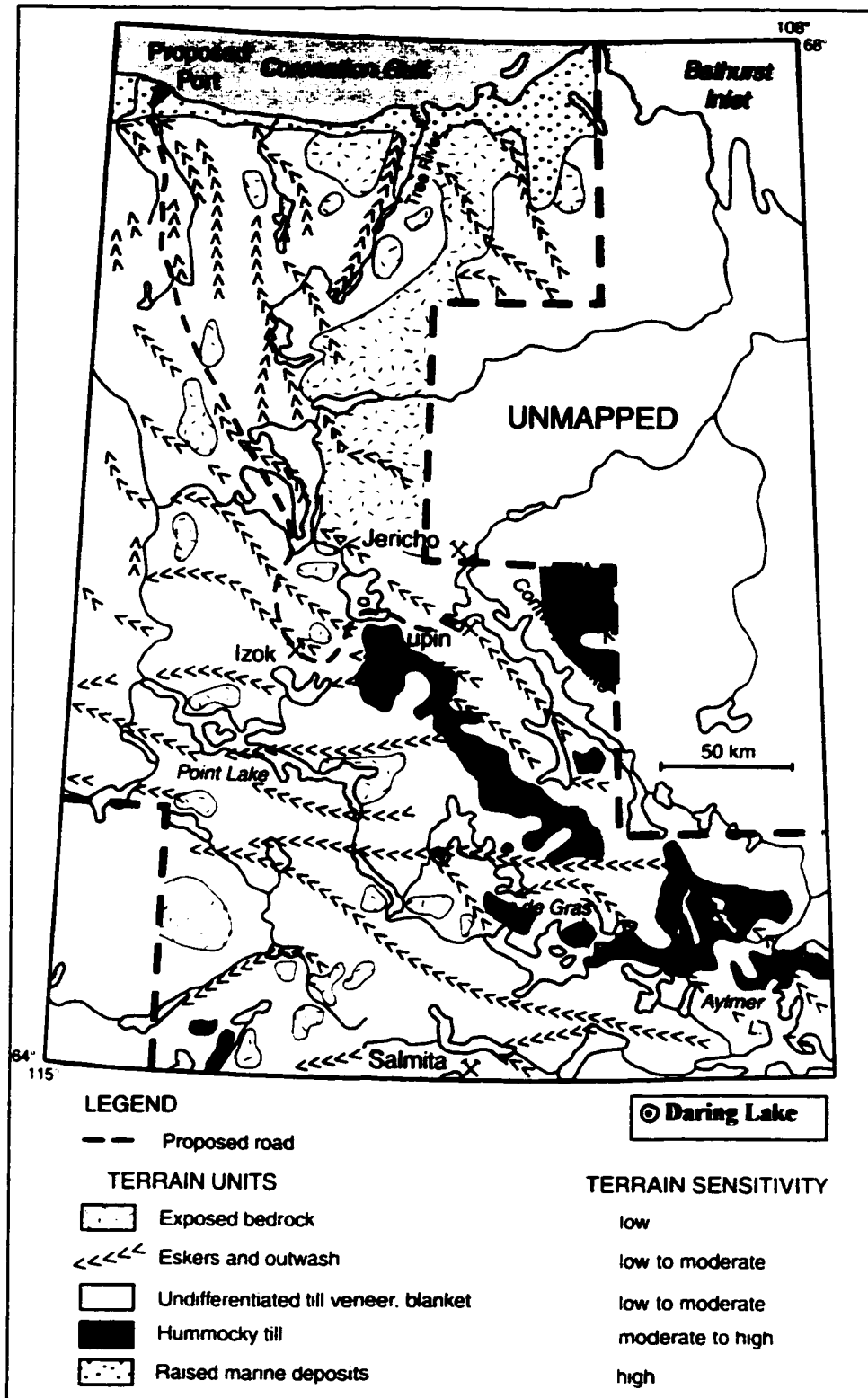
### **2.4 - TILL DEPOSITS**

All features in the Slave Province are related to the Late Wisconsinan glaciation. Till veneers, undulating till blankets and streamlined rocks and till forms that include drumlins and eskers are the principal landforms in the area (Figure 2.3). These features are indicative of warm-based ice conditions thus accounting for the relatively shallow depth of permafrost in the region. (Dredge et al., 1999). Only one stratigraphic unit of



(Dredge *et al.*, 1999)

**Figure 2.2** – Bedrock types and southern limit of continuous permafrost in the Slave Geological Province



(Dredge *et al.*, 1999)

**Figure 2.3** – Surficial sediments, eskers, and terrain sensitivity in the Slave Geological Province -28-

till has been recognized in the Slave Province which can be divided into 3 units based on thickness and surface morphology: (1) thin veneer, (2) blanket deposits up to 10 m thick, and (3) hummocky till up to 30 m thick. The Kakawi Lake basin is characterized by geological predominance of esker sediments composed of sand, silt and gravel which corresponds with the second of the three till units. This till can range from silty sand to sand with low percentages of clay. Grain size varies according to the bedrock source and the amount of meltwater associated with the deposition (Geological Survey of Canada, Map 1870A) .

## **2.5 - ESKERS**

Eskers are one of the most predominant glaciofluvial deposits in the Slave Province. Trunk and tributary eskers mark the location of major and minor meltwater conduits within the late-glacial ice sheet (Dredge et al., 1999). Eskers in this region range from small, sinuous ridges to large more linear features and contribute to the majority of topographic relief in the area (Geological Survey of Canada, Map 1870A) . They can range in form from those which have rounded profiles with sandy features to those which are sharp crested and have bouldery surfaces with or without slump features along the flanks (Dredge et al., 1999). Most eskers appear to be well drained near the surface and may have low ice contents. However, within the Lac de Gras area, southeast of the study site, massive ice in excess of 5 m thick is known to occur within an esker (Dredge et al., 1999).

A wide ranging network of small, generally northwest trending eskers feeds into a

large, approximately east-west trending trunk esker along the southern shore of Yamba and Exeter lakes (Geological Survey of Canada, Map 1870A) (Figure 2.3). The Kakawi Lake study basin lies at the confluence of this trunk esker and a tributary esker trending north towards Yamba Lake. The trunk esker is 30 m in height along the Kakawi Lake basin and is characterized by a broad, flat ridge with numerous boulders flanking the top. Dredge et al., 1999 reported from observations on 46 esker sites and five sections south of Lac de Gras that some eskers contain high proportions (70-90% by volume) of thinly stratified fine-grained material ranging in grain size from silty sand to clayey silt. These eskers tend to be 15-25 m high and have broad crests ranging from 20-80 m across similar to the esker lining the Kakawi Lake basin. Eskers play a significant role in terms of hydrology as they trap large quantities of snow in their downwind side and in any depressions within the feature. Therefore, they are significant features of surface and most probably groundwater recharge. Surficial geology maps and ground truthing efforts in the Daring Lake basin indicate that till deposits outside what may be considered to be the boundary of esker influence are structurally similar to the esker deposits.

## **2.5 - GENERAL VEGETATION AND CLIMATE**

Treeline is approximately 75 km to the southwest of Daring Lake. The Daring Lake area is characterized as a Low-Shrub vegetation zone on the "Canadian Transect and Mapping for the Circumpolar Arctic Vegetation Map" (Gould et al., 2000). This zone is found entirely on the mainland in Canada and is characterized by low-shrub vegetation, primarily *Betula glandulosa* on acidic soils and *Salix glauca* on non acidic soils.

*Eriophorum vaginatum* tussock tundra can be dominant on acidic substrates this zone. A variety of tall shrubs are found in riparian and sheltered areas. Wetlands show considerable peat development. Vegetation cover is continuous except on exposed ridges and areas of the Canadian Shield with mineral surficial deposits (Gould et al., 2000).

Mean annual total precipitation for the Daring Lake area is approximately 300 mm per year (Environment Canada, 1986), 50% of which occurs in the form of snow in the Daring Lake area (Environment Canada, 1986). Snowfall accumulation begins in mid-August and remains on the ground until the end of May and even early June in some years. Yearly average temperature as recorded from 1956 to 1981 at Contwoyoto Lake, N.W.T. (65° 29' N, 110° 29' W) is -7.8°C with mean temperatures of -35.1°C and 4.8°C for January and June respectively.

---

---

## **CHAPTER 3 - METHODOLOGY**

---

---

### **3.1 - KAKAWI LAKE VEGETATION CHARACTERIZATION**

Vegetation is an important controlling factor on both the hydrology and energy partitioning in arctic environments. In order to better understand the effects of specific types of vegetation on active layer development a detailed inventory of dominant vegetation types was completed within the Kakawi Lake basin. First, all dominant species of plants, peat and lichens were documented as well as the environments in which they were found to be most common. Tables 3.1, 3.2, and 3.3 list the major types of plants, peat and lichens respectively including their common name and scientific name. Tables 3.2 and 3.3 also describe the general environment in which each specific type of peat and lichen grow.

Based on a detailed inventory of Kakawi Lake vegetation types and visual inspection of the basin a series of 7 vegetation classes were assigned which served to generalize the basin into specific areas with respect to dominant vegetation type. These 7 vegetation classes include:

- (1) Closed birch
- (2) Open Birch
- (3) Birch dominant
- (4) Lichen
- (5) Hummocky sedge
- (6) Peat and cloudberry
- (7) Sedges and weeds

These vegetation classes were first outlined on a map of Kakawi Lake basin and then later incorporated into a detailed survey of the basin.

**TABLE 3.1 - Kakawi Lake Basin Vegetation**

<b><u>FAMILY</u></b>	<b><u>COMMON NAME</u></b>	<b><u>SCIENTIFIC NAME</u></b>
BETULACEAE - Birch Family	Dwarf Birch	<i>Betula glandulosa</i>
SALICACEAE - Willow Family	Least Willow	<i>Salix herbacea</i> (L.)
EMPETRACEAE - Crowberry Family	Crowberry	<i>Empetrum nigrum</i> (L.)
ERICACEAE - Heath Family	Alpine Bear Berry	<i>Arcostaphylos aplina</i> (L.) (Spreng.)
ERICACEAE - Heath Family	Dry Ground Cranberry	<i>Vaccinium vitis-idaea</i> (L.)
ERICACEAE - Heath Family	Alpine Bilberry (blueberry)	<i>Vaccinium uliginosum</i> (L.)
ROSEACEAE - Rose Family	Cloudberry	<i>Rubus chameamorus</i> (L.)
ERICACEAE - Heath Family	Labrador Tea	<i>Ledum decumbens</i> (L.)
ERICACEAE - Heath Family	Bog Laurel	<i>Kalmia polifolia</i> (Wang.)
ERICACEAE - Heath Family	Bog Rosemary	<i>Andromeda polifolia</i> (L.)

**TABLE 3.2 - Kakawi Lake Basin Peatland Species**

<b><u>COMMON NAME</u></b>	<b><u>SCIENTIFIC NAME</u></b>	<b><u>DESCRIPTION</u></b>
Rusty Peat Moss	<i>Sphagnum fuscum</i>	- most common in basin - orange (brown/green) colour - found on hummocks
Slender Hair Cap	<i>Polytrichum strictum</i>	- green in colour - closely assoc. with sphagnum - found atop hummocks
Tall Clustered Thread Moss	<i>Pryom pseudotriquetrum</i>	- less common in basin - green to red in colour - grows in cushions, mats or as individuals

**TABLE 3.3 - Kakawi Lake Lichen Species**

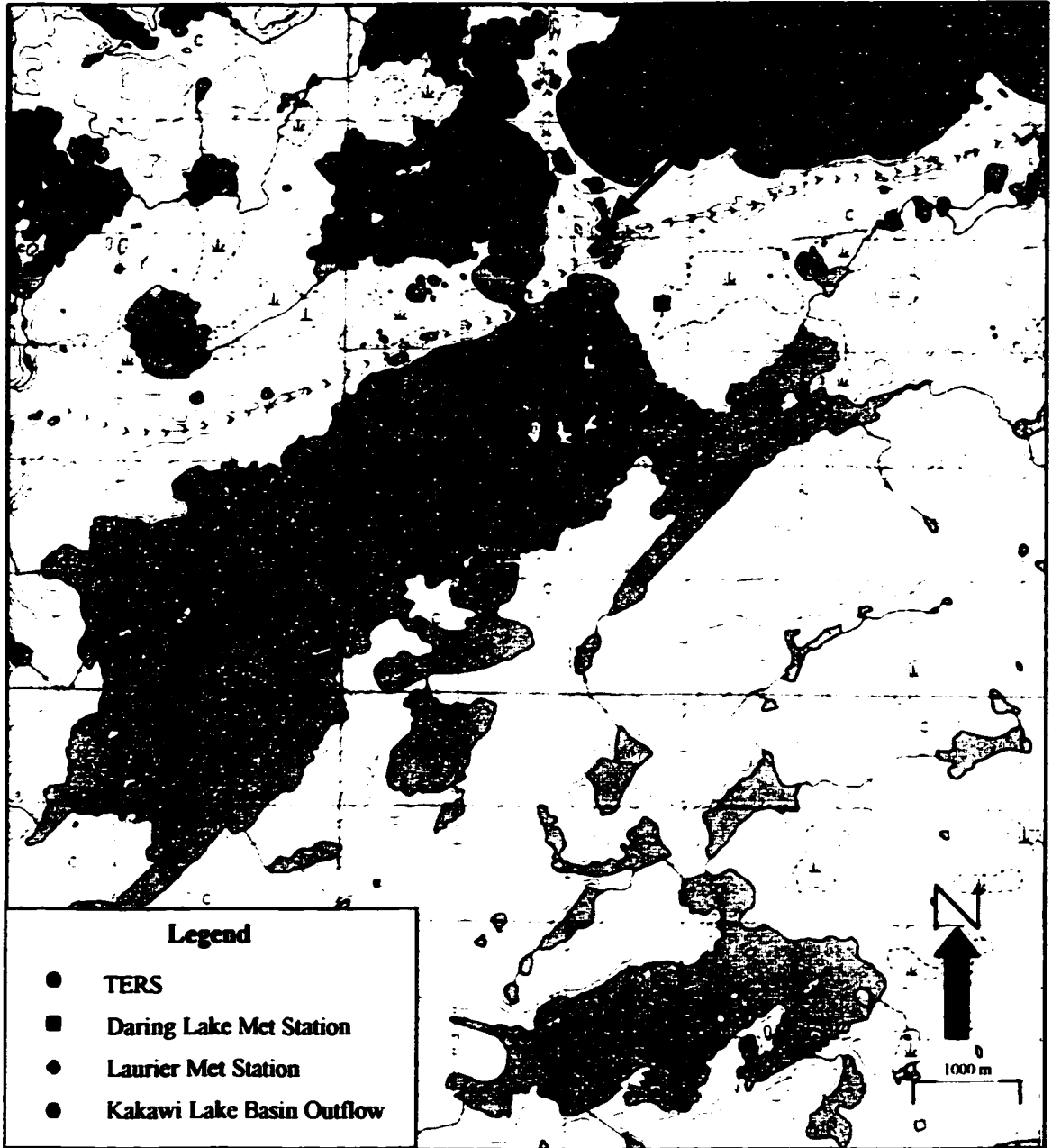
<b><u>SCIENTIFIC NAME</u></b>	<b><u>COMMON NAME</u></b>	<b><u>DESCRIPTION</u></b>	<b><u>LOCATION / ENVIRONMENT</u></b>
<i>Rhizocarpon geographicum</i>	Map Lichen	- black with light yellow/green spots	*- rocks
<i>Parmeliopsis ambigua</i>		- whitish yellow	*- rocks
<i>Umbilicaria</i> sp.	Rock Tripe	- black and flaky	*- rocks
<i>Flavocentraria nivalis</i>	Flattened Snow Lichen	- white colour	- random
<i>Flavocentraria cucullata</i>	Curled Snow Lichen		**
<i>Cladina mitus</i>		- yellow	** - common - on most hillslopes
<i>Nephroma arcticum</i>		- yellow ( like above - broader leaves)	** - common - on most hillslopes
<i>Thamnola sobuliformis</i>	Worm Lichen	- small, white - looks like antlers	****- most hillslopes
<i>Masonhalea richardsonii</i>	Antler Lichen	- small, brown - looks like antlers	****- most hillslopes
<i>Stereocaulon tomentosum</i>	Woolly Coral	- white	****- commonly interspersed with yellow lichen
<i>Bryocaulon divergens</i>		- small, black, twig-like	
<i>Cladonia borealis</i>	Red Pixie-Cup	- thick yellow antler with red bead on top	

### **3.2 - METEOROLOGICAL STATIONS**

Three meteorological stations were used for this study to monitor air temperature, relative humidity, wind speed and direction, solar radiation, precipitation, soil moisture and temperature, lake temperature and lake level. Each met station was positioned to take in account microclimatic spatial and temporal variability encountered within and in close proximity to the study basin.

The Daring Lake met site was established in 1995 approximately 300 m from the east shore of Daring Lake by the Department of Indian Affairs and Northern Development (DIAND) and is located on gently sloping terrain characterized by hummocky sedge, dwarf birch and grasses (Figure 3.1). The Laurier met station was erected at the beginning of the 1999 field season at the top of the esker lining the southern boundary of the Kakawi Lake basin (Figure 3.2). The area surrounding this met site is relatively flat and is characterized by bouldery open gravelly sand areas which are interspersed with patches of dwarf birch and lichen. As well, at the beginning of the 1999 field season the Kakawi Lake met station was also constructed along the southern shore of Kakawi Lake downslope of the Laurier met station (Figure 3.2). This met station's primary function is to monitor lake levels and wind speeds at the base of the Kakawi Lake basin.

Specific details regarding instruments used to measure variables at each meteorological station are detailed in Tables 3.4, 3.5 and 3.6.



*Source:* NTS Map 76 D/11

*Scale:* 1:50,000

**Figure 3.1 – Kakawi Lake study basin and greater Daring Lake area**



Top View

Figure 3.2 Kakawi Lake Basin Instrumentation

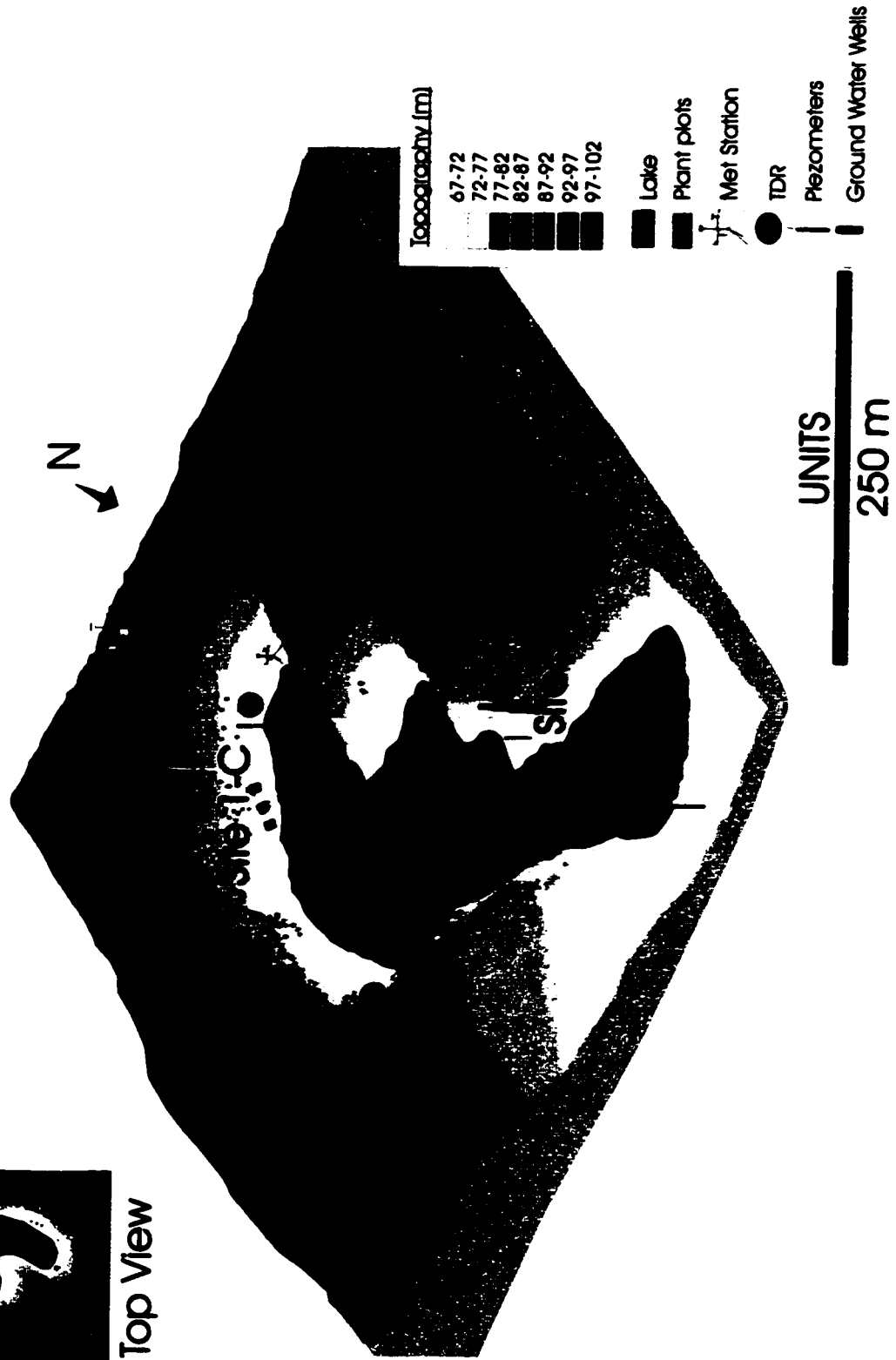


**Table 3.4 - Daring Lake Met Station**

<b>VARIABLE</b>	<b>HEIGHT / DEPTH (m)</b>	<b>INSTRUMENT TYPE</b>
Air temperature and Relative Humidity	2.4	Vaisala HMP35CF [error: $\pm 0.4^{\circ}\text{C}$ ]
Wind Speed	2.9	Met One Model 013A Anemometer [error: $\pm 0.11 \text{ m s}^{-1}$ ]
Wind Direction	2.9	NRG Type 200P Wind Vane [error: $\pm 5^{\circ}$ ]
Solar Radiation	2.5	LiCor LI200S Pyranometer [error: $\pm 2\%$ ]
Precipitation	3.3	Texas Electronics TE525M tipping bucket rain gauge [error: $\pm 1\%$ ]
Snow Depth		Campbell Scientific UDG01 [error: $\pm 1\%$ ]
Soil Moisture	0.10, 0.30	Campbell Scientific CS615 Water Content Reflectrometry Sensors [error: $2\%$ ]
Soil Temperature	0, 05, 0.10, 0.20, 0.40	107B Fenwal thermistors [error: $\pm 0.2^{\circ}\text{C}$ ]

**Table 3.5 - Laurier Met Station**

<b>VARIABLE</b>	<b>HEIGHT / DEPTH (m)</b>	<b>INSTRUMENT TYPE</b>
Air Temperature and Relative Humidity	0.87, 2.54	Vaisala HMP35CF [error: $\pm 0.4^{\circ}\text{C}$ ]
Wind Speed	2.87	Met One Model 014A Anemometer [error: $\pm 0.11 \text{ m s}^{-1}$ ]
Wind Direction	2.9	NRG Type 200P Wind Vane [error: $\pm 5^{\circ}$ ]
Solar Radiation	1.37	Kipp and Zonen NRLite Net Radiometer (1.19 m above veg - dwarf birch) [error: $\pm 5\%$ ]
Precipitation	3.27	Texas Electronics TE525M tipping bucket rain gauge [error $\pm 1\%$ ]
Soil Moisture	0.13, 0.52	Campbell Scientific CS615 Water Content Reflectometry Sensors [error: 2%]
Soil Temperature	0.10, 0.30, 0.83	107B Fenwal thermistors [error: $\pm 0.2^{\circ}\text{C}$ ]

**Table 3.6 - Kakawi Lake Level Station**

<b>VARIABLE</b>	<b>HEIGHT / DEPTH (m)</b>	<b>INSTRUMENT TYPE</b>
Water Level	Lake bottom	Keller 169 Transducer [error: $\pm 0.25\%$ ]
Water Temperature	Lake bottom	107B Fenwall Thermistor [error: $\pm 0.2^{\circ}\text{C}$ ]
Soil Temperature	3 @ 0.2	107B Fenwal thermistors [error: $\pm 0.2^{\circ}\text{C}$ ]
Wind Speed	1.2	NRG Type 40 Anemometer [error: $\pm 1\%$ ]

### **3.3 - HILLSLOPE AND SITE SELECTION**

Three hillslope transects were selected within the Kakawi Lake study basin. Each transect was representative of a specific aspect including north-, south-, and east-facing, referred to in this paper as transects 1, 2 and 3 respectively (Figure 3.2). Vegetation cover was also taken into consideration in the selection of hillslope transects by ensuring that the location of each transect corresponded with vegetation types that were representative of both the Kakawi Lake basin and larger surrounding area.

On each hillslope transect three sites were selected for intensive monitoring of soil characteristics, active layer development, soil temperature and moisture variability. Three sites were selected on each hillslope; one site at the top of the hillslope (10 m downslope from ridge), one site at the approximate middle of the hillslope, and one site at the bottom (5-10 m upslope from lake edge). These sites will be further referred to as sites A, B, and C respectively throughout this paper.

### **3.4 - SURVEY AND GIS ANALYSIS**

A Leica Total Station surveying system was used to survey the Kakawi Lake basin. The three main purposes of this survey were: (1) to measure surficial topographic relief, (2) to determine the basin divide and (3) to delineate the major vegetation zones located within the basin ecosystem.

With respect to the surficial topographic relief and the basin divide, hillslope topography was documented as well as significant micro-scale features and the lake edge boundary. The three sites on each hillslope transect were incorporated into the survey as

well as the location of the two meteorological stations. Using the vegetation classification system developed upon initial inspection of the basin, zone boundaries were surveyed with each particular zone receiving a unique survey data label. These zones include:

**Basin Survey Zones:**

- (1) Lake
- (2) Open Gravel
- (3) Beach
- (4) Open
- (5) Discharge Area
- (6) Closed birch
- (7) Open Birch
- (8) Birch dominant
- (9) Lichen
- (10) Hummocky sedge
- (11) Peat and cloudberry
- (12) Sedges and weeds
- (13) Boulder and lichen

ArcInfo and Arcview GIS software was utilized at the University of Waterloo and at Wilfrid Laurier University to analyze data obtained from the intensive field survey of the Kakawi Lake basin. The data file created using the total station surveying equipment consisted of a series of 2875 points (Figure 3.3), each of which has attributes including northing, easting, relative elevation, and survey zone classification. Thiessen Polygon analysis was used to interpolate between these points thus creating a polygon map with each polygon representing a specific survey zone (Figure 3.4). This polygon map which included 2666 polygons was then simplified using ArcInfo to produce a map consisting of 725 polygons. Reduction in the number of polygons was conducted in order to perform analyses on areas within the basin that were larger than those displayed in the original



**Figure 3.3 – Kakawi Lake Basin survey point locations**

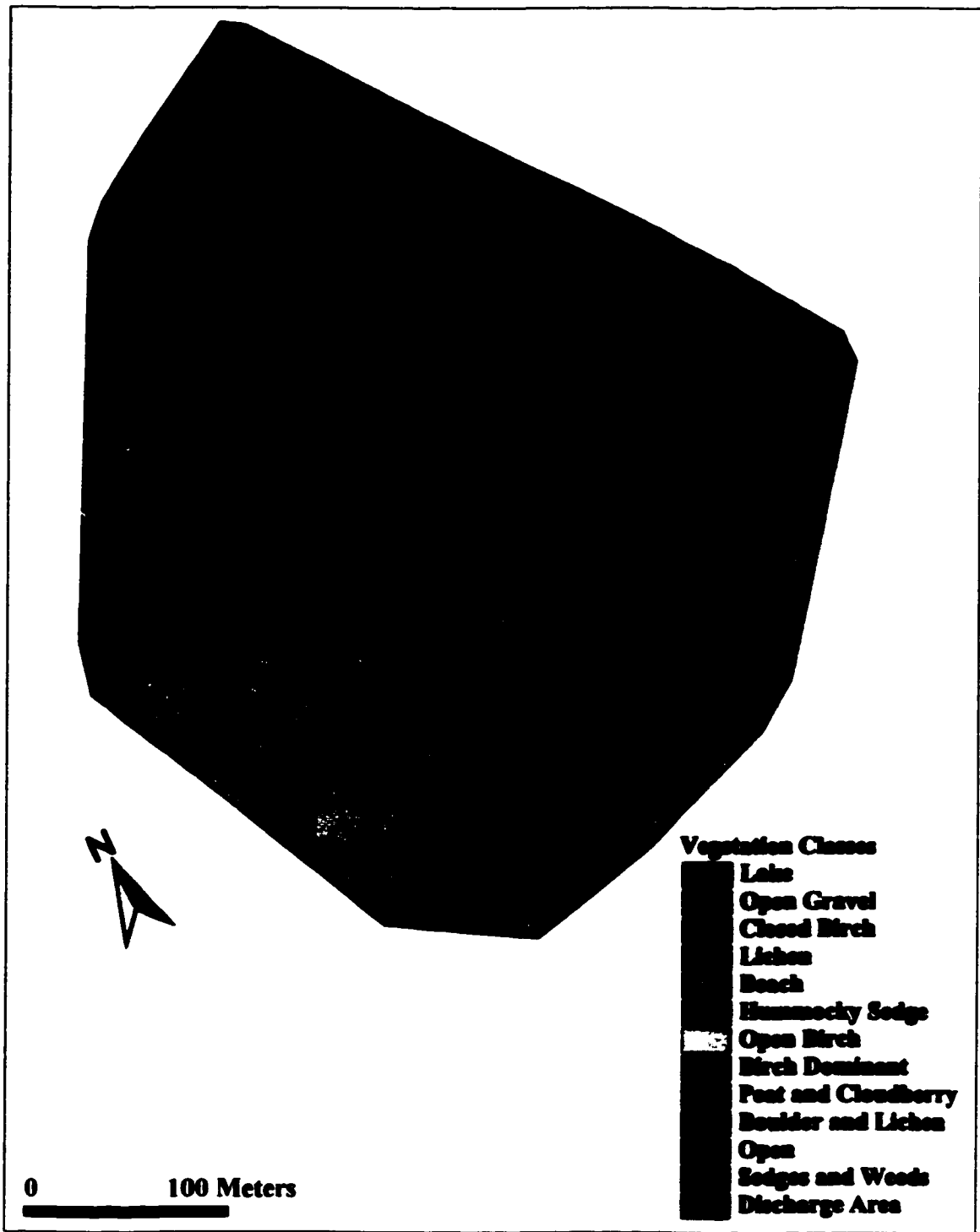


**Figure 3.4 - Kakawi Lake Basin vegetation polygon map**

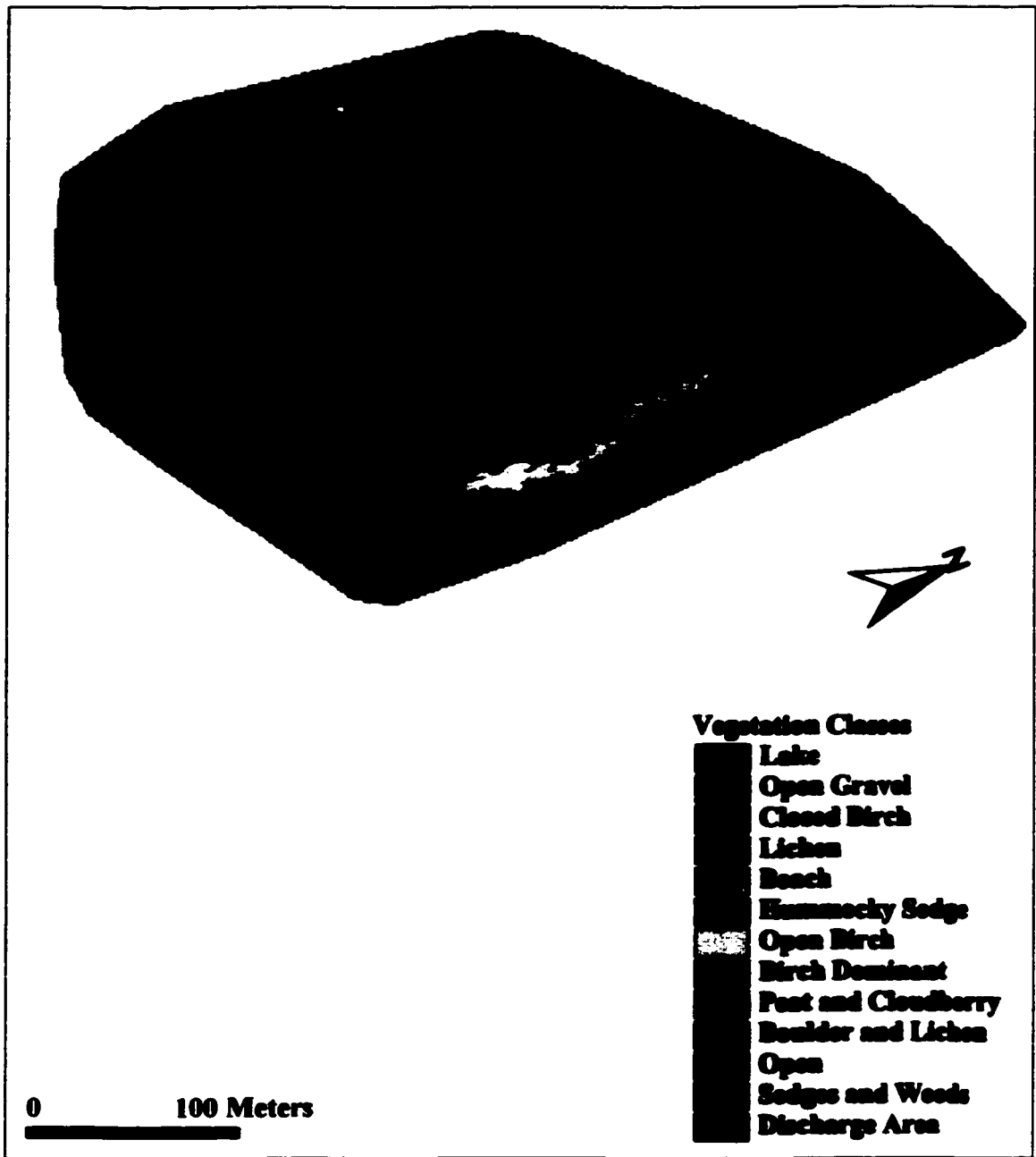


**Figure 3.5 - Kakawi Lake Basin 3-D orthographic image with vegetation overlay**

map. This reduced complexity of the map with respect to the number of individual polygon attributes that would be used in subsequent calculations.

For the purposes of this study, a further simplification was required to allow for analysis of areas that were larger in size than those created using the dissolve command in ArcInfo. Consideration of trends produced by the ArcInfo analysis along with detailed local knowledge of basin characteristics was further utilized to divide the 325 polygon map into a more generalized map of 130 polygons. This map serves as the basis for comparing areas within the Kakawi Lake basin taking slope, aspect, vegetation cover and topographic relief into consideration.. Polygons of this scale are more representative of hillslope sites studied in this paper with respect to size, topographic relief, and aspect.

Quantitative analysis of this map using Arcview software allows the user to obtain information specific to each individual polygon. Useful to this study is the average slope, the average aspect, and the area of each polygon as well as the area of the lake surface and the total area of the Kakawi Lake basin. These attributes were calculated for each polygon and utilized in subsequent analysis. As well, an orthographic image of the Kakawi Lake basin was produced with the vegetation layer overlaid on top to provide a visual representation of the basin with respect to spatial distribution of vegetation types (Figure 3.5).

### **3.5 - SOIL SAMPLING AND ANALYSIS**

Nine soil pits were excavated on the hillslopes including one site directly adjacent to the Laurier met site location. Soil pits extended from ground surface to the permafrost

table and averaged 1 m x 1 m in area. The upslope soil pit face was then analysed visually to produce a qualitative description which included: soil horizon depths, maximum depth of rooting systems, type and amount of organic material present, and soil characteristics (i.e. relative particle size and colour for each horizon). Depth to the permafrost table and the presence of large rocks or boulders were also included in this analysis.

Prior to completing the qualitative analysis of the soil pits, samples were extracted from the pit face to obtain physical properties including bulk density, porosity and percent carbon. Metal tubes of known length and volume were inserted horizontally into the upslope soil pit face until completely filled with soil. They were then extracted with care to ensure that samples remained intact and relatively undisturbed before being wrapped in plastic and securely taped for transport back to the Tundra Ecosystem Research Station (TERS) laboratory. For soil bulk density, soil tubes (23 cm in length and 254.03 cm<sup>3</sup>) were used to collect samples from each of the main soil horizons. Soil porosity sample tubes were smaller in length and volume (5 cm in length and 55.9 cm<sup>3</sup>). For sites 1-C, 2-B and 2-C a total of 3 distinct soil horizons were identified and sampled whereas for all remaining sites only 2 soil horizons were identified and sampled due to a more homogenous soil profile.

In the TERS laboratory soil within the bulk density cores was removed and weighed to determine the initial volume of the in situ soil including moisture. The samples were then placed in an oven and dried for 24 hours at 105°C to remove moisture from the samples. The samples were then weighed again and the bulk density (g/cm<sup>3</sup>)

was calculated by dividing the weight of the dried sample (g) by the volume of the core tube ( $\text{cm}^3$ ). Average bulk densities and standard deviations were then calculated for each soil horizon.

Also in the TERS laboratory soil porosity cores were handled with care to ensure that samples were disturbed as little as possible during the transportation and unpacking process. Once in the lab, perforated tape was placed over one end of the core tubes and they were placed tape side down in a vertical position in aluminum cooking trays measuring 7 cm in depth. Once all cores were in place water was added to the cooking trays up to a level equal to the top of the core tubes without allowing water to enter the top opening of the core tubes. The samples were left in the aluminum trays for 24 hours to allow water to enter the bottom of the core tubes and move upwards through the sample under positive pressure. After the 24 hour soaking time, cores were removed individually and the weight of the core tube, sample contents and water was recorded. The contents of the soil tubes were then placed in an oven and dried for 24 hours at  $105^\circ\text{C}$ . With the weight of the core tube accounted for, the weight of the dry sample subtracted from the weight of the saturated sample (g) was used to calculate the amount of water occupying the pore space within the soil sample. Therefore, this volume of water divided by the total volume of the core tube and subsequently multiplied by one hundred is equal to the porosity. Average soil porosities and standard deviations were then calculated for each soil horizon.

Finally, soil carbon analysis was carried out at Wilfrid Laurier University using bulk soil samples collected from each soil pit at both shallow ( $\approx 10\text{-}20$  cm) and deep

(=50-70 cm) depths below the surface. From each bulk sample, three subsamples of approximately 15 g were placed in individual petrie dishes and dried for 24 hours at 90°C to evaporate any moisture in the soil. The weights of the dried soil plus petrie dishes were recorded. Dried samples were then placed in an oven for 30 minutes at 800°C in order to burn off any carbon that existed within the samples. Prior to cooling, the weights of the burned soil plus petrie dishes were recorded once again. The weight of the burned sample subtracted from the weight of the dried sample is equal to the percent carbon for each individual sample. Percent carbon values for each of the three subsamples were then averaged and a standard deviation calculated.

### **3.6 - SOIL TEMPERATURE**

Soil temperature was recorded continuously at the Laurier met station throughout the summer 1999 and spring 2000 field seasons. Measurements of soil temperature were averaged hourly and recorded using a Campbell Scientific CR10X data logger at depths of 10, 30 and 83 cm below the surface using 107B Fenwal thermistors. Soil temperature was also manually recorded approximately 3 times daily at various depths at each of the 9 hillslope sites to account for diurnal variations in soil temperature measurements. These measurements were taken from calibrated Fenwal 107B thermistors sealed with silicon and covered in water tight heat shrink tubing constructed at Wilfrid Laurier University. Probes were calibrated in the laboratory by placing them in ice water, 0°C water and room temperature water and recording resistance from each individual thermistor measured in ohms using a standard multimeter. From these data, a regression equation was calculated

for each thermistor probe based on the resistance-temperature relationship that has previously been demonstrated to be a linear one. At each site thermistor probes were inserted horizontally into the upslope face of an excavated soil pit which was later backfilled in order to obtain in situ soil temperature measurements. Subsequent resistance measurements (ohms) from each probe were calibrated using their unique regression equation to ascertain temperature in degrees C.

Sporadic subsurface temperature measurements taken at the 9 hillslope sites were regressed against continuous met site readings to construct a continuous record of soil temperature for each thermistor. Regression analysis was completed separately for the 1999 and 2000 field seasons to account for seasonal variations in the soil temperature record thus producing a unique equation for each probe for each of the two field seasons. Sporadic hillslope site measurements (2 - 4 times daily) taken between 0 and 20 cm depth were regressed against the 10 cm met site soil temperature series whereas hillslope site measurements taken between 20 - 55 cm and >60 cm were regressed against the 30 cm and 83 cm temperature series' respectively. Resulting regression equations were then used to produce continuous records of soil temperature at depth for each hillslope site. Corresponding r-squared values were also calculated to validate the significance of each regression analysis.

Surface temperature measurements were recorded at the Daring Lake met site as well as at each site within the hillslope #3 transect. Surface temperature measurements were found to have a strong correlation with air temperature (2.40 m) at the Daring Lake met site ( $r^2=0.80$ ). Due to the fact that vegetation cover at the Daring Lake met site was

similar to that of hillslope transects #1 and #2 (dwarf birch, grass and lichen) a regression equation was calculated and applied to these sites to obtain a surface temperature record based on air temperature measured at 2.54 m above the ground surface ( $y = 4.309 + 0.569x$ ).

### 3.7 - SOIL MOISTURE

Soil moisture was recorded continuously at the Laurier met site throughout the summer 1999 and spring 2000 field seasons. Soil moisture readings were averaged hourly and recorded by Campbell Scientific CR10 data logger at depths of 13 cm and 52 cm using Campbell Scientific CS615 Water Content Reflectometry sensors inserted horizontally into the soil profile. Daily soil moisture measurements were also recorded via time domain reflectometry (TDR) at each of the 9 hillslope sites using probes constructed at Wilfrid Laurier University. These 2-wire TDR probes consisted of a ferrite balun connected to two 1/8", 18 cm stainless steel welding rods which serve as the waveguides. Also attached to the balun is RG6 coaxial transmission cable. The balun and connections were fully encapsulated in electrical potting epoxy.

Time domain reflectometry is based on the relationship between the soil volumetric water content ( $\theta$ ) and the dielectric constant of the porous media. The dielectric constant of a soil is strongly dependent on the volumetric water content ( $\theta$ ) and essentially independent of other soil properties including soil texture, bulk density and temperature (Topp *et al.*, 1980). The dielectric constant is determined from the analysis of TDR trace from two-wire (parallel transmission line) probes previously referred to as

waveguides (Topp *et al.*, 1980). The dielectric constant is determined using the following expression:

$$K_a = 1.01 \left[ \frac{l}{L} \right]^2 \quad (1)$$

where

$K_a$  = is the dielectric constant

$l$  = is the electrical length of the TDR trace (m)

$L$  = is the physical length of the waveguide pair (m)

The constant 1.01 is the inverse of the wave propagation speed

Determination of the electrical length of the TDR trace was completed in the field by connecting each probe to the Tectronix 1502B TDR and recording the start and end points of the curve measured in feet (ft) as displayed on the instrument screen. The start length subtracted from the end length results in the electrical length of the TDR trace (ft) which was later converted to a volumetric water content (%) using WAT-TDR software developed at the University of Waterloo.

At the met site and at each hillslope site two TDR probes were inserted horizontally into the upslope face of the excavated soil pits. Horizontal installation was chosen so that the calculated water contents ( $\theta$ ) would be representative of a specific depth in the soil profile. The coaxial transmission cable extended from each probe to the soil surface where it was encased in protective PVC tubing in between field measurements.

Water content measurements taken two to four times daily at the 9 hillslope sites were regressed against continuous met site readings to construct a continuous record of

soil moisture for each TDR probe.

### **3.8 - MEASUREMENT OF ACTIVE LAYER / PERMAFROST TABLE**

Measurements of depth to permafrost table were taken daily at each site during the 1999 field season in order to monitor active layer development throughout the summer months. These depths were measured by inserting a 1.75 m rebar pounding rod vertically through the soil profile until resistance from the permafrost table was reached. Due to the presence of a rocky esker substrate the pounding rod was often impeded by materials other than ice. This, however, was distinguishable at the surface by the unique sound produced by the pounding rod when it hit either rock or ice and by the cooling of the pounding rod end upon contact with the PFT. This procedure was repeated five times within a 2 m<sup>2</sup> quadrat at each site. These five measurements were averaged in order to assign one representative active layer depth to each site. Variation about the mean was expressed as 1 standard deviation.

For measurements taken at each site on hillslope 2 active layer measurements of >1.5 m were not recorded due to the initiation of active layer development and subsequent thawing greater than the depth of the pounding rod prior to the study period. Active layer depths at sites on hillslopes 1 and 3 however were less than 1.5 m throughout the study period. An effort was made to estimate the depth to permafrost table at various locations throughout the basin at the end of the 1999 field season by selecting random sites to insert the pounding rod. However once again due to the presence of numerous subsurface rocks and boulders this effort was abandoned due to a lack of confidence in

depth measurements.

During the spring 2000 field season measurement of active layer depth commenced on May 30 (Julian Day 150) and continued daily through to June 19 (Julian Day 170). Due to the presence of snowcover throughout the basin at the beginning of the field season active layer measurements were only taken at sites on which snow had completely melted. Therefore, a spatial and temporal record of initiation of active layer development and subsequent thaw rates throughout the basin was recorded during the spring 2000 field season. Only hillslope 3 sites B and C had substantial snow cover at the end of the measurement period resulting in no record of active layer depth or development during this time.

### **3.9 - RADIATION BALANCE**

Incoming shortwave radiation ( $K_t$ ) was measured at the Daring Lake met site and was assumed to be equal at the Laurier met site due to the close proximity (500 m) of each site to one another and the horizontal plane on which each site was located. However, each study site within the Kakawi Lake basin differed substantially with respect to both slope and aspect thus rendering the met site radiation measurements inaccurate at these sites. Therefore, radiation geometry equations were utilized to obtain the incoming solar radiation at each site based on their respective position within the basin as described in Oke (1987).

In terms of the solar radiation received on the horizontal, the direct-beam solar radiation on a slope is given by:

$$\hat{S} = S \cos \hat{\Theta} / \cos Z \quad (2)$$

where:  $\hat{S}$  = direct-beam solar radiation on a slope  
 $S$  = direct-beam solar radiation received on horizontal  
 $\hat{\Theta}$  = angle of incidence between the normal to the slope and the solar beam  
 $Z$  = solar zenith angle

Spherical trigonometry gives the following relationships which are used to solve for  $\hat{S}$  in equation (1):

$$\cos \hat{\Theta} = \cos \hat{\beta} \cos Z + \sin \hat{\beta} \sin Z \cos(\Omega - \hat{\Omega}) \quad (3)$$

where:  $\hat{\beta}$  = study site slope inclination  
 $\Omega$  = solar azimuth angle  
 $\hat{\Omega}$  = study site azimuth

$$\cos Z = \sin \phi \sin \delta + \cos \phi \cos \delta \cos h \quad (4)$$

where:  $\phi$  = latitude  
 $\delta$  = solar declination  
 $h$  = hour angle

$$\begin{aligned} \cos \Omega &= (\sin \delta \cos \phi - \cos \delta \sin \phi \cos h) / \sin Z; t < 12 \\ &= 360^\circ - (\sin \delta \cos \phi - \cos \delta \sin \phi \cos h) / \sin Z; t > 12 \end{aligned} \quad (5)$$

where:  $t$  = local apparent solar time (using 24 hour clock)  
 $h$  = hour angle ( $h = 15(12 - t)$ )

Using equation (1) the incoming solar radiation ( $K_b$ ) was calculated for each site on an hourly basis using the measured value of  $K_t$  from the Daring Lake met site in combination with radiation geometry calculations as outlined by Oke (1987).

Consequently,  $K_{\downarrow}$  measurements for both the 1999 and 2000 field seasons served as the basis for calculating the radiation balances for each of the hillslope sites within the Kakawi Lake basin.

During the 2000 field season a number of albedo measurements were taken over a variety of vegetation types and at each of the study sites within the Kakawi Lake basin. Albedo ( $\alpha$ ) is defined as the ratio of the amount of solar radiation reflected by a body ( $K_{\uparrow}$ ) to the amount incident upon it ( $K_{\downarrow}$ ). Albedo was measured using a pyranometer which was first placed in a horizontal position 1 m over the vegetation to measure the  $K_{\downarrow}$ , followed by inverting it to a face-down position so that the  $K_{\uparrow}$  could be measured immediately after. Dividing the  $K_{\downarrow}$  by the  $K_{\uparrow}$  results in an albedo measurement specific to the surface type located directly under the instrument. A number of measurements were taken at each site throughout the field season and were subsequently averaged in order to assign an albedo value to each type of vegetation and, more specifically, to each study site.

The total amount of energy emitted by a surface can be determined using the Stefan-Boltzmann Law:

$$L_{\uparrow} = \epsilon \sigma T_0^4 \quad (6)$$

where:  $\epsilon$  = surface emissivity

$\sigma$  = Stefan-Boltzmann proportionality constant ( $5.67 \times 10^{-8} \text{ W m}^{-2} \text{ K}^{-4}$ )

$T$  = surface temperature (K)

Surface temperature measurements on an hourly basis for each site were used to calculate  $L_{\uparrow}$  using equation (6) assuming an emissivity of 0.96 as is commonly used for arctic

environments (Rouse and Bello, 1983; Bailey et al., 1989; Rouse, 1984).

The surface radiation budget is the sum of the individual short- and long-wave streams:

$$Q^* = K \downarrow - K \uparrow + L \downarrow - L \uparrow = K^* + L^* \quad (7)$$

where  $Q^*$  = net all-wave radiation

$K \downarrow$  = short-wave (incident) radiation

$K \uparrow$  = short-wave radiation reflected from the surface

$L \downarrow$  = incoming long-wave radiation emitted by the atmosphere

$L \uparrow$  = outgoing long-wave radiation from the surface

$K^*$  = net short-wave radiation

$L^*$  = net long-wave radiation

The final component of the radiation balance measured at the Laurier met site was  $Q^*$ .

Due to the fact that  $K \downarrow$ ,  $K \uparrow$ ,  $L \downarrow$  and now  $Q^*$  were measured or calculated at the Laurier met site  $L \downarrow$  was determined as the residual component from radiation balance equation:

$$L \downarrow = Q^* - K \downarrow + K \uparrow + L \uparrow \quad (8)$$

This value was then assumed to be constant at all sites within the Kakawi Lake basin due to the fact that macroclimatic variations were minimal within the basin. As stated by Oke (1987), it is generally acceptable to assume that  $L \downarrow$  arrives equally from all parts of the sky hemisphere. Subsequently, by assuming  $L \downarrow$  to be constant at all sites the radiation balance for the Laurier met site can be calculated as well as that of each individual site within the study basin. Each of the individual radiation balance components and the corresponding radiation balance was determined for each study site for both the 1999 and 2000 field seasons on an hourly basis.

### 3.10 - GROUND HEAT FLUX

The soil heat flux  $Q_G$  can be treated as the sum of the storage of sensible heat  $Q_S$  and latent heat  $Q_L$  giving,

$$Q_G = Q_S + Q_L \quad (9)$$

$Q_S$  for a soil depends on the soil's heat capacity and the change in temperature for a given volume of substrate. Due to the complexity introduced to the ground heat flux from permafrost soils,  $Q_G$  in this study is calculated using the calorimetric method (Halliwell & Rouse, 1987; Petrone, 1999). This method incorporates both the ground temperature profile and the contribution of latent heat of fusion  $Q_L$  during the melt period.

$Q_S$  was determined on an hourly basis for each study site by dividing the soil profile into layers with each thermistor representing the centre of each layer. The total heat stored in the column of soil is given by,

$$\sum_{i=1}^N Q_{S_i} = \sum_{i=1}^N C_{S_i} (T_{S_i} - T_{S_i(t-1)}) \Delta z \quad (10)$$

where:  $N$  = layer in the soil profile centred on respective thermistor

$C_{S_i}$  = volumetric heat capacity for that layer

$T_{S_i}$  = temperature at that depth at current time step

$T_{S_i(t-1)}$  = temperature at that depth at the previous time step

$\Delta z$  = thickness of the substrate layer  $N$

Soil heat capacity ( $C$ ) can be calculated by addition of the heat capacities of the various constituents, weighed according to their volume fractions. Since the density of air is only

about 1/1000 that of water, its contribution to the specific heat of the composite soil can generally be neglected (Hillel, 1980). Thus, the value of  $C$  is determined using the following relationship:

$$C = f_m C_m + f_o C_o + f_w C_w \quad (11)$$

where:  $C$  = constituent heat capacity  
 $f$  = volume fraction of each phase  
 $m$  = mineral matter  
 $o$  = organic matter  
 $w$  = water

From Hillel (1980), heat capacities for each phase including  $m$ ,  $o$  and  $w$  are  $2.0 \times 10^6 \text{ J m}^{-3} \text{ K}$ ,  $2.5 \times 10^6 \text{ J m}^{-3} \text{ K}$ , and  $4.2 \times 10^6 \text{ J m}^{-3} \text{ K}$ , respectively. Due to the fact that soil physical characteristics required for the calculation of heat capacity were not measured on hillslope 3, values of  $1.4 \times 10^6 \text{ J m}^{-3} \text{ K}$ ,  $3.1 \times 10^6 \text{ J m}^{-3} \text{ K}$ , and  $4.8 \times 10^6 \text{ J m}^{-3} \text{ K}$  were used for water contents of  $0.0 \text{ m}^3/\text{m}^3$ ,  $0.4 \text{ m}^3/\text{m}^3$ , and  $0.8 \text{ m}^3/\text{m}^3$  cited in reference to peat soils (Hillel 1980).

It is also important in permafrost environments to account for heat flowing out of the bottom of the soil profile. This flux is determined using the gradient between the bottom two thermistors in the profile (Petroni, 1999),

$$Q_{Grad} = -K \frac{(T_z - T_{z-1})}{\Delta z} \quad (12)$$

where:  $K$  = thermal conductivity of the substrate  
 $T_z$  = temperature of the bottom thermistor  
 $T_{z-1}$  = temperature of the thermistor above the bottom thermistor, separated by  $\Delta z$

### 3.11 - SURFACE ENERGY BUDGET

The surface energy balance is given by

$$Q^* = Q_G + Q_H + Q_E \quad (13)$$

where:  $Q^*$  = net radiative flux at the surface

$Q_G$  = ground heat flux

$Q_H$  = sensible heat flux

$Q_E$  = latent heat flux

The sensible and latent heat fluxes can be calculated using a time-averaged flux-gradient approach

$$Q_H = -\rho C_p K_H \frac{\Delta T_a}{\Delta z} \quad (14)$$

$$Q_E = -\rho \frac{C_p}{\gamma} K_w \frac{\Delta e}{\Delta z} \quad (15)$$

where:  $\rho$  = density of air ( $\text{kg m}^{-3}$ )

$C_p$  = specific heat of air ( $\text{MJ kg}^{-1} \text{K}^{-1}$ )

$\gamma$  = psychrometric constant ( $\text{kPa K}^{-1}$ )

$K_H$  = turbulent transfer coefficient for sensible heat ( $\text{m}^2 \text{s}^{-1}$ )

$K_w$  = turbulent transfer coefficient for latent heat ( $\text{m}^2 \text{s}^{-1}$ )

$T_a$  = air temperature (K)

$z$  = height above ground surface (m)

$e$  = vapour pressure (kPa)

The density of air and psychrometric constant were determined based on values given in Oke (1987). The specific heat of air is  $1.01 \text{ J kg}^{-1} \text{K}^{-1} \times 10^{-3}$  (Oke, 1987). The

turbulent transfer coefficients for sensible and latent heat were calculated by averaging temperature dependent values stated in Oke (1987) for the molecular diffusion coefficients in air of heat and water vapour. Finally, vapour pressure was calculated by multiplying the relative humidity (RH/100) measured at the meteorological station with the saturation humidity of water (Pa) which is temperature dependent (Oke, 1987).

At the Daring Lake meteorological station the Bowen ratio ( $\beta$ ) was determined using the following relationship:

$$\beta = \frac{Q_H}{Q_E} \quad (16)$$

### **3.12 - IRRIGATION EXPERIMENTS**

Due to a lack of significant precipitation events throughout the 1999 field season a series of irrigation experiments were carried out to attempt to quantify the effects of precipitation on soil temperature and water content at depth for each transect. At the same time of day and under nearly identical antecedent conditions a 20 mm rainfall event was simulated on Hillslopes 1, 2 and 3: August 6, August 8 and August 12 respectively.

At each site on the hillslope soil temperature and water content were recorded at depth as a measure of antecedent subsurface conditions prior to the simulated rainfall event. Once these measurements were recorded 2.0 L of Kakawi Lake water was introduced to each site from a graduated cylinder through a perforated container onto a marked 1 m<sup>2</sup> quadrat ensuring even dispersal of water. Ten minutes after application of water to each site, soil temperature and water content was again measured to record any

changes resulting from the introduced water. This procedure was repeated for each site every 0.5 hours over a 3.5 hour time frame thus simulating a 20 mm rainfall event. Measurements of soil temperature and water content were also recorded approximately 1 hour, 3 hours and 6 hours after completion of the experiment to identify any lag in effects of precipitation on the subsurface conditions.

### 3.13 - BASIN HYDROLOGY

The hydrological balance of a lake is expressed using the following equation:

$$\text{Lake Mass Water Balance} = P + I - O - E - \Delta S \quad (17)$$

where:  $P$  = total volume of precipitation falling on the lake surface.  
 $I$  = volume of lateral surface and subsurface inflow,  
 $O$  = volume of surface and subsurface outflow,  
 $E$  = lake evaporation  
 $\Delta S$  = volumetric change in lake storage

Precipitation was monitored on an hourly basis at the Laurier meteorological station. Outflow from the Kakawi Lake basin occurs via groundwater flow through the sand berm located at the north end of the basin. Outflow from the sand berm is channelled into a small stream where discharge is subsequently monitored. Outflow was monitored at a discharge weir (Figure 3.1) where daily measurements of stream stage and periodic readings of outflow velocity were recorded to produce a stage-discharge relationship to quantify daily fluxes. Due to a low range in flow at the discharge weir, stage was recorded daily while actual flow was measured weekly with extra measurements taken during times of peak flow associated with rainfall events. Volumetric change in lake storage was recorded via a pressure transducer installed in the lake bed and wired to the Kakawi Lake meteorological station (Table 3.6).

Lake evaporation was not measured at the Kakawi Lake study basin. However, due to the similar lake size, location (100 km north of Kakawi Lake) and landscape of a basin studied by Gibson et al. (1996), evaporation values reported in their study may be used to estimate the water mass balance of the Kakawi Lake basin. In their study, Gibson et al. (1996) calculated evaporation for a lake of similar size to Kakawi to be 180 mm and 181 mm for a 54 day study period in summer 1992 and a 71 day study period in summer 1993 respectively. This was achieved by calculating  $E$  as the residual of the water mass balance equation (16). Such values serve as an approximation of evaporation rates for Kakawi Lake to be used in subsequent water balance calculations.

Piezometers were installed within the Kakawi Lake basin to monitor hydraulic gradients in subsurface materials. Piezometers used in this study were stainless steel drive-points consisting of a conical shaped tip head and a 15.0 cm screened length. Attached to the head was a threaded 150 cm length of stainless steel pipe with a 2.54 cm outside diameter. The screened length of the stainless steel drivepoint piezometer head was attached to a 170 cm long, 0.95 cm inside diameter polyethylene tubing which ran up inside the steel pipe. Three piezometers were driven approximately 70 cm into the lake sediment, 1 m from the shore at the base of each hillslope. At each site on hillslope 3 one piezometer was installed to monitor hydraulic conductivity through the peat. Four piezometers were installed at depths of 33 cm, 62 cm, 82 cm, and 108 cm in the lake 1 m from the discharge berm.

Bail tests were performed periodically on each piezometer to determine *in situ* hydraulic conductivity. This method involves causing an instantaneous change in the

water level in a piezometer through a sudden introduction of a known volume of water and measuring the recovery of the water level with time (Freeze and Cherry 1979).

Piezometer recovery data is interpreted using the Hvorslev equation:

$$K = \frac{r^2 \ln(L / R)}{2LT_o} \quad (18)$$

where:  $K$  = hydraulic conductivity

$r^2$  = radius of piezometer head squared

$L$  = length of piezometer intake

$R$  = radius of piezometer intake tube

$T_o$  = slope of recovery versus time relationship

Several wells were also installed on hillslope transect 3 to monitor the timing and magnitude of the water-table response to precipitation events in the peatland area. Wells were each constructed from 5.1 cm inside diameter polyvinylchlorine (PVC) pipe. Each well was approximately 150 cm in length and was slotted along the entire length with several 0.3 cm drill holes. At each of the three sites on hillslope 3, water wells were installed in the middle of the site perpendicular to the hillslope transect where peat depths were the greatest, as well as on both sides of the perpendicular transect (i.e. left and right sides; facing upslope). Wells were monitored daily to determine the depth of the water table and more frequently during and after rainfall events.

## CHAPTER 4 - METEOROLOGICAL TRENDS

Summer (June-August) 1999 was cooler than average with the most significant difference occurring in July which was 4.2°C cooler than the 5 year average of 13.8°C (Figure 4.1). Average air temperature for August was 0.8°C cooler than the 5 year average of 10.6°C while the June average was 0.2°C warmer than the 5 year average of 8.0°C. Spring 2000 was average compared to the other four years of data with a mean monthly temperature in May of -2.61°C. This is the first month of the year in which air temperatures begin to rise above 0.0°C signifying the onset of spring melt in the Yamba Lake region.

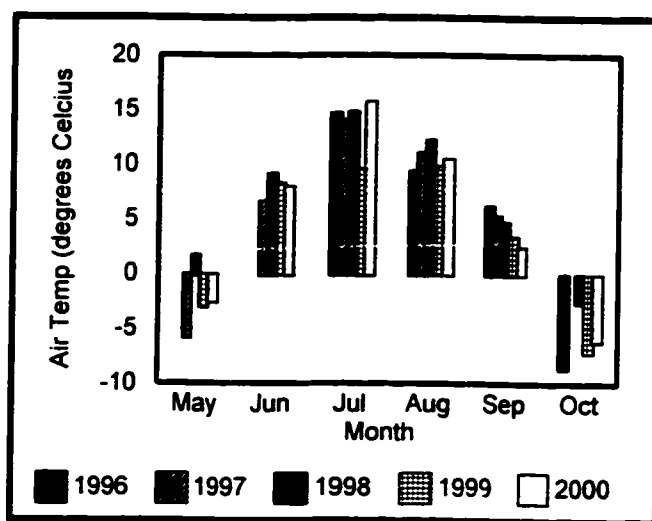


**Figure 4.1** - Mean monthly air temperature recorded at the Daring Lake meteorological station from May to October for years 1996 to 2000.

As well as being a cooler summer, 1999 was also a wetter than average summer with a total rainfall of 219.8 mm recorded for the months of May to October (Figure 4.2).

This value is larger than the 1996 to 2000 average of 164.8 mm with the most significant increase occurring in the month of May in which 23 mm more than the average of 9.97 mm fell in the Kakawi Lake basin. Monthly rainfall totals were greatest in 1999 from May to August with the exception of a considerably wet August in 1996.

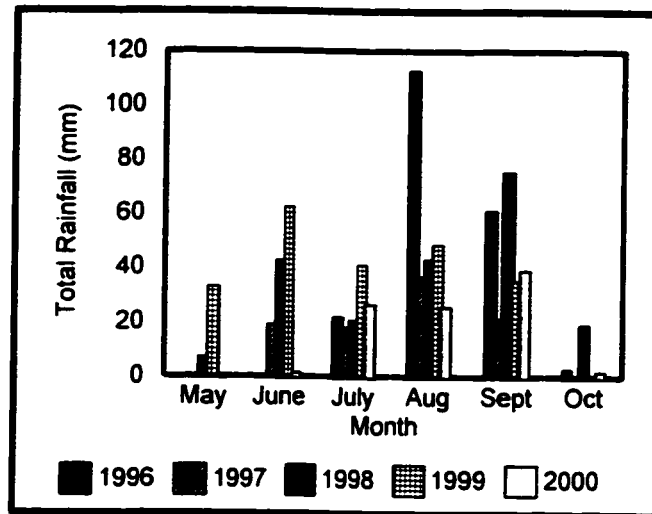


**Figure 4.2 - Mean monthly rainfall (mm) recorded at the Daring Lake meteorological station for years 1996 to 2000.**

Snow accumulation in the Daring Lake area generally reaches its maximum depth near the end of April followed by the onset of the melt period which ends in early June. During the past 5 years of recorded snowfall at the Daring Lake meteorological station, 1999 had the shallowest depth at 24.0 cm (JD 144) while 1997 had the most with 53.1 cm (JD 155) (Figure 4.3). Snow reached a maximum accumulation of 32.3 cm in 2000 while a maximum depth of 41.0 cm was recorded for 1998.

Snowmelt occurs rapidly at the Daring Lake meteorological station (Figure 4.3). The 1999 record indicates that maximum snow depth was recorded on JD 155 followed

by the melt period which lasted for 18 days. The 1999 melt period was the shortest of the 5 year record due to less snow accumulation and a warmer mean monthly air temperature as illustrated in Figure 4.1. During the 2000 study period the spring melt was longer than average, lasting approximately 23 days, despite the fact that maximum snow depth at the Daring Lake meteorological station was only 32.2 cm.

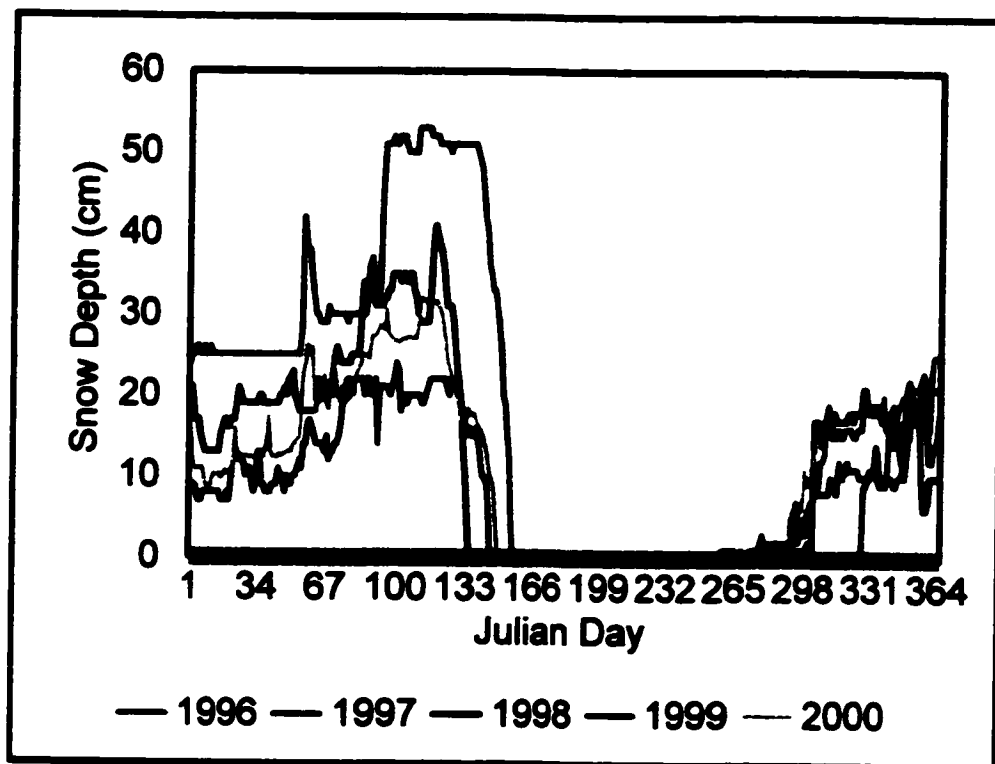
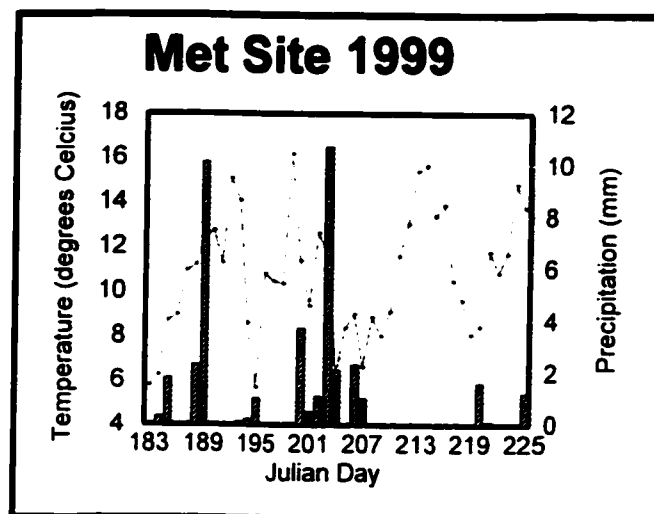


Figure 4.3 - Mean daily snow depths recorded at the Daring Lake meteorological station from 1996 to 2000.

Mean daily snow depths illustrated in Figure 4.3 were recorded at the Daring Lake meteorological station located on a horizontal surface less than 100 m from the shore of Daring Lake. Due to the steep slopes and convex shape of the Kakawi Lake

basin it should be noted that these snow depths are indicative of annual snowfall trends for the larger Daring Lake area and are not representative of site specific snow depths in the study basin. For this reason, during the spring 2000 field season snow depth and density measurements were taken at numerous sites within the Kakawi Lake basin to account for spatial and temporal differences in snow accumulation.

During the 1999 field season daily air temperature fluctuated considerably. As illustrated in Figure 4.4 daily average air temperature ranged from 5.68°C to 16.19°C with an average of 10.76°C throughout the 43 day study period. Only two precipitation events were documented that produced more than 10 mm of rainfall. The first significant rainfall event began on JD 188 and ended on JD 189 producing 12.4 mm of rainfall. The second significant event began on JD 202 and extended through to JD 204 producing 13.9 mm of rainfall. Associated with the second significant rainfall event was a decrease in daily air temperature of approximately 6°C which lasted for approximately 1 week.



**Figure 4.4** - Average daily temperature and daily total precipitation at Kakawi Lake basin during 1999 study period.

During the 1999 study period two major cooling trends were recorded which were not directly associated with rainfall events. Daily average air temperature decreased nearly 10°C from JD 192 to JD 195 and decreased nearly 6°C from JD 216 to JD 219.

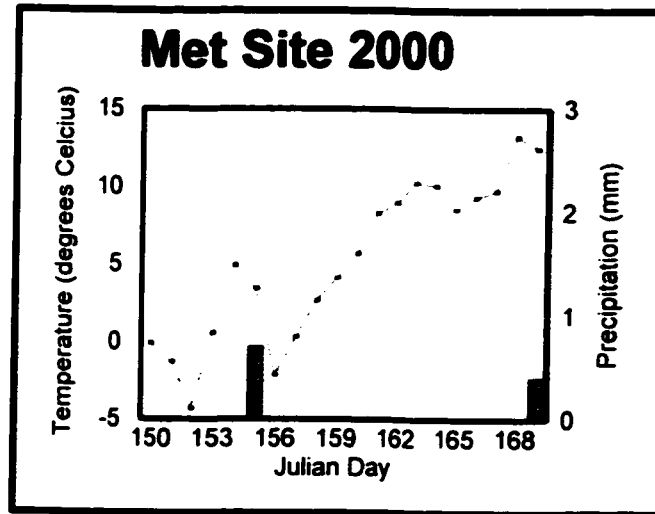


**Figure 4.5** - Average daily temperature and daily total precipitation at Kakawi Lake basin during 2000 study period.

During the 2000 study period air temperatures began to rise above the freezing point on JD 153 (Figure 4.5) as measured at the Kakawi Lake meteorological station. Daily average air temperature increased to 4.95°C on JD 154 but was followed by a decrease in air temperature and the first of two measurable rainfall events which produced 0.7 mm of rainfall. From JD 156 air temperature increased steadily rising above the 12°C mark. The second of the two measurable rainfall events occurred on JD 169 producing 0.4 mm of rainfall in the Kakawi Lake basin.

---

## CHAPTER 5 - RADIATION BALANCE

---

### 5.1 - INCOMING SHORT-WAVE RADIATION

The radiation received by a surface is usually the major determinant of its climate (Oke, 1987). This input of radiant energy is composed of direct-beam, diffuse, and long-wave radiation. Of these components only the direct-beam short-wave radiation receipt is dependent upon the angle at which it strikes the receiving surface (Oke, 1987). Using methodology outlined in Oke (1987), measured values of incoming short-wave radiation measured on a horizontal plane at the Daring Lake meteorological station were extrapolated to each of the hillslope transects using radiation geometry calculations. This methodology requires data including the angle of the slope relative to a horizontal plane, the azimuth angle of the slope and both the azimuth and zenith angles of the Sun in order to calculate radiation receipt on a sloping surface. A slope that faces the Sun most directly receives the most radiation whereas minimal radiation is received when the Sun only skims the surface.

Differences in incoming radiation received at the surface with respect to aspect are illustrated in Figure 5.1 using data from a typical day, Julian Day 212 (JD 212), during the 1999 field season. At a slope angle of 10 degrees (Figure 5.1a) it is clear that the south-facing slope receives the maximum daily total amount of incoming radiation followed by the west-, east-, and north-facing slopes respectively. This difference in incoming radiation receipt with respect to aspect is more clearly defined when the slope angle of each slope is increased from 10 to 30 degrees (Figure 5.1b). In this case, not

only is there a marked difference in the amount of total daily radiation received at each slope similar to that depicted in Figure 5.1a but there is also a notable difference in the diurnal distribution of short-wave radiation receipt. Following the Sun's path, the north-facing slope is the first to receive short-wave radiation followed by the east-, south- and west-facing slopes respectively.

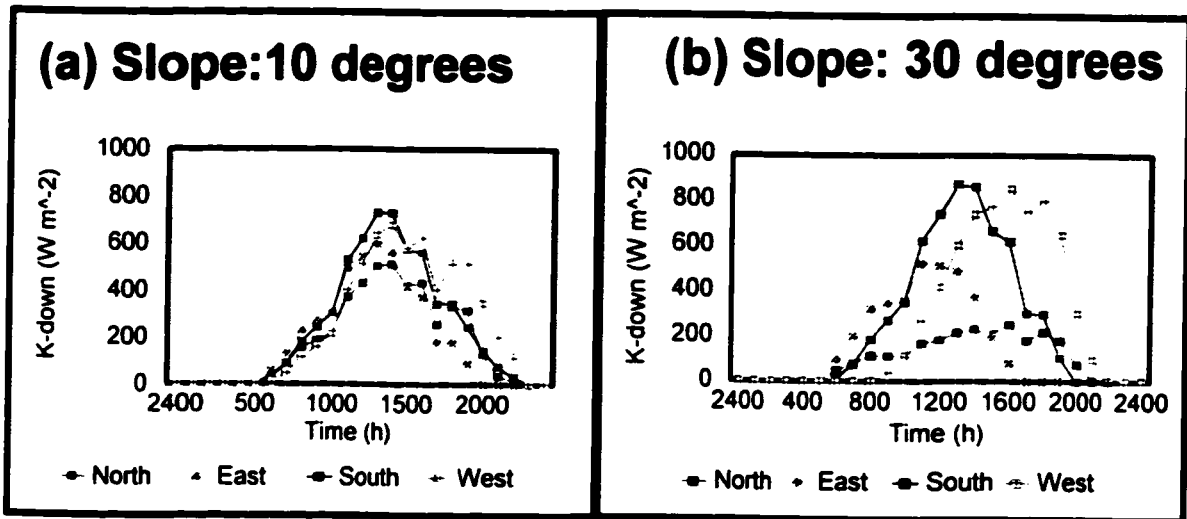


**Figure 5.1** - Diurnal variation of direct-beam solar radiation on surfaces with varying slopes (10 and 30 degrees) and aspect (north-, south-, west-, and east-facing) for YD 212.

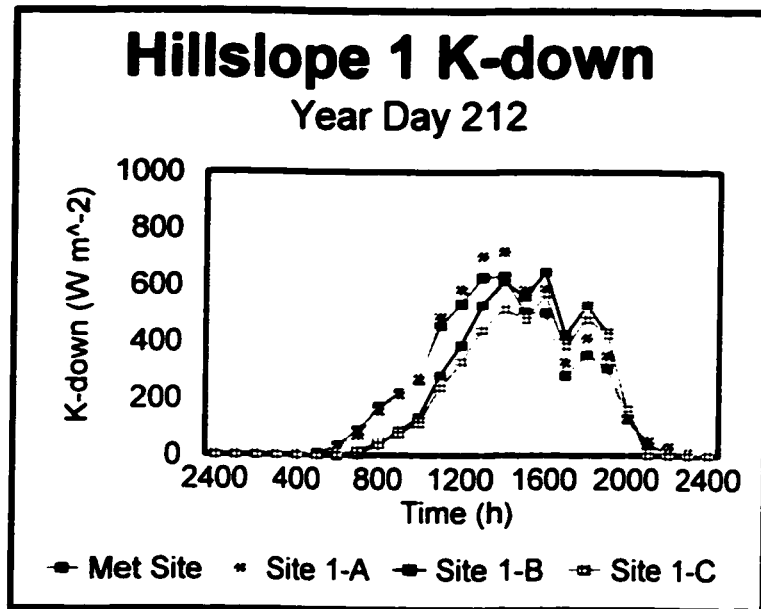
Applying radiation geometry calculations to the Kakawi Lake study sites required initial determination of site specific attributes including slope and aspect. This was determined from analysis using a GIS in which the intensive survey of the Kakawi Lake basin using Leica Total Station surveying equipment was entered and subsequently analyzed (Figure 3.4). The slope and aspect values associated with each study site as determined using the GIS are presented in Table 5.1. These values are used in the calculation of hourly short-wave radiation receipt on each study hillslope.

Figure 5.2 illustrates the diurnal variation of direct-beam solar radiation upon hillslope transect #1 sites as well as at the Kakawi Lake meteorological station for JD 212 of the 1999 field season. As compared to the diurnal variation of incoming short-wave radiation at the meteorological station which received a daily total of 5163.9 Wm<sup>-2</sup>, site 1-A received approximately 10% more with a daily total of 5709.3 Wm<sup>-2</sup>. Alternatively, Sites 1-B and 1-C received less total

**Table 5.1 - Slope and aspect values for each study site**

	Site	Slope	Aspect
<b>Transect #1</b>	A	7.3	211.2
	B	20.6	294.0
	C	22.2	313.3
<b>Transect #2</b>	A	26.9	220.4
	B	29.2	222.8
	C	25.2	196.7
<b>Transect #3</b>	A	9.2	239.9
	B	12.4	96.1
	C	13.9	71.4

daily direct-beam radiation receiving 4822.7 and 4275.6 Wm<sup>-2</sup> respectively. This difference in diurnal variation of incoming short-wave radiation is due to the fact that sites 1-B and 1-C have similar slopes as well as similar north-westerly facing slopes whereas site 1-A has approximately 13° less slope and a predominantly south-westerly facing slope (Table 5.1).



**Figure 5.2** - Diurnal variation of direct-beam solar radiation upon Hillslope #1 on YD 212.

Hillslope 2 study sites are characterized as having very similar aspects ranging only 26° amongst all 3 and by having the steepest average slope at 27.1° as compared to hillslope transects 1 and 3 which have average slopes of 16.7° and 11.8° respectively. As such, these predominantly south-westerly facing sites receive much greater direct-beam solar radiation on a daily basis as compared to the met site as illustrated in Figure 5.3. On JD 212, sites 1-A, 1-B received the highest total daily short-wave radiation input at 6608.6 W m<sup>-2</sup> and 6691.1 W m<sup>-2</sup> while site 1-C received slightly less at 6270.2 W m<sup>-2</sup>. These values are all significantly higher than the amount of radiation received on a horizontal plane as measured at the met site which totalled 5163.9 W m<sup>-2</sup>.

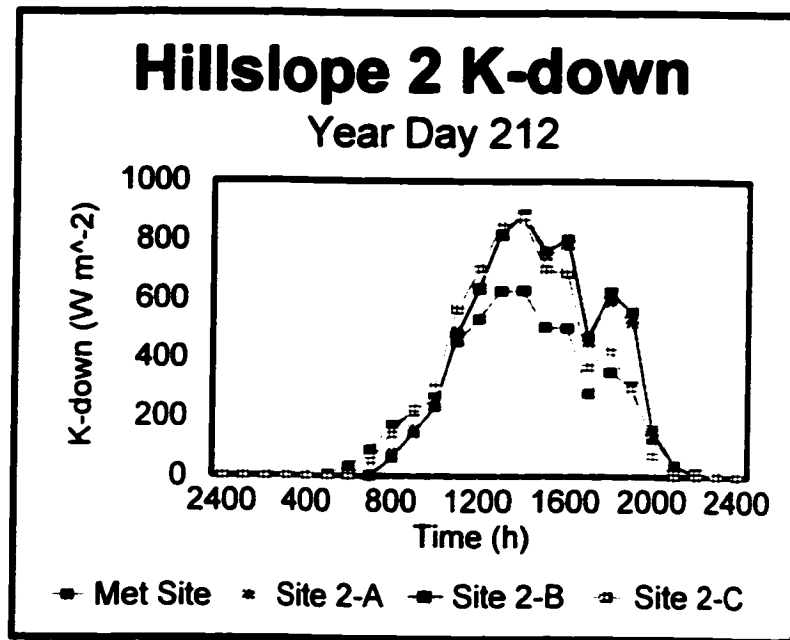


**Figure 5.3** - Diurnal variation of direct-beam solar radiation upon Hillslope #2 on YD 212.

Compared to Hillslope transects #1 and #2, transect #3 is characterized by having relatively gradual sloping study sites with an average slope of 11.8° (Figure 5.4). Site 3-A which has a predominantly south-westerly facing aspect receives the most radiation of the three study sites on hillslope 3 with a daily total of 5781.6 W m<sup>-2</sup> on JD 212. This is larger than the amount of radiation received at the met site which totals 5163.9 W m<sup>-2</sup> and is significantly greater than direct-beam radiation received at hillslope sites 3-B and 3-C which total 4340.9 W m<sup>-2</sup> and 3940.9 W m<sup>-2</sup>.

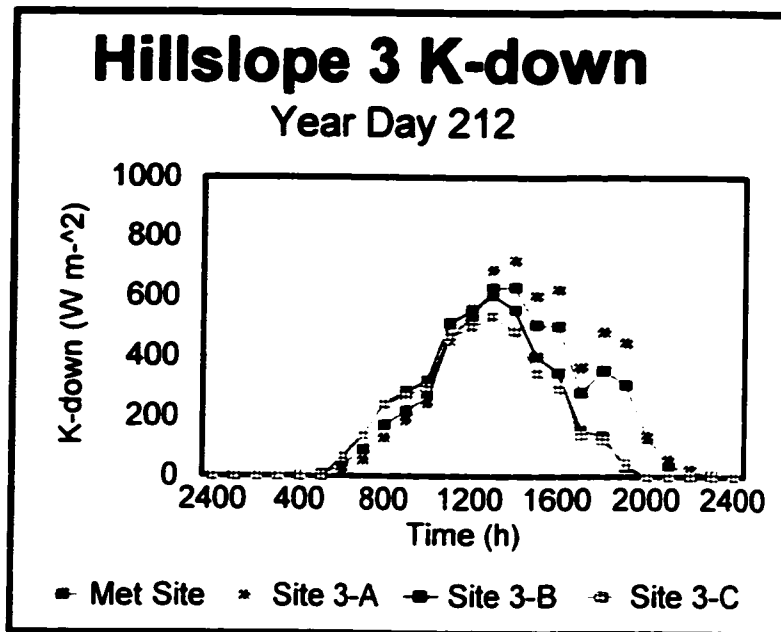


**Figure 5.4** - Diurnal variation of direct-beam solar radiation upon Hillslope #3 on YD 212.

## 5.2 - RADIATION BALANCE

In order to define the radiation balance for each study site all of the individual components including net radiation ( $Q^*$ ), incoming long-wave radiation ( $L_{\downarrow}$ ), emitted long-wave radiation from the surface ( $L_{\uparrow}$ ), incoming short-wave radiation ( $K_{\downarrow}$ ), and short-wave radiation reflected by the surface ( $K_{\uparrow}$ ) must be known. The three factors that determine differences in radiation balance amongst each of the study sites include: (1) the slope and aspect of the study site which controls receipt of  $K_{\downarrow}$ , (2) the surface temperature which determines  $L_{\uparrow}$ , and (3) the albedo which is used to calculate  $K_{\uparrow}$ . The meteorological data calculations taken from Oke (1987) and the Stefan-Boltzmann Law

were used to calculate  $K_i$  and  $L_i$ , respectively. This leaves  $\alpha$  as the final controlling factor in determination of study site radiation balances. Measurements of albedo taken at various times throughout the study period were used to assign a specific albedo value to each of the study sites (Table 5.2).

**Table 5.2 - Albedo values for each study site**

	Site	Vegetation Cover	Albedo	Standard Deviation
<b>Transect #1</b>	A	open gravel	0.17	$\pm 0.01$
	B	lichen	0.12	$\pm 0.03$
	C	lichen	0.16	$\pm 0.01$
<b>Transect #2</b>	A	gravel, lab tea	0.13	$\pm 0.03$
	B	lichen	0.15	$\pm 0.01$
	C	lichen, birch	0.13	$\pm 0.03$
<b>Transect #3</b>	A	hummocky peat	0.14	$\pm 0.01$
	B	hummocky peat	0.14	$\pm 0.01$
	C	hummocky peat	0.14	$\pm 0.01$

Albedo measurements taken within the Kakawi Lake basin varied spatially due to differences in the amount and types of vegetation overlying each site. In general, dark lichen had the lowest albedo ( $0.12 \pm 0.01$ ) followed by peat ( $0.14 \pm 0.01$ ), birch ( $0.15 \pm 0.02$ ), lichen and Labrador tea ( $0.17 \pm 0.01$ ) and open gravel ( $0.17 \pm 0.02$ ). Albedo values for each of the study sites as summarized in Table 5.2 indicate that albedo ranged from 0.13 to 0.17 with minimal deviation at each site. Albedo measurements taken under wet

(post-rainfall) and dry conditions had no notable difference at any of the study sites. Compared to values cited for studies conducted in similar environments (Table 5.3) measurements taken within the Kakawi Lake basin fall within a similar range of values. As reported by Babarauckas and Schmidlin (1997), Bailey et al.(1989), Rouse (1984) and Lafleur et al. (1993) average daily albedo measurements remain essentially constant throughout the snow-free season. Similar to Rouse (1984) and Bailey et al. (1989), seasonal development of vegetation did not effect albedo in the Kakawi Lake basin. There was also no relationship found in this study between soil moisture and albedo as also reported by Bailey et al. (1989).

**Table 5.3 - Albedo measurements as cited for studies in arctic and alpine environments**

Reference	Location	Surface Type	Albedo
Babrauckas and Schmidlin, 1997	Mount Washington, New Hampshire	alpine tundra	0.20
Bailey et al., 1989	Plateau Mountain, Alberta	alpine tundra	0.17
Rouse, 1984	Churchill, Manitoba	snow	0.78
		grass, lichen and lab tea	0.12
Lafleur et al., 1993	Churchill, Manitoba	snow	0.87 ± 0.10
		tundra	0.17 ± 0.02
Rouse and Bello, 1983	Churchill, Manitoba	upland tundra	0.14 to 0.15
		lowland swamp	0.08 to 0.12
Duguay et al., 1999	Churchill, Manitoba	hummocky sedge	0.08 to 0.09
		lichen ridge	0.14 to 0.15
		willow	0.13 to 0.16

Although daily albedos remain relatively constant throughout the snow-free season, as reported here and in the literature, it should be noted that slight diurnal variations in albedo do occur with larger albedos occurring at larger zenith angles. Albedo is maximal at sunrise and sunset as quantified by Babrauckas and Schmidlin (1997) who reported albedo measurements ranging from 0.18 at the highest solar angles to 0.23 near sunrise and sunset. This subtle difference is noted on days of cloudless, cloud-bright and overcast conditions according to Bailey et al., (1989). The authors offered several explanations for this diurnal variation which included:

- (1) large variability in pyranometer response at high solar zenith angles is expected from the innate variability in cosine responses at these positions when solar irradiances are low;
- (2) slope of surface may play a role. Slope in this case was 1.5 degrees. Corrections to the data due to slopes of this magnitude proved to be of no consequence;
- (3) sensor thermopiles may not be in complete accordance with the spirit level on the sensor; and
- (4) upward shift of the relationship in the afternoon may arise in response to changes in the spectral transmissivity of the atmosphere.

Albedo measurements in this study were taken manually with a pyranometer at various times during the day under different meteorological and seasonal conditions. A continuous record of albedo was not available during the study and precision of the portable measuring device was limited to two decimal places. These factors, in combination with the fact that incoming short-wave radiation is minimal at sunrise and

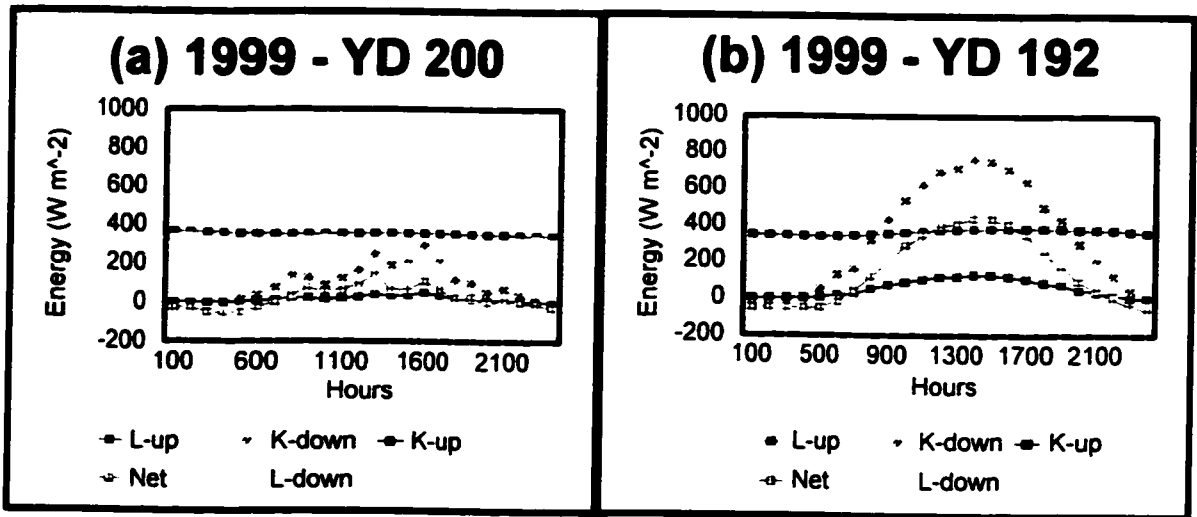


**Figure 5.5** - Diurnal radiation balance for met site on (a) cloudy and (b) cloudless day.

sunset as compared to times with larger zenith angles have therefore required that an average daily albedo be assigned to each specific study site for subsequent radiation balance calculations. Rouse (1994) reported diurnal variations in albedo ranging from 0.16 to 0.26 on a sunny day. Similarly, Bailey et al. (1989) reported a similar range of 0.18 to 0.24 also under sunny conditions. Diurnal variations in albedo however are much less pronounced under cloudy conditions as reported by Babarauckas and Schmidlin (1997) citing a diurnal range of 0.18 to 0.22. Albedo measurements in this study were taken mainly during the midday hours and are therefore representative of the time at which incoming solar radiation is at a daily maximum.

Using measured values of  $Q^*$  and  $K\downarrow$  and estimates of  $L\downarrow$  and  $K\uparrow$  for the Daring Lake meteorological station the remaining component of the radiation balance,  $L\uparrow$  was calculated as the residual of the radiation balance equation (Equation 8). This value was

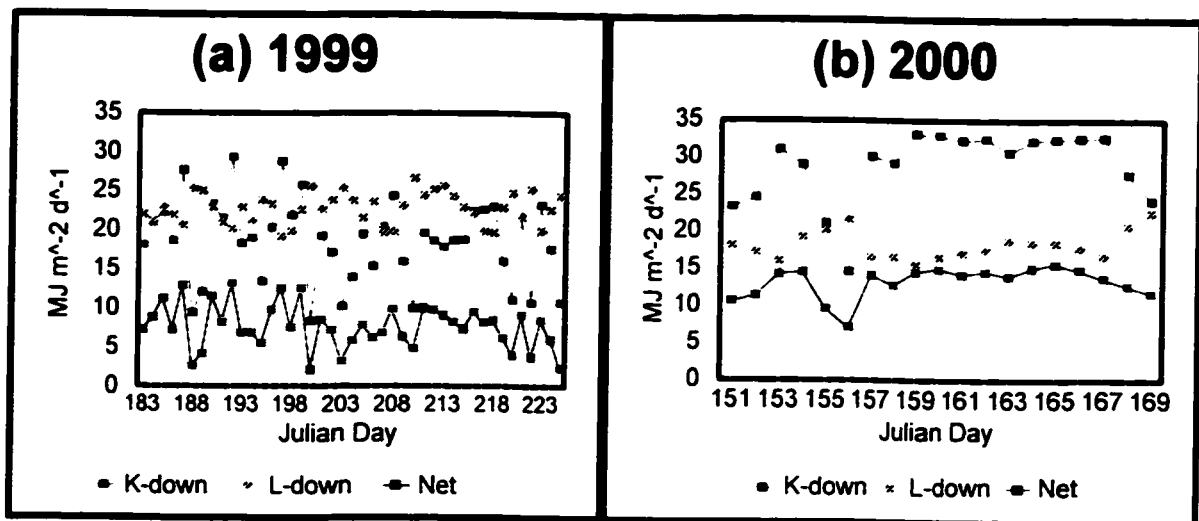
assumed to be constant throughout the Kakawi Lake study basin and therefore used in the calculation of site specific radiation balances. Illustrated in Figure 5.5 are the diurnal radiation balances for the Daring Lake met site on the days with the lowest and highest total daily  $K_{\downarrow}$  days corresponding with cloudy and cloudless days respectively.

In comparing the diurnal radiation balance at the Daring Lake meteorological site between a day with cloud cover and one without (Figure 5.5) the most notable difference is a reduction in daily total  $K_{\downarrow}$ . Figure 5.5b illustrates that  $K_{\downarrow}$  begins to increase at approximately 500h, continues to increase until a peak of just less than  $800 \text{ W m}^{-2}$  in the early afternoon, followed by a steady decrease until sunset late in the day. On a cloudy day such as the one illustrated in Figure 5.5a however,  $K_{\downarrow}$  peaks at approximately  $300 \text{ W m}^{-2}$  with a significant decrease in daily total  $K_{\downarrow}$ . The amount of shortwave radiation reflected by the surface ( $K_{\uparrow}$ ) also varies according to weather conditions and, as such, is reduced on days with increased cloud cover.

Differences in the diurnal long wave radiation balance are less prominent than those of the short-wave radiation balance with  $L_{\downarrow}$  remaining virtually unchanged both diurnally and from day-to-day despite notable differences in weather conditions (Figure 5.5). There is, however, a slight increase in  $L_{\downarrow}$  from midday through the afternoon due to heating of the soil surface as illustrated in Figure 5.5b under cloudless conditions. Figure 5.5b illustrates that  $L_{\downarrow}$  is inversely proportional to  $K_{\downarrow}$  on clear days whereas on days with cloud cover daily total  $L_{\downarrow}$  is comparatively larger. This results in a well-defined relationship between global solar radiation and net radiation as reported by Bailey et al. (1989). Diurnal fluctuations in  $K_{\downarrow}$  and  $L_{\downarrow}$  are more erratic on days with

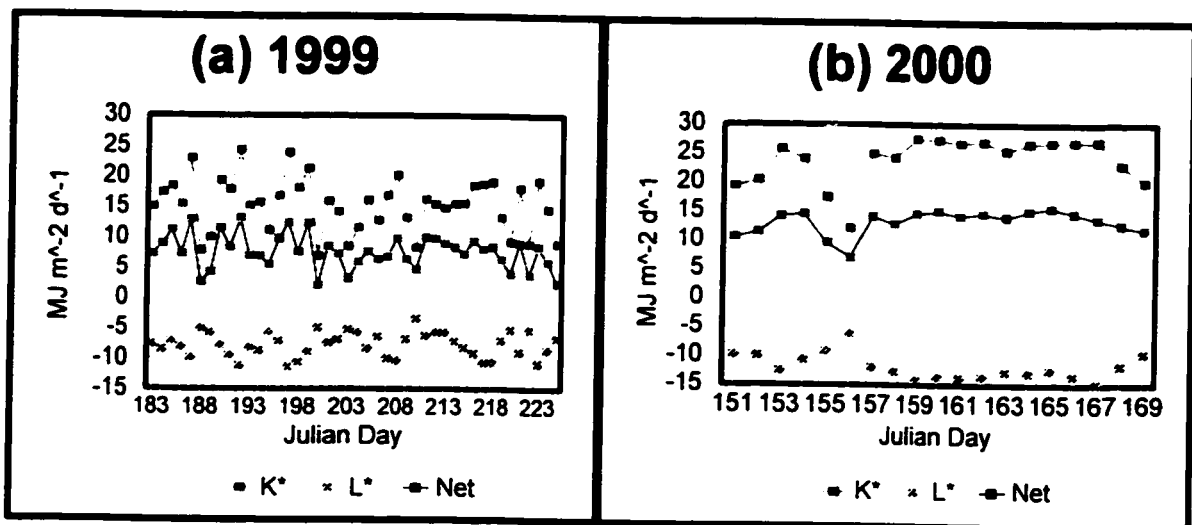
cloud cover as compared to clear days due to constantly changing cloud patterns which absorb, scatter and re-emit radiation as exemplified in Figure 5.5a. Net radiation is strongly influenced by  $K_d$  and, as such, exhibits a similar diurnal flux with values remaining around the  $0 \text{ W m}^{-2}$  mark and even becoming slightly negative due to heat loss from the soil from dusk to dawn and reaching maximum daily values when the zenith angle is the greatest.

Figure 5.6 illustrates that increases in  $L_d$  are associated with decreases in  $K_d$  on a day-to-day basis. During the 1999 field season incoming short-wave radiation ranged from a minimum daily total of  $8.3 \text{ MJ m}^{-2} \text{ d}^{-1}$  to a maximum of  $29.3 \text{ MJ m}^{-2} \text{ d}^{-1}$  with an average value of  $18.5 \pm 5.3 \text{ MJ m}^{-2} \text{ d}^{-1}$  (Figure 5.6a). Long-wave radiation daily totals varied less than short-wave values with a mean value of  $22.7 \pm 2.0 \text{ MJ m}^{-2} \text{ d}^{-1}$  and maximum and minimum daily totals of  $26.6 \text{ MJ m}^{-2} \text{ d}^{-1}$  and  $19.1 \text{ MJ m}^{-2} \text{ d}^{-1}$  respectively.



**Figure 5.6** - Daily incoming longwave, shortwave and net radiation values at met site for (a) 1999 and (b) 2000 field seasons.

Daily incoming short-wave radiation remained relatively constant on a daily basis throughout the 2000 field season with the exception of a notable drop from JD 154 through to JD 157 (Figure 5.6b). Similar to the 1999 field season, incoming short-wave radiation values during the 2000 field season deviated more significantly from the mean than did long-wave values with averages of  $28.8 \pm 5.1 \text{ MJ m}^{-2} \text{ d}^{-1}$  and  $18.2 \pm 2.0 \text{ MJ m}^{-2} \text{ d}^{-1}$  respectively. This is similar to findings documented by Rouse and Bello (1983) in which seasonal  $L\downarrow$  did not vary more than  $\pm 10\%$  about the mean, whereas  $K\downarrow$  varied by up to  $\pm 50\%$ . Of particular interest in Figure 5.6 is the fact that there is an increase in  $Q^*$  during the 2000 study period given higher basin albedos. This is related to a much higher  $K\downarrow$  due to reduced cloud cover as compared with the 1999 field and, therefore, lower daily  $L\downarrow$ .



**Figure 5.7** - Daily shortwave, longwave and net radiation balance values at met site for (a) 1999 and (b) 2000 field seasons.

Analysis of the net short-wave and long-wave radiation balance indicates that on

days with minimal incoming short-wave radiation, long-wave radiation emitted from the surface can drive the net radiation balance towards zero (Figure 5.7). Due to the fact that surface albedos in the Kakawi Lake basin are low, much of the incoming short-wave radiation is absorbed by the ground resulting in a positive  $K^*$  value throughout both the 1999 (Figure 5.7a) and 2000 (Figure 5.7b) study seasons. Alternatively,  $L^*$  values are constantly negative thus reducing the effects of  $K^*$  on the net radiation balance. Similar to trends exhibited with incoming radiation (Figure 5.6) variation in  $K^*$  about the mean is more substantial than that of  $L^*$  with mean values of  $15.37 \pm 4.38 \text{ MJ m}^{-2} \text{ d}^{-1}$  and  $7.78 \pm 2.02 \text{ MJ m}^{-2} \text{ d}^{-1}$  respectively for the 1999 study period and  $23.88 \pm 4.19 \text{ MJ m}^{-2} \text{ d}^{-1}$  and  $11.90 \pm 2.14 \text{ MJ m}^{-2} \text{ d}^{-1}$  respectively for the 2000 study period.

Table 5.4 summarizes the total flux of each individual radiation balance component for the entire 1999 field season. As previously indicated  $K_{\downarrow}$  varies between hillslopes with hillslope transect #2 receiving the highest amount followed by hillslope transect #1 and hillslope transect #3. Variation in  $K_{\downarrow}$  follows the same trend as that of  $K^*$  although differences are less substantial due to low albedos and therefore less reflected short-wave radiation. Long-wave radiation components do not vary between hillslope sites due to the diffuse nature of  $L_{\downarrow}$  throughout the study basin and similar surface temperatures on hillslopes #1 and 2 resulting in minimal variation in  $L_{\downarrow}$ . The longwave radiation balance does however affect  $Q^*$  in that its negative flux counters the strongly positive  $K^*$  thus lowering the net balance. Of the total radiation incident at the surface during the measurement period at the met site 55% comprises  $L_{\downarrow}$  which is similar to Rouse and Bello (1983) who reported 59%.

**Table 5.4** - Total incoming and outgoing radiation balance components and net shortwave, longwave and total radiation values for the 1999 study period at each site ( $\text{MJ m}^{-2}$ ).

1999							
SITE	K↓	K↑	L↓	L↑	K*	L*	Q*
<i>Met Site</i>	796.4	-135.4	974.6	-1309.0	661.0	-334.4	326.6
<i>1-A</i>	823.2	-139.9	974.6	-1309.0	683.3	-334.4	348.8
<i>1-B</i>	800.3	-128.1	974.6	-1309.0	672.2	-334.4	337.8
<i>1-C</i>	726.5	-116.2	974.6	-1309.0	610.3	-334.4	275.8
<i>2-A</i>	946.8	-142.0	974.6	-1309.0	804.7	-334.4	470.3
<i>2-B</i>	957.2	-143.6	974.6	-1309.0	813.6	-334.4	479.2
<i>2-C</i>	898.7	-134.8	974.6	-1309.0	763.9	-334.4	429.5
<i>3-A</i>	841.2	-117.8	974.6	-1270.8	723.4	-296.2	427.3
<i>3-B</i>	656.4	-91.9	974.6	-1300.1	564.5	-325.5	239.0
<i>3-C</i>	605.3	-84.8	974.6	-1300.1	520.6	-325.5	195.1

**Table 5.5** - Total incoming and outgoing radiation balance components and net shortwave, longwave and total radiation values for 2000 study period at each site ( $\text{MJ m}^{-2}$ ).

2000							
SITE	K↓	K↑	L↓	L↑	K*	L*	Q*
<i>Met Site</i>	546.6	-92.9	345.5	-571.5	453.7	-226.0	227.7
<i>1-A</i>	554.4	-94.2	345.5	-571.5	460.1	-226.0	234.1
<i>1-B</i>	544.4	-146.8	345.5	-571.5	397.6	-226.0	171.5
<i>1-C</i>	504.0	-80.6	345.5	-571.5	423.4	-226.0	197.3
<i>2-A</i>	615.2	-128.0	345.5	-571.5	487.1	-226.0	261.1
<i>2-B</i>	620.0	-204.4	345.5	-571.5	415.6	-226.0	189.6
<i>2-C</i>	584.4	-173.6	345.5	-571.5	410.8	-226.0	184.8
<i>3-A</i>	565.6	-194.3	345.5	-514.5	371.3	-169.0	202.3
<i>3-B</i>	455.7	-196.0	345.5	-514.5	259.8	-169.0	90.8
<i>3-C</i>	429.1	-184.5	345.5	-514.5	244.6	-169.0	75.6

Radiation balance totals for the 2000 field season are presented in Table 5.5. Although total values are smaller than those in Table 5.4 due to a shorter study period they do follow the same general trend in that differences in  $Q^*$  are clearly controlled by incoming short-wave radiation. Of the radiative factors  $K_{\downarrow}$  is the main variable accounting for differences in surface temperatures over time and between one surface and another (Rouse and Bello, 1983). Although  $K_{\downarrow}$  is primarily responsible for diurnal fluctuations in  $Q^*$  on a daily and seasonal basis as illustrated in this study it represents less than one half (41%) of the radiative supply to surfaces as documented by Rouse and Bello (1983).

It is important to quantify differences in net radiation between study sites because it represents the energy available for evaporation, for heating the air, and for melting the permafrost active layer. As such it is important for plant survival and growth, for determining the depth of active layers in the permafrost terrain and for the hydrologic regime. All of these features are strongly variable with terrain type (Rouse and Bello, 1983).

### **5.3 - POTENTIAL SOURCES OF ERROR**

In this study surface temperature was not directly measured in the Kakawi Lake basin on hillslope transects 1 and 2. As a result, a regressed value based on the Daring Lake meteorological station air temperature versus surface temperature relationship was applied to sites on these hillslopes leading to potential error in subsequent calculation of  $L_{\downarrow}$  using the Stefan-Boltzman equation. As such, surface temperature measurements were

taken during the 2000 field season using a portable temperature probe at each of the 9 sites between 1200 and 1300 hours. The probe was inserted 5 cm into the ground within a 2 m<sup>2</sup> quadrat a total of 6 times then averaged. Average surface temperatures are summarized in Table 5.6.

Table 5.6 - Average surface temperature for each study site

<b>Hillslope 1</b>		<b>Hillslope 2</b>		<b>Hillslope 3</b>	
Site	Surface Temperature (°C)	Site	Surface Temperature (°C)	Site	Surface Temperature (°C)
<i>1-A</i>	7.2	<i>2-A</i>	8.9	<i>3-A</i>	5.3
<i>1-B</i>	5.6	<i>2-B</i>	9.0	<i>3-B</i>	5.7
<i>1-C</i>	6.6	<i>2-C</i>	9.6	<i>3-C</i>	5.5

Surface temperatures varied less than 5°C between the 9 study sites. Using the Stefan-Boltzman equation a difference of 5°C equals a difference of 25 W m<sup>-2</sup> while a difference of 10°C equals a 50 W m<sup>-2</sup> difference. Furthermore, a difference of 5°C, or 25 W m<sup>-2</sup> over a 24 hour period is equivalent to 2.2 MJ d<sup>-1</sup> while a 10°C difference equals 4.3 MJ d<sup>-1</sup>. The average hourly flux of L↓ was determined to be 380 W m<sup>-2</sup>. Therefore, a difference of 5°C and 10°C corresponds with an error of 6.5% and 13% respectively. These errors are not significant in the overall calculation of the radiation balance but are acknowledged as potential sources of error in such calculations in this paper. It should also be noted that error is also introduced when using the Stefan Boltzman equation because any error becomes magnified when taken to the fourth power (Rouse, 1984).

Bailey et al. (1989) noted through error analysis that when  $L_{\downarrow}$  and  $L_{\uparrow}$  are not directly measured an error of approximately 13% and 30% is introduced for each, respectively. Also, surface temperature measurements taken in the field included the thin vegetation layer that lies above the soil profile which also could result in an underestimation of  $L_{\uparrow}$  due to the fact that vegetation cools the surface temperature.

As noted by Rouse (1984) it is difficult to assess the accuracy of the instrumental measurement because there are no absolute standards.  $K_{\text{down}}$ ,  $K_{\text{up}}$  and  $Q^*$  will give the greatest accuracy in intercomparisons among surfaces, and the derived fluxes such as  $L_{\text{down}}$  and  $L_{\text{up}}$  will have greater error. According to Latimer (1972) typical errors for radiation instruments under field use are  $\pm 5\%$  for  $K_{\text{down}}$  and  $K_{\text{up}}$  and  $\pm 7\%$  for  $Q^*$ .  $L^*$  assumes a larger error because it is calculated as the residual in equation 8. Given the typical errors in  $K_{\text{down}}$  and  $K_{\text{up}}$  and  $Q^*$  Lafleur et al. (1993) assigned a root mean square error of  $\pm 10\%$ . Duguay et al. (1999) estimated maximum relative errors of field measurements at  $\pm 10\%$  for  $Q^*$ ,  $\pm 5\%$  for  $K_{\downarrow}$  and  $K_{\uparrow}$  and  $\pm 1\%$  for surface temperature.

Finally, another potential source of error in determination of the radiation balance in this study is associated with the fact that calculations for  $K_{\downarrow}$ , based on Oke (1987), do not take into account shadow effects. Although the Kakawi Lake basin has a gently sloping terrain the steep nature of some hillslope segments does result in shading. This effect was observed to be most prominent early in the day when low zenith angles cause lower portions of the west-facing hillslopes to be shaded. During the hours in which incoming short-wave radiation receipt is at its maximum, shadow effects are limited to small, isolated pockets of topographic relief.

# CHAPTER 6 - SOIL MICROCLIMATE

## 6.1 - SOIL ANALYSES

Analyses of soil samples obtained from each of the study sites were undertaken to determine physical and thermal characteristics of the soil within the Kakawi Lake basin. In general, soil bulk density increased with depth at each site (Figure 6.1) corresponding to a decrease in organic content from the surface towards the permafrost table (Figure 6.3). Hillslope transect 1 showed the greatest variation in intra-hillslope bulk density ranging from 0.364 g cm<sup>-1</sup> at site C, 5 cm depth to 0.852 g cm<sup>-1</sup> at site B, 45 cm depth. Hillslope transect 2 has the least intra-hillslope variability but is similar to hillslope transect 1 in average bulk density values. Due to the much higher organic content of hillslope transect 3 bulk density values are much lower than those of hillslopes 1 & 2.

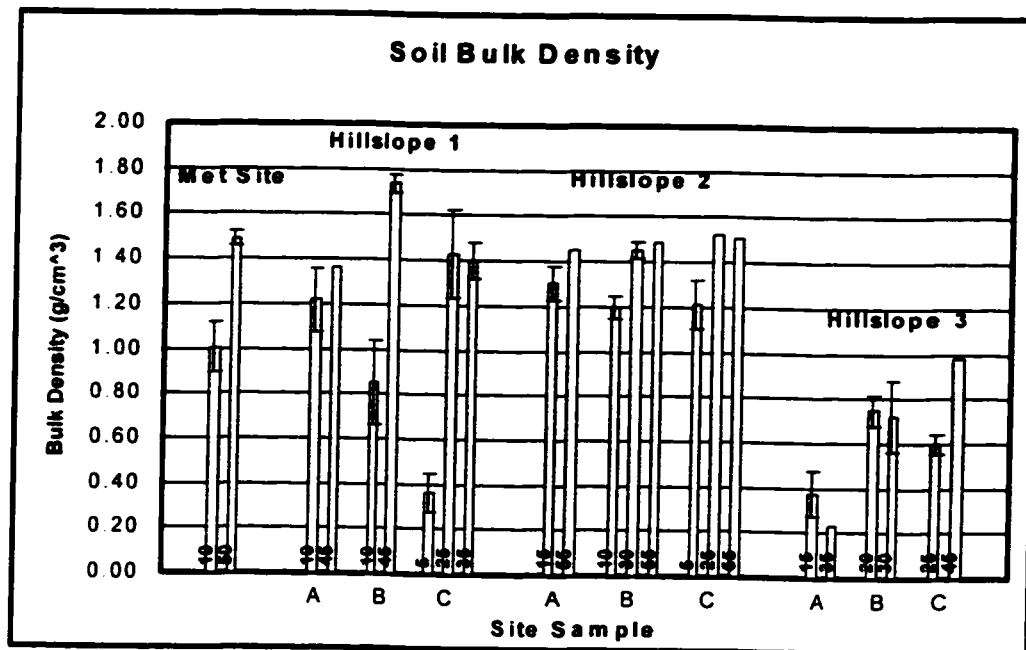


**Figure 6.1** - Soil bulk density measurements for each site. Hillslope transects and site locations are indicated directly above and below each column respectively; depths (cm) of each sample below ground surface are displayed at the base of column. Error bars are included for sites at which three samples were averaged.

Soil bulk density values obtained in the Kakawi Lake basin are similar to those of other arctic and subarctic sites (Hinzman et al., 1991; Shilkomanov and Nelson, 1999; Petrone et al., 2000). Hinzman et al. (1991) reported bulk density values in the organic layer (0 to 10 cm depth) between 0.13 and 0.18 g cm<sup>-3</sup> with an increase in bulk density to 1.57 g cm<sup>-3</sup> at 40 cm in the Imnavait watershed, Alaska. Similarly, Petrone et al. (2000) reported increases in bulk density with depth of the same order of magnitude in both dry and wetland study sites near Churchill, Manitoba. Shilkomanov and Nelson (1999) cited bulk density values of 0.15 g cm<sup>-3</sup> for dry organic matter and 1.35 and 1.37 g cm<sup>-3</sup> at sites comprised of sandy loam and silty sand respectively in the Kuparuk River Basin, Alaska.

Soil porosity measurements obtained from hillslope transects 1 & 2 indicate a general decrease in porosity with depth as illustrated in Figure 6.2. Porosity values

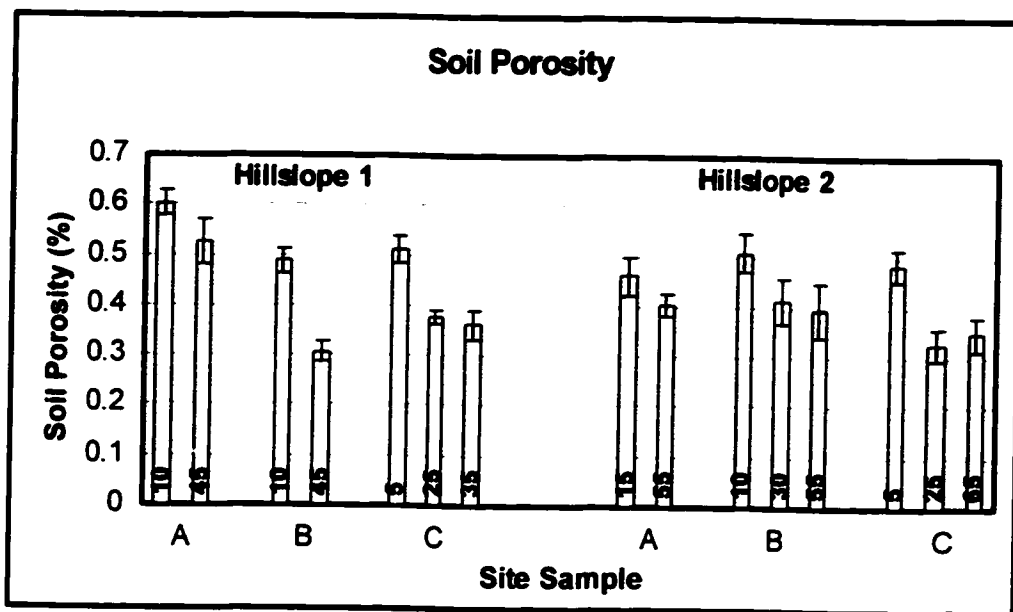


**Figure 6.2** - Soil porosity measurements for hillslopes 1 and 2. Transects and site locations are indicated directly above and below each column respectively; depths (cm) of each sample below ground surface are displayed at the base of each column. Error bars included for sites at which three samples were averaged.

obtained within the upper 10 cm of the soil profile showed a greater variation with an average value of  $0.52 \pm 0.21$  as compared to measurements taken at depths greater than 10 cm where the average value was  $0.38 \pm 0.06$ . Porosity values obtained from the Kakawi Lake study basin are similar to those cited in similar studies in arctic and subarctic environments in which porosity values decrease with increased depth corresponding to an increase in mineral content and decrease in organic matter (Hinzman et al., 1991; Woo and Xia, 1996; Putkonen, 1998; Petrone et al., 2000).

Loss on ignition (LOI) experiments indicated very low soil carbon values at all sites on hillslope transects 1 & 2 (Figure 6.3). Maximum percent carbon values were obtained within the upper 10 cm of the soil profile at each of the sites with an average of  $3.6 \pm 1.4$  % for all sites. These values decreased considerably below 10 cm (mean value

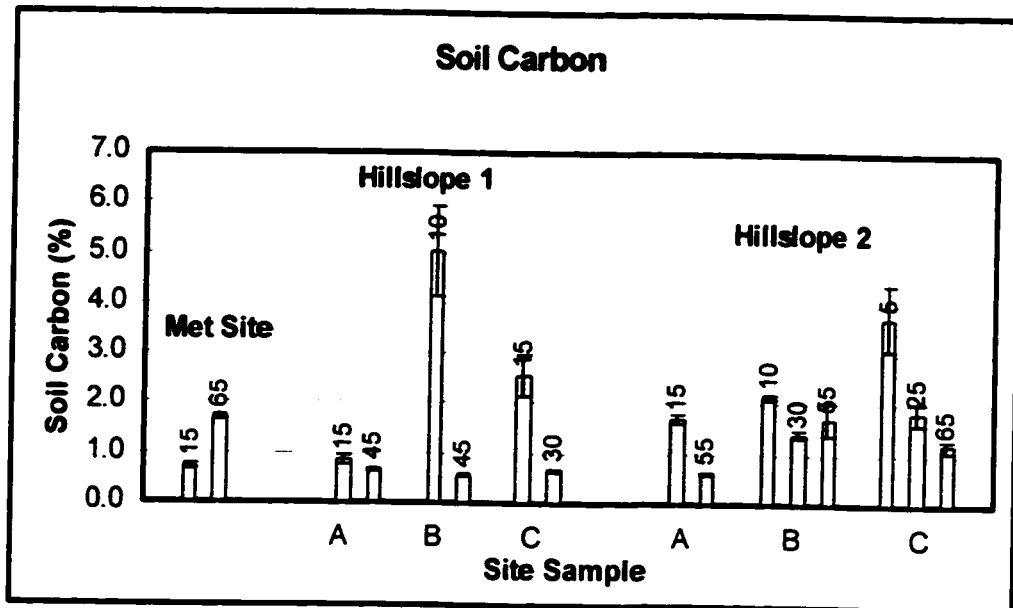


**Figure 6.3** - Soil carbon measurements for met site and for hillslopes 1 and 2. Transects and site locations are indicated directly above and below each column respectively; depths (cm) of each sample below ground surface are displayed directly above each column. Error bars are included for sites at which three samples were averaged.

1.3 ± 0.63 %) due to a very shallow rooting system of plant species growing on these hillslope transects.

The heat capacity of a soil depends upon its mineral composition and organic mater content, as well as on the volume fractions of water and air (Hillel, 1980). Taking these factors into consideration as outlined above, heat capacity measurements were obtained for hillslope transects 1 and 2 as well as at the meteorological site at various depths as illustrated in Figure 6.4. Heat capacity values for hillslope transect 3 were obtained from Hillel (1980) and were based on standard values of volumetric heat capacity of peat with varying volumetric wetness which was measured in the field.

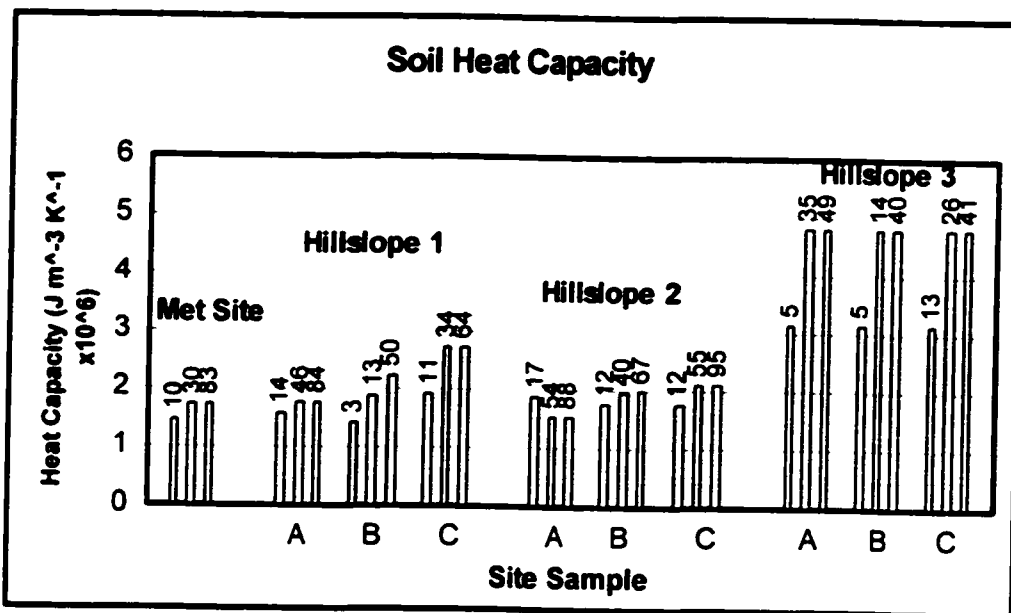


**Figure 6.4** - Soil heat capacity for each study site. Transects and site locations are indicated directly above and below each column respectively; depths (cm) of each sample below ground surface are displayed directly above each column.

Soil heat capacity values for hillslope transects 1 and 2 as well as for the meteorological station were very similar with a mean value of 1.9 ± 0.35 MJ m<sup>-3</sup> K<sup>-1</sup>. Very

little variation occurred at these sites with depth due to low water contents and relatively homogenous soil physical properties. Variations in heat capacity at hillslope 3 are attributed to a much wetter organic soil profile dominated by peat. These values correspond well with those cited in the literature summarized in Table 6.1.

**Table 6.1 - Heat capacity values for different materials**

<b>Reference</b>	<b>Location</b>	<b>Material</b>	<b>Heat Capacity MJ m<sup>-3</sup> K<sup>-1</sup></b>
Romanovsky and Osterkamp (2000)	Barrow, Alaska	peat and silt	2.6 to 3.0
		moss (living and dead)	1.7
		silt	1.9 to 2.9
Halliwell and Rouse (1987)	Churchill, Manitoba	peat	2.5
		clay	1.9
Woo and Xia (1996)	Resolute, N.W.T.	mineral	1.9
		organic	2.5
Oke (1987)		sandy soil - dry to wet	1.3 to 3.0
		clay soil - dry to wet	1.4 to 3.1
		peat - dry to wet	0.6 to 4.0

## **6.2 - ACTIVE LAYER DEVELOPMENT**

Measurements of depth to permafrost table commenced on Julian Day 186 and proceeded through to Julian Day 221 during the 1999 field season. Throughout this period attempts to record active layer depth on hillslope transect 2 revealed that the depth to permafrost table was greater than the length of the measuring device. Therefore active layer depths were recorded only on hillslope transects 1 & 2.

As illustrated in Figure 6.5-a active layer measurements on hillslope transect 1 at the completion of the 1999 field season were shallowest at the top of the hillslope, site 1-A (61.4 cm), followed by the bottom and middle of the hillslope transect, sites 1-C (85.9 cm) and 1-B (104.6 cm) respectively. Throughout the study period however site 1-C had the greatest increase in active layer depth increasing by 30.4 cm as compared to that of sites 1-A and 1-B that increased by 0.3 cm and 24.3 cm respectively.

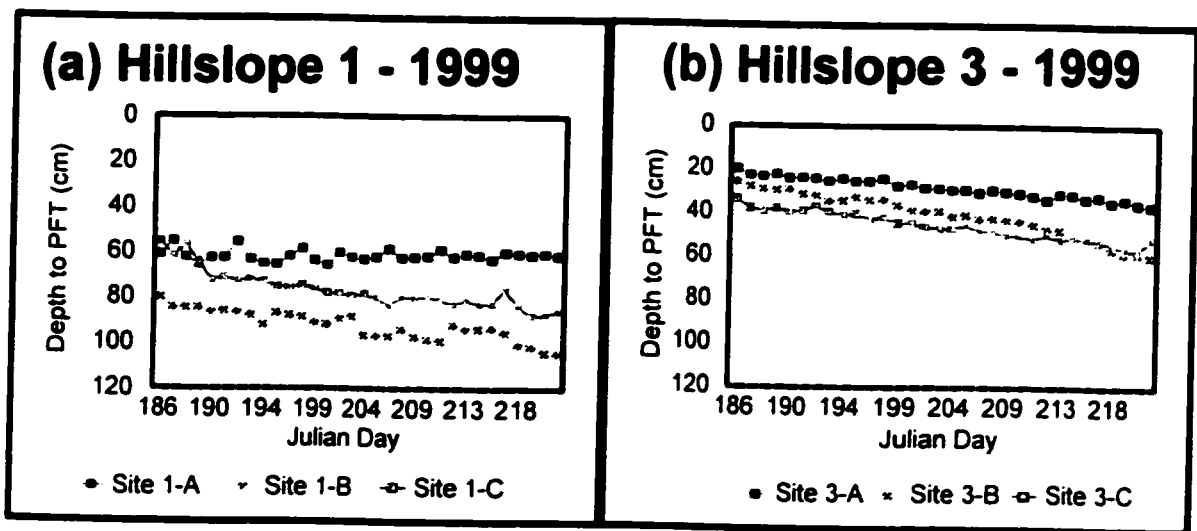


**Figure 6.5** - Active layer development for (a) hillslope transect 1 and (b) hillslope transect 3 during the 1999 field season

Average active layer depths on hillslope transect 3 (49.2 cm), which remained in the peat and did not extend to the mineral soil beneath, were much shallower than those of hillslope 1 (83.9 cm) by an average of 34.7 cm (Figure 6.5-b). Similar to hillslope 1, at the completion of the 1999 field season the shallowest active layer depth was recorded at the top of the hillslope, site 3-A (35.4 cm) followed by the bottom of the hillslope, site 3-C (51.8 cm) and finally the middle, site 3-B (59.3 cm). During the study period the

active layer increased the most at site 3-B (33.5 cm), followed by site 3-C and 3-A. 18.2 cm and 16.7 cm respectively.

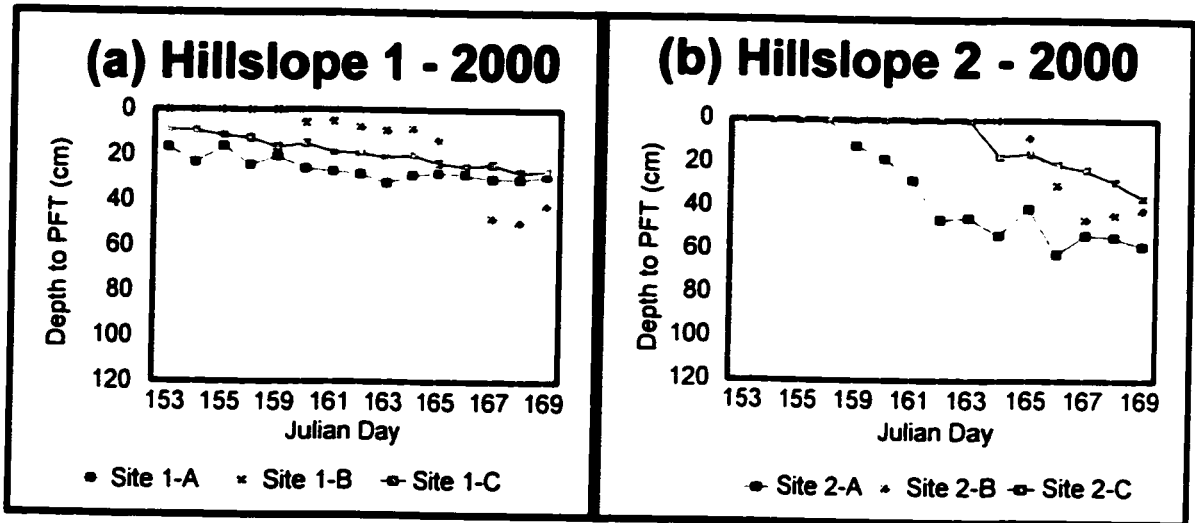


**Figure 6.6** - Active layer development for (a) hillslope transect 1 and (b) hillslope transect 2 during the 2000 field season.

Initiation of active layer development occurred first on hillslope 1 followed by hillslope 2 during the 2000 study period as illustrated in Figure 6.6. Hillslope 3 remained snow covered and consequently frozen for the majority of the time and thus is not included in this discussion. Upon initial measurement on hillslope 1, site 1-A had the deepest active layer at 16.5 cm followed by site 1-C measuring 8.7 cm and site 1-B which hadn't yet begun to melt (Figure 6.6-a). The active layer melted at a relatively uniform rate at sites 1-A and 1-C throughout the study period however site 1-B remained frozen for approximately 1 week longer and then melted over 40.0 cm in the following 10 days.

As compared to hillslope 1, hillslope 2 remained frozen for a longer period of time but had deeper active layer at all sites at the outset of the field season as illustrated in

Figure 6.6-b. Site 2-A was the first to begin melting on Julian Day 158 followed by site 2-C (JD 163) and 2-B (JD 164). At the end of the 2000 measurement period site 2-A had the deepest active layer at 57.7 cm followed by sites 2-B and 2-A which measured 41.0 and 35.5 cm respectively.

In continuous permafrost areas seasonal thawing of the active layer makes it possible for many hydrological processes to occur including groundwater storage and flow, infiltration of rainwater and evapotranspiration of the soil moisture (Woo, 1988). Therefore, the thickness and rate of change of this layer and the duration of thaw are important to the hydrology of the Kakawi Lake basin. As noted by Woo (1988) hydrological conditions also affect the ground thaw. Heat input into the active layer is supplied by the energy flux at the surface and is used to warm the active layer and to thaw the permafrost below. Heat transfer and the melting of ground ice are influenced strongly by the status of the soil.

Correlation between surface characteristics including topography, vegetation, and aspect and depth to frozen ground cannot be assumed to be constant across different areas despite essentially identical general climatic conditions and location (Leverington, 1995). Data presented here and in other studies (Romanovsky and Osterkamp, 1995; Woo and Xia, 1996; Gomersall and Hinkel, 2001) indicate that differences in depth to frozen ground can vary considerably even in sites that are relatively close to one another. Subsurface soil temperatures and  $Q_i$  are a function of the solar radiation, soil texture, soil moisture content and state, and the surface vegetation and weather conditions.

Hinzman et al. (1991) stated the importance of thermal conductivity as the main

mechanism of heat transfer in frozen soils. This varies with the soil moisture content, both in frozen and unfrozen states. Hinzman et al. (1991) found that thermal conductivity of a saturated organic soil decreased by 50% upon thawing while the saturated mineral soil decreased by about 30% after thawing. Regardless of the temperature or moisture content, Hinzman et al. (1991) note that the organic soil has a lower thermal conductivity than the mineral soil and will serve as a layer of insulation to the permafrost. Therefore it is important to have a thorough understanding of soil physical properties in order to begin to quantify subsurface thermal processes.

Soil heat flux is a minor component of the surface energy balance comprising only 10 per cent of the net all-wave radiation absorbed at the surface (Halliwell and Rouse, 1987). However, in permafrost terrain the release of latent heat resulting from phase change between water and ice represents a major energy sink or source and the magnitude of the soil heat flux can increase considerably. The standard method of measuring soil heat flux uses a heat flux plate buried close to the surface. Rouse (1984) suggested that heat flux plates seriously underestimate the soil heat flux in permafrost terrain. Halliwell and Rouse (1987) found this error to be as large as 50%. Therefore, in this study the calorimetric method for determining  $Q_c$  is used (Halliwell and Rouse, 1987; Carey and Woo, 2000; Petrone et al., 2000). The heat value given by the calorimetric method is composed of three parts: (1) the sensible heat content between the surface and base depth, (2) latent heat stored in this layer and, (3) heat flux at the base depth (Halliwell and Rouse 1987).

### **6.3 - SOIL TEMPERATURE**

Sporadic soil temperature measurements taken at each of the nine study sites were regressed against continuous measurements recorded at the meteorological station in order to produce an hourly record of soil temperature at each study site for the 1999 and 2000 field seasons. Effort was made to measure soil temperature at the nine study sites at times in which daily maximum and minimum temperatures would be expected (i.e. early morning, solar noon, and late evening) to ensure an accurate representation of temperature range for subsequent regression analysis. Regression equations and r-squared values for each thermistor probe are summarized in Appendix A. Figures illustrating the diurnal fluctuation in soil temperature at each of the study sites are included for reference in Appendix B. Soil temperature descriptive statistics for each study site derived from the regressed continuous record are summarized in Tables 6.2 and 6.3 for the 1999 and 2000 study periods respectively.

In general, soil temperatures are warmest on hillslope 2 followed by hillslope 1 and hillslope 3 as summarized in Table 6.2 and Appendix B for the 1999 field season. Soil temperatures at all sites on hillslope 2 varied considerably throughout the duration of the study period both diurnally and seasonally as indicated by the range of values (maximum temperature - minimum temperature) and the standard deviation of the mean seasonal temperature at each depth. Hillslope 3 temperature measurements showed a similar overall gradient in temperature from the shallowest to the deepest measurement as hillslope 2 but were comparatively cooler due to the increased insulative properties of the peat and the decreased receipt of incoming direct-beam solar radiation as discussed in

**Table 6.2** - Descriptive statistics for 1999 study period soil temperature (°C)

Met Site															
	10cm	30cm	83cm												
<b>Avg</b>	7.5	5.4	2.1												
<b>St.dev</b>	1.3	1.0	0.8												
<b>Max</b>	10.7	7.3	4.12												
<b>Min</b>	4.3	3.2	0.5												
Site 1-A			Site 1-B				Site 1-C								
	14 cm	46 cm	84 cm	3 cm	13 cm	50 cm	11 cm	34 cm	64 cm						
<b>Avg</b>	10.4	9.7	6.5	11.8	5.7	0.4	7.2	5.2	1.9						
<b>St.dev</b>	0.6	0.6	0.6	1.1	0.8	0.9	1.0	1.1	1.4						
<b>Max</b>	11.9	10.8	8.1	14.3	7.2	2.8	9.7	7.4	5.6						
<b>Min</b>	8.9	8.4	5.2	8.4	4.0	-1.5	4.7	2.8	-0.8						
Site 2-A			Site 2-B				Site 2-C								
	17 cm	54 cm	88 cm	12 cm	40 cm	67 cm	12 cm	55 cm	95 cm						
<b>Avg</b>	13.5	11.5	9.5	11.3	9.6	7.3	12.5	9.4	8.0						
<b>St.dev</b>	1.2	1.1	1.1	2.0	2.9	3.6	1.3	1.3	0.8						
<b>Max</b>	16.3	14.4	12.3	15.3	17.0	16.7	15.5	12.6	10.0						
<b>Min</b>	10.5	9.3	7.4	6.9	3.9	0.2	9.5	6.9	6.5						
Site 3-A				Site 3-B					Site 3-C						
	3.5 cm	9 cm	37.5 cm	49.5 cm	5 cm	14 cm	40 cm	48.5 cm	13 cm	26 cm	41 cm				
<b>Avg</b>	8.4	3.8	1.0	-0.6	10.0	3.9	2.4	2.5	4.6	4.1	3.0				
<b>St.dev</b>	1.6	1.1	0.1	0.2	1.7	2.5	2.0	2.0	1.0	1.1	0.5				
<b>Max</b>	12.2	6.4	1.1	-0.2	14.0	8.8	7.5	7.6	6.6	6.3	4.2				
<b>Min</b>	4.5	1.2	0.9	-0.9	5.9	-1.6	-1.5	-1.4	2.4	1.6	1.7				

**Table 6.3 - Descriptive statistics for 2000 study period soil temperature (°C)**

	Met Site								
	10 cm	30 cm	83 cm						
<b>Avg</b>	3.6	0.8	-0.2						
<b>St.dev</b>	2.0	0.9	0.2						
<b>Max</b>	7.8	2.9	0.1						
<b>Min</b>	0.2	-0.1	-0.7						
	Site 1-A			Site 1-B			Site 1-C		
	14 cm	46 cm	84 cm	3 cm	13 cm	50 cm	11 cm	34 cm	64 cm
<b>Avg</b>	4.5	5.0	1.6	1.4	-0.9	-0.8	2.8	-0.6	-0.2
<b>St.dev</b>	3.5	2.6	2.1	1.6	0.8	0.0	2.4	0.3	0.2
<b>Max</b>	12.8	11.2	6.6	4.8	0.7	-0.8	7.8	0.1	0.1
<b>Min</b>	0.9	2.4	-0.5	-1.4	-2.3	-0.9	-1.4	-0.9	-0.6
	Site 2-A			Site 2-B			Site 2-C		
	17 cm	54 cm	88 cm	12 cm	40 cm	67 cm	12 cm	55 cm	95 cm
<b>Avg</b>	4.7	1.2	0.8	5.4	3.5	2.3	3.0	0.1	1.8
<b>St.dev</b>	5.6	2.8	1.3	3.3	2.2	0.7	2.6	0.0	0.0
<b>Max</b>	18.1	8.0	3.9	12.4	8.3	3.5	8.4	0.2	1.8
<b>Min</b>	-1.0	-1.7	-0.5	0.6	0.3	0.6	-0.8	0.1	1.7
	Site 3-A								
	3.5 cm	9 cm	37.5 cm	49.5 cm					
<b>Avg</b>	2.8	-0.5	-0.2	3.6					
<b>St.dev</b>	1.8	0.1	0.1	0.1					
<b>Max</b>	6.5	-0.4	-0.1	3.8					
<b>Min</b>	-0.4	-0.6	-0.4	3.4					

the previous chapter. Finally, average soil temperatures on hillslope 1 were in between those of hillslopes 2 and 3. Hillslope 1 also had the smallest range of temperatures at each specific depth throughout the 1999 field season.

Table 6.3 and Appendix (B) summarize and illustrate the diurnal and seasonal fluctuation in soil temperature for the 2000 study period. Due to the fact that snow remained present on sites 2-B, 2-C and hillslope 3 well into the study period, italicised values in Table 6.3 represent data from Julian Day 164 to 170 only. All other values in Table 6.3 represent the entire study 2000 study period (JD 150-170). Similarly, in Appendix B data illustrated to the left of the vertical bar are extrapolated data which are not considered to be reliable and therefore are not included in this discussion. As summarized in Table 6.3 soil temperatures at the meteorological station site decreased by 2.8°C from 10 cm to 30 cm in depth and remained frozen at 83.0 cm which was the deepest temperature reading. Diurnal variations in soil temperature were also greatest at 10 cm, were less prominent at 30 cm and did not exist at 83 cm (Appendix B).

On hillslope 1 the highest average soil temperatures occurred at site 1-A followed by sites 1-B and 1-C which experienced similar warming near the surface but remained near the freezing point at the intermediate and deepest depths. On hillslope 2 the shallowest temperature measurements at all sites increased notably throughout the 2000 study period while deeper measurement points also began to warm above the freezing point. Site 2-B had significantly warmer temperatures at 40 cm and 67 cm as compared to measurements taken at similar depths at sites 2-A and 2-C as indicated by the higher average temperatures.

Finally, site 3-A differed considerably in comparison to the other two hillslope transects in that temperature increased as opposed to decreasing with depth in the soil profile. Soil temperatures increased daily with a pronounced diurnal fluctuation but remained around the freezing point at 9.0 cm and 37.5 cm. At 49.5 cm, the deepest measurement point, the average soil temperature was greater than all three of the shallower measurement points remaining around 3.5°C with no diurnal fluctuation throughout the 7 days of measurement following snowmelt on the surface.

As illustrated in this study the thermal properties of the active layer do not remain constant throughout the year because of thawing and freezing and the difference in thermal conductivity between thawed and frozen ground causing a 'negative thermal offset'. This is defined as the difference between the mean annual permafrost surface temperature (MAPST) and mean annual ground surface temperature (MAGST) (Romanovsky and Osterkamp, 1995). As a result, the mean annual ground temperature usually decreases with depth in the active layer. Negative thermal offset depends on soil thermal properties and is usually largest within a peat layer as described above. Summer temperature conditions on the ground surface also have a significant influence on the thermal offset value (Romanovsky and Osterkamp, 1995).

As summarized in Tables 6.2 & 6.3 near-surface temperatures more closely reflect the air temperature fluctuations as compared to those which are at depths greater than approximately 30 cm. Similarly, Woo and Xia (1996) concluded that temperature profiles showed larger temperature gradients in the top 10.0 cm of the soil profile being two or three times larger than the gradient below. The amplitude of the daily temperature

wave decreases rapidly with depth aided by decreased thermal diffusivity and increased heat capacity (Halliwell and Rouse, 1987). Rouse (1984) reported that in tundra soils near Churchill the annual temperature range at the surface is 38°C, at 0.5 m is 20°C and at 2 m is 6°C. Furthermore, in a comparison study of a dry polar desert site versus a moist fen site Woo and Xia (1996) noted significant differences in average temperature gradients with depth as summarized in Table 6.4.

**Table 6.4 - Average temperature gradients at polar desert site and fen site in continuous permafrost area of Arctic Canada; Resolute, Cornwallis Island, N.W.T. (Woo and Xia 1996)**

<b>POLAR DESERT SITE</b>		<b>FEN SITE</b>	
Depth (m)	Temperature Gradient (°C/m)	Depth (m)	Temperature Gradient (°C/m)
0.02 - 0.10	37.1	0.02 - 0.10	67.6
0.10 - 0.25	18.4	0.10 - 0.20	20.0
0.25 - 0.50	11.6	0.20 - 0.30	11.7

Most significant is the difference in temperature gradient at near surface depths between the fen and polar desert site. Woo and Xia (1996) noted that surface peat had lower thermal conductivity than underlying silty clay at the fen site because of its low mineral content and high porosity. Upon thaw, water replaces ice and reduces its conductivity sharply. At the polar desert site surface thaw occurs sooner when infiltrated meltwater filled many of the voids. As drying followed, air began to replace water and the conductivity decreased at the surface layer. Such findings are similar to the present study in which temperature gradients at near surface depth are higher on hillslope 3 (similar to fen site) as compared to hillslopes 1 and 2 due to surface peat.

## 6.4 - SOIL MOISTURE

Soil moisture, as measured at the Laurier meteorological station located at the top of the Kakawi Lake basin, decreased at a steady rate during the 1999 study season with the exception of two significant rainfall events (Figure 6.7-a). The first event occurred on JD 188 and totalled 12.4 mm resulting in an immediate increase in soil moisture from  $0.18 \text{ m}^3/\text{m}^3$  to  $0.31 \text{ m}^3/\text{m}^3$  at 13 cm depth. The same event caused little increase in soil moisture content at 52 cm in depth. Soil moisture content at 13 cm decreased back near its pre-event content within 3 days. The second rainfall event on JD203 was slightly larger than the first totalling 13.9 mm but occurred over a period of 2 days therefore causing less of an immediate increase in soil moisture (from  $0.13 \text{ m}^3/\text{m}^3$  to  $0.17 \text{ m}^3/\text{m}^3$ ) at 13 cm and a longer period of time in which soil returned to the pre-event water content. Once again, soil moisture as measured at 52 cm depth indicated a minimal increase as a

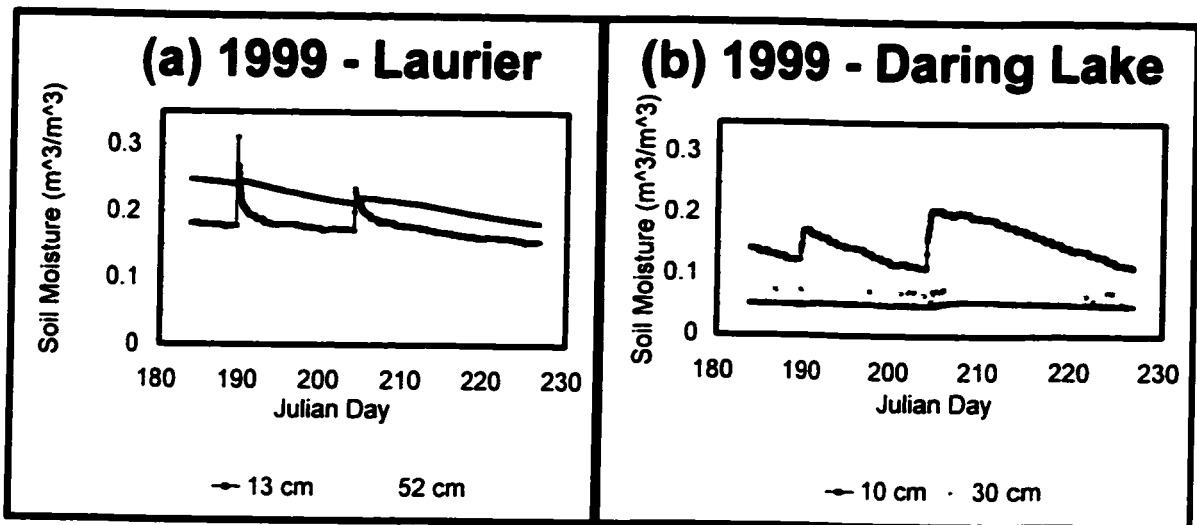


Figure 6.7 - Daily soil moisture contents measured at depth at (a) Laurier met site (hillslope) and (b) Daring Lake met site (relatively flat ground) during 1999 field season.

result of the second precipitation event.

In contrast to the Laurier meteorological station, which is located at the top of the Kakawi Lake study basin 26 m above the Kakawi Lake water level, the Daring Lake station is located approximately 100 m inland from the east shore of Daring on relatively flat ground only a few metres in elevation above the Daring Lake water level. As such, the subsurface response in soil moisture content to precipitation events is significantly different at this site as illustrated in Figure 6.7-b. At the beginning of the 1999 study period soil moisture contents were similar at shallow depths for both the Daring Lake and Kakawi met site locations. In response to the first significant precipitation event the Daring Lake site experienced a smaller increase in soil moisture than the Kakawi site increasing only  $0.05 \text{ m}^3/\text{m}^3$  as compared to  $0.14 \text{ m}^3/\text{m}^3$  at the Kakawi site. The second major precipitation event of the 1999 study season (JD 203), which was 1.5 mm larger than the first event, caused a larger increase in soil moisture at shallow depth at the Daring Lake site ( $0.10 \text{ m}^3/\text{m}^3$ ) as compared to the Kakawi site ( $0.06 \text{ m}^3/\text{m}^3$ ).

Soil moisture content at 30 cm depth at the Daring Lake met site shows an interesting relationship in response to precipitation. Soil moisture at this depth remained consistent throughout the 1999 study season with the exception of a series of minor very short term increases ( $0.02 \text{ m}^3/\text{m}^3$ ) in response to precipitation events, for example, a precipitation event on JD 185 totalled 2.1 mm while the next event on JD 189 experienced 12.4 mm. Despite the notable difference in precipitation input between these two events response in soil moisture at 30 cm depth, as for all such events, was the same. This leaves doubt as to the reliability of the soil moisture content measurements recorded at this depth, possibly due to instrument error.

Figure 6.7 illustrates that soils drain much more rapidly at the Kakawi site as compared to the Daring Lake site due to its positioning at the crest of the Kakawi Lake basin divide and subsequent downslope drainage of soil water. Due to low elevation gradients water percolating into the soil at the Daring Lake site takes longer to drain resulting in an increased lag in the soil moisture curve.

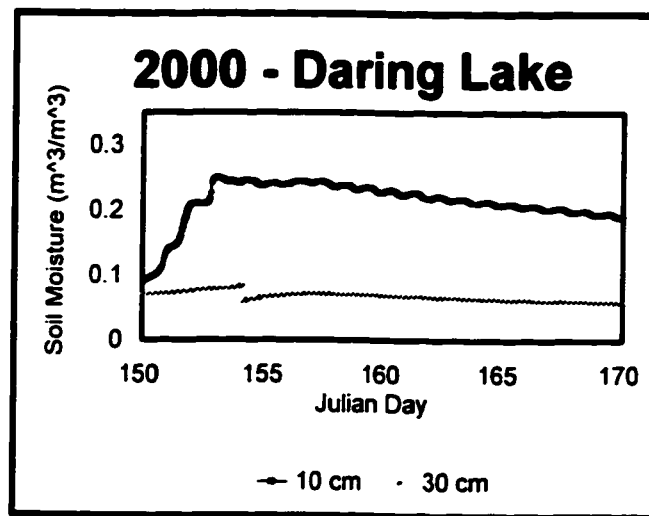


Figure 6.8 - Daily soil moisture content measured at depth at the Daring Lake met site during 1999 field season.

Illustrated in Figure 6.8 are the soil moisture contents as measured at the Daring Lake meteorological station at 10 cm and 30 cm depth during the spring 2000 study period. Upon the onset of spring melt soil water content at 10 cm rose over  $0.25 \text{ m}^3/\text{m}^3$  until JD 154 when the snow had melted and the soil water began to drain and evaporate at shallow depth. Soil moisture as measured at 30 cm depth showed little change throughout the study period and was consistent with measurements taken the previous year. Soil moisture probes failed to operate at the Kakawi Lake meteorological station, therefore no record of soil moisture is included in this discussion.

Due to errors involving measurement of soil moisture content at each of the 9 study sites in the first half of the 1999 study season, soil water content data are only available on a daily basis from Julian Day 212 to 226. Average water contents as summarized in Table 6.5 for this time period indicate very little variation due, in part, to minimal accumulation of precipitation.

**Table 6.5** - Average soil moisture content (Julian Day 212 to 226) for 1999 field season

Hillslope	Site and Depth (cm)	Average Soil Moisture (m <sup>3</sup> /m <sup>3</sup> )
Hillslope #1	A - 17.0	0.18 ± 0.02
	A - 52.0	0.21 ± 0.03
	B - 27.0	0.09 ± 0.01
	B - 61.0	0.20 ± 0.02
	C - 17.0	0.22 ± 0.01
	C - 37.0	0.35 ± 0.02
Hillslope #2	A - 13.5	0.20 ± 0.02
	A - 62.0	0.18 ± 0.01
	B - 11.2	0.19 ± 0.02
	B - 51.5	0.18 ± 0.03
	C - 15.6	0.18 ± 0.01
	C - 85.0	0.19 ± 0.01
Hillslope #3	A - 7.0	0.25 ± 0.01
	A - 13.0	0.61 ± 0.01
	B - 4.5	0.56 ± 0.01
	B - 15.0	0.73 ± 0.01

At all sites on hillslope 1 soil moisture increased with depth whereas in hillslope 2 soil moisture contents were very similar at all sites and at each depth due to uniform texture of surficial material . The greatest soil moisture contents were present on hillslope 3 where peat soils have increased porosity and lower thermal conductivity resulting in increased attenuation and decreased evaporation as compared to hillslopes 1 and 2 which are dominated by mineral soils.

## **6.5 - IRRIGATION EXPERIMENT**

Due to the fact that precipitation events were minimal and total rainfall accumulation was only 40 mm for the entire 1999 field season an irrigation experiment was conducted on each hillslope to quantify the effect of rainfall on subsurface soil water content and temperature. A 20 mm rainfall event was simulated on each hillslope over a 3.5 hour time frame and soil temperature and moisture content were monitored for 6 hours upon completion of the experiment.

Summarized in Table 6.6 are the changes in soil temperature and soil water content on hillslope transects 1 and 2 resulting from irrigation experiments. On both hillslope transects changes in temperature occurred at all shallow depths for sites; all of which were less than 1°C over the 6 hour period. Due to the diurnal fluctuation in soil temperature at such depths as previously discussed such changes in temperature cannot be attributed to either rainfall or diurnal trends therefore concluding that rainfall has no significant effect on soil temperature. Soil water content increased slightly at shallow depths at sites 1-B, 1-C, 2-A, 2-B, and 2-C with the largest increase occurring at site 1-C

**Table 6.6** - Soil temperature and water content differences from 1999 field season irrigation experiments.

Site	Start Temp. (°C)	End Temp. (°C)	Temp. Difference (°C)	Site	Start Water Content (m <sup>3</sup> /m <sup>3</sup> )	End Water Content (m <sup>3</sup> /m <sup>3</sup> )	Water Content Difference (m <sup>3</sup> /m <sup>3</sup> )
1-A-14	10.6	11.1	0.5	1-A-17	0.16	0.16	0.00
1-A-46	10.1	10.1	0.0	1-A-57	0.20	0.20	0.00
1-A-84	7.7	7.7	0.0				
1-B-3	10.4	11.2	0.8	1-B-27	0.11	0.11	0.00
1-B-13	7.0	7.3	0.3	1-B-61	0.20	0.20	0.00
1-B-50	2.5	2.5	0.0				
1-C-11	7.8	8.7	0.9	1-C-17	0.21	0.24	0.03
1-C-34	7.4	7.4	0.0	1-C-37	0.37	0.38	0.01
1-C-64	3.9	3.9	0.0				
2-A-17	14.4	14.6	0.2	2-A-13.5	0.19	0.21	0.02
2-A-54	13.6	13.6	0.0	2-A-62	0.19	0.19	0.00
2-A-88	11.3	11.3	0.0				
2-B-12	13.7	14.2	0.5	2-B-11.2	0.15	0.16	0.01
2-B-40	12.6	12.9	0.3	2-B-51.5	0.22	0.22	0.00
2-B-67	11.5	11.5	0.0				
2-C-12	12.9	13.2	0.3	2-C-15.6	0.17	0.18	0.01
2-C-55	11.2	11.4	0.2	2-C-85	0.19	0.19	0.00
2-C-95	9.07	9.07	0.0				

at +0.03 m<sup>3</sup>/m<sup>3</sup>. Soil water content also increased slightly from 0.37 m<sup>3</sup>/m<sup>3</sup> to 0.38 m<sup>3</sup>/m<sup>3</sup> at 37 cm depth at site 1-C although, differences of this magnitude are within the error of

measurement (Table 12) and are therefore inconclusive.

Although changes in soil microclimate resulting from irrigation experiments were minimal on hillslopes 1 and 2, site 3-A did show an increase in soil temperature and water content as illustrated in Figures 6.9. At site 3-A soil temperature began to increase 1.0 hour into the experiment at 3.5 cm in depth and continued to increase a total of 6.3°C

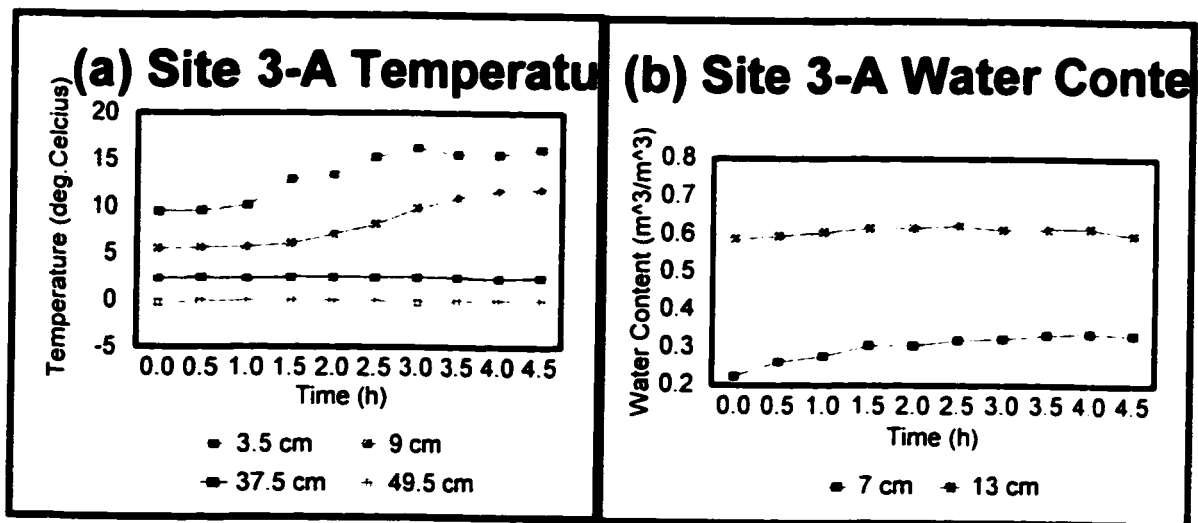


Figure 6.9 - Irrigation experiment Site 3-A changes in (a) soil temperature and (b) soil water content.

after 4.5 hours. Similarly, soil temperature at 9 cm depth increased a total of 5.8°C during the irrigation experiment. Soil temperature as measured at 37.5 cm and 49.5 cm in depth remained unchanged throughout the duration of the irrigation experiment. Figure 6.9-b illustrates the increase in water content as a result of the introduction of water at the surface. Soil water content increased 11.0 ( $m^3/m^3$ ) at a depth of 7 cm but remained relatively unchanged at 13 cm. It is also interesting to note that although temperature

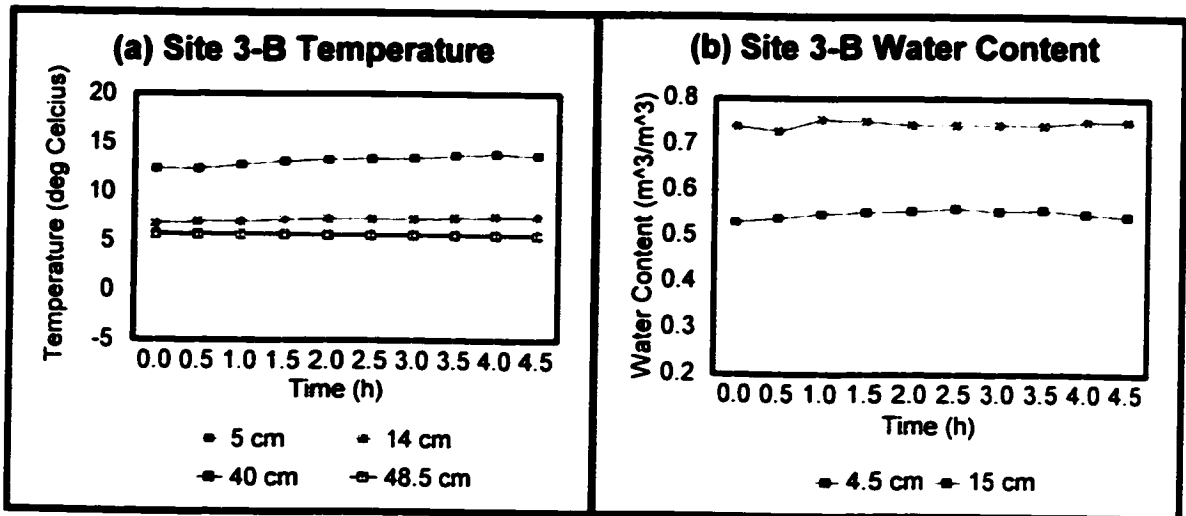


Figure 6.10 - Irrigation experiment Site 3-B changes in (a) soil temperature and (b) soil water content.

increased by approximately 7°C at 9 cm in depth there was no significant change in water content at 13 cm, which was measured only 4 cm below the soil temperature probe.

Unlike site 3-A, site 3-B had a similar response to hillslope transects 1 and 2 in that neither soil temperature or soil moisture varied as a result of the simulated 20 mm rainfall event. Soil temperature increased only 1.5°C at 5 cm depth during the 4.5 hour experiment while soil moisture content measured at 4.5 cm below the soil surface initially increased by 0.02 m<sup>3</sup>/m<sup>3</sup> after 2.5 hours followed by a 0.01 m<sup>3</sup>/m<sup>3</sup> decrease resulting in an overall increase of 0.01 m<sup>3</sup>/m<sup>3</sup> due to simulated rainfall. Neither soil temperature or water content varied as a result of the irrigation experiment at depths greater than 15 cm.

Due to the fact that irrigation experiments resulted in no notable increase in soil moisture or temperature at all sites with the exception of site 3-A average soil moisture contents listed in Table 6.5 may be used with confidence in subsequent calculations of diurnal and seasonal ground heat flux at each of the study sites. This is further supported

by findings reported by Putkonen (1998) in which soil moisture content at the study site near Ny-Alesund, northwestern Spitsbergen, Svalbard did not vary appreciably during the course of the summer after initial thaw resulting in the use of average soil moisture values in seasonal heat transfer calculations. With respect to the influence of rainfall on ground heat transfer, Woo and Xia (1996) noted that rain convected heat was minimal, mainly because of the low rainfall magnitude similar to conditions noted at the Kakawi Lake study basin for both the 1999 and 2000 field seasons. Furthermore, in a follow-up study to Woo and Xia (1996), Carey and Woo (2000) quantified this relationship and concluded that convection from rainfall accounted for less than 3% of the ground heat flux. These studies further increase confidence in the use of average water contents for subsequent ground heat flux calculations and the insignificance that rainfall events of magnitudes reported here have on such calculations.

## **6.6 - SUBSURFACE LATENT HEAT ( $Q_L$ )**

Development of the active layer occurred at a relatively steady rate at all sites during the 1999 and 2000 field seasons. However, daily measurements derived as an average of 5 depth readings at each site did have standard deviations that ranged on average between 5 and 10 cm. This error results from difficulties in obtaining accurate measurements of permafrost table depth in an area that is underlain by discontinuous bouldery surficial material. This daily deviation decreases confidence in quantifying specific changes in active layer development measurements from one day to the next. Due to the fact that temperature measurements were found to have little if any daily fluctuation throughout the study period at depths greater than 30 cm it may be assumed

that depth to permafrost table measurements also do not vary diurnally. As such, to eliminate error in calculations of daily subsurface latent heat ( $Q_L$ ) resulting from fusion of ice at the permafrost table, active layer development measurements were regressed against Julian Day to eliminate daily fluctuations but keep the slope of the active layer development vs. time relationship the same (refer to Appendix C).

Figure 6.11 illustrates the regressed active layer development for hillslope transect 1 and transect 3 during the 1999 field season. Figures 6.12-a and 6.12-b illustrate the regressed active layer development for hillslope transects 1 and 2 during the 2000 field season. Note that actual as opposed to regressed data were used for site 2-B during the 2000 field season due to the non-linear development of the active layer. Finally, summarized in Table 6.7 are the daily  $Q_L$  totals released as a result of active layer development and the related totals for all sites during both the 1999 and 2000 study seasons.

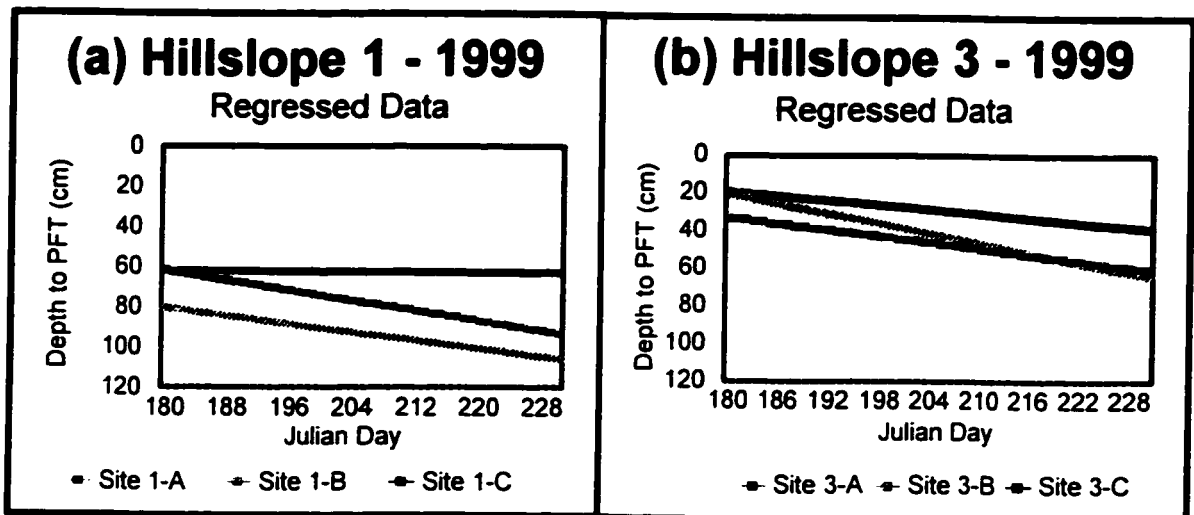


Figure 6.11 - Regressed active layer development for (a) hillslope transect 1 and (b) hillslope transect 3 during the 1999 field season

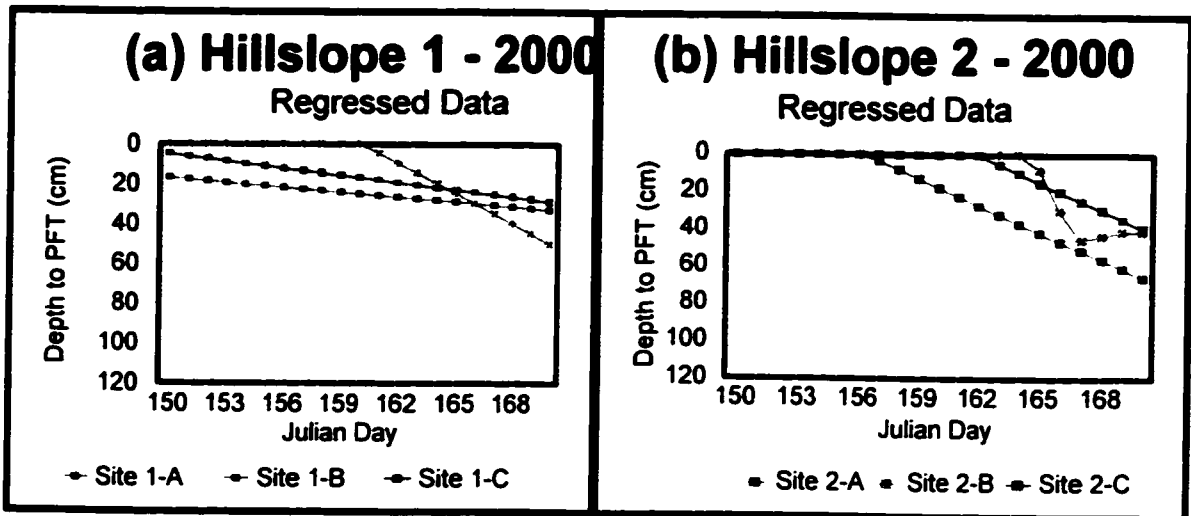


Figure 6.12 - Regressed active layer development for (a) hillslope transect 1 and (b) hillslope transect 2 during the 2000 field season

Latent heat is largest at the beginning of the thaw season when there is rapid active layer development but is later reduced as ground thaw slackens (Woo and Xia, 1996). This trend is evident in Table 6.7 in that total latent heat flux for the 2000 field season was nearly the same as 1999 and in some cases exceeds the 1999 measured  $Q_L$  despite the fact that the later period was 25 days longer. During the 1999 field season hillslope transect 3 had the largest total latent heat flux due to the high thermal conductivity of the peat.

The role of ground ice plays an important role in affecting active layer thaw. Woo and Xia (1996) found that for a fen soil with large ice content throughout its profile, its maximum seasonal thaw depth was only 60% of the polar desert soil which has a lower ice content. This relationship is similar to that found in the Kakawi Lake study basin during the 1999 field season. During this time the average active layer depth on hillslope transect 3 (49.2 cm) dominated by peat and a high water content was only 59% of the

**Table 6.7 - Daily and seasonal total  $Q_L$  for each site during 1999 and 2000 field seasons. Number of days in 2000 field season are noted in brackets**

	Site	Daily Total $Q_L$ (MJ $m^{-2}$ )	Field Season Total $Q_L$ (MJ $m^{-2}$ )
1999	1-A	0.01	0.54
	1-B	0.31	13.44
	1-C	0.68	29.09
	3-A	0.72	30.96
	3-B	1.93	83.04
	3-C	1.22	52.55
2000	1-A	0.50	9.57 (n=20)
	1-B	3.12	27.62 (n=20)
	1-C	1.29	24.48 (n=20)
	2-A	1.18	7.09 (n=6)
	2-B	x	23.81 (n=6)
	2-C	2.89	17.35 (n=6)
	3-A	x	23.50 (n=6)

average active layer depth on hillslope 1 (83.9 cm). Woo and Xia (1996) further noted that soils in poorly drained sites, which are often rich in ice, retard the development of a deep active layer. Storage of summer moisture is confined as a result of shallow thaw and therefore augments the ice content when the water freezes in winter. This feature is common in arctic wetlands and indicates a feedback between the hydrological and thermal aspects of the active layer (Woo and Xia, 1996).

## 6.7 - SUBSURFACE SENSIBLE HEAT ( $Q_s$ )

Based on measurements of subsurface temperature, water content and soil physical properties the sensible heat flux ( $Q_s$ ) was determined for each site for the 1999 and 2000 study periods. Illustrated in Figure 6.13 is the  $Q_s$  flux for sites on Hillslope 1. During the 1999 field season site 1-B had the highest average daily sensible heat flux at  $0.46 \pm 0.21 \text{ MJ m}^{-2} \text{ d}^{-1}$  while site 1-A had the lowest averaging  $0.03 \pm 0.29 \text{ MJ m}^{-2} \text{ d}^{-1}$ . Average daily  $Q_s$  at site 1-C was mid range as compared to the other two sites on hillslope 1 but had a notably larger standard deviation averaging  $0.25 \pm 0.54 \text{ MJ m}^{-2} \text{ d}^{-1}$ .

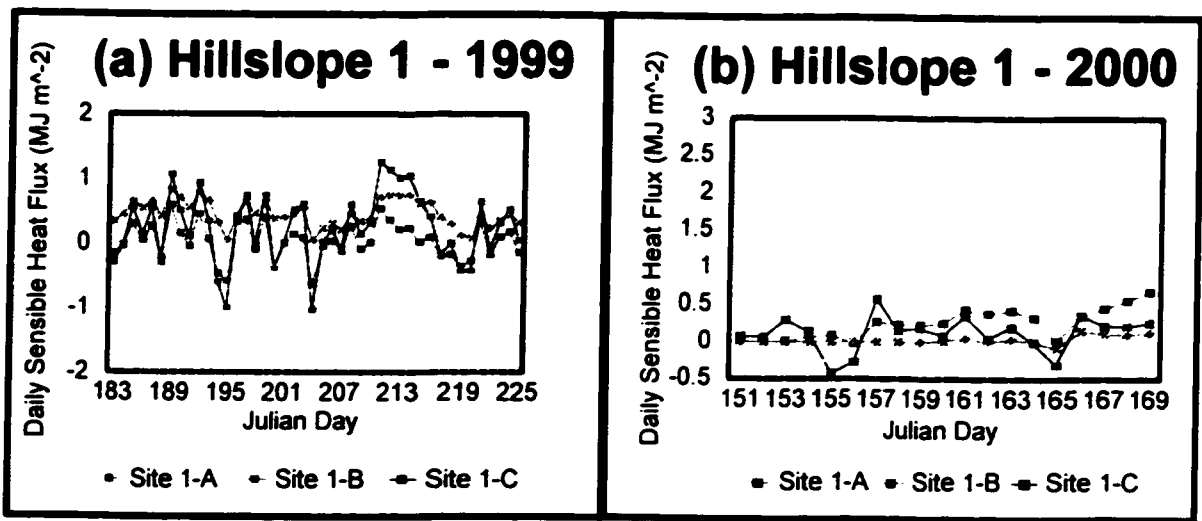


Figure 6.13 - Subsurface  $Q_s$  on hillslope 1 for (a) 1999 and (b) 2000 study seasons.

In general, reductions in daily average  $Q_s$  are related to cooling trends in air temperature as measured at the Kakawi Lake met site during 1999. Specifically, the three most notable cooling periods occurred from JD 191-193, JD 199-203 and JD 214-218 in which average air temperature decreased by approximately  $10^\circ\text{C}$ ,  $10^\circ\text{C}$  and  $8^\circ\text{C}$  respectively. Regression analysis comparing average air temperature (independent variable) and average  $Q_s$  (dependent variable) concluded that site 1-B had the highest

correlation coefficient followed by site 1-C and 1-A; 0.52, 0.38 and 0.36 respectively.

During the spring 2000 study period site 1-B remained frozen for longer than the other sites in hillslope 1 due to snowpack influence resulting in a lower average  $Q_s$  ( $0.03 \pm 0.06 \text{ MJ m}^{-2} \text{ d}^{-1}$ ) as compared to the other two sites (Figure 6.13-b). Site 1-A had the largest  $Q_s$  flux averaging  $0.24 \pm 0.21 \text{ MJ m}^{-2} \text{ d}^{-1}$  while site 1-C once again had the greatest deviation about the mean averaging  $0.11 \pm 0.24 \text{ MJ m}^{-2} \text{ d}^{-1}$ . Average daily air temperature measured at the Kakawi Lake met station indicated a steady increase from JD 156 to 168 with the exception of a  $2^\circ\text{C}$  decrease on YD 165 which is reflected at all sites in Figure 6.14-b in terms of a negative  $Q_s$ .

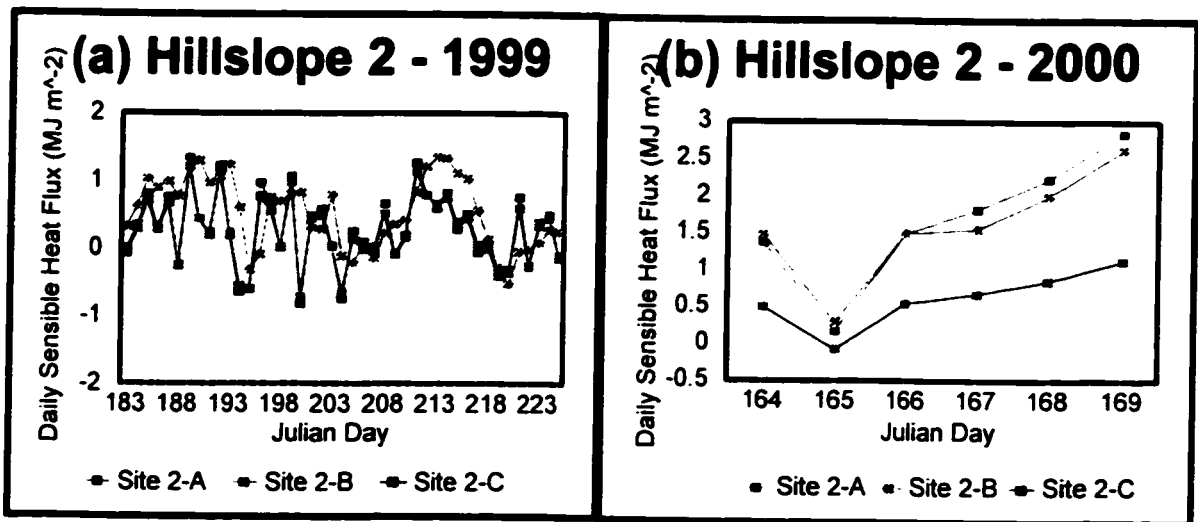


Figure 6.14 -  $Q_s$  on hillslope 2 for (a) 1999 and (b) 2000 study periods.

As compared to hillslope 1, hillslope 2 had much greater deviation about the mean in  $Q_s$  as illustrated in Figure 6.14. During the 1999 study season site 2-B had the highest  $Q_s$  averaging  $0.53 \pm 0.52 \text{ MJ m}^{-2} \text{ d}^{-1}$ . Site 2-A and 2-C had a lower average  $Q_s$  measuring  $0.28 \pm 0.54 \text{ MJ m}^{-2} \text{ d}^{-1}$  and  $0.25 \pm 0.49 \text{ MJ m}^{-2} \text{ d}^{-1}$  respectively.

During the spring 2000 study season  $Q_s$  in hillslope 2 was significantly larger than

that of 1999 as well as compared to other study sites due to increased receipt of incoming shortwave radiation. Sites 2-A and 2-B had the largest average  $Q_s$  of  $1.66 \pm 0.91 \text{ MJ m}^{-2} \text{ d}^{-1}$  and  $1.58 \pm 0.77 \text{ MJ m}^{-2} \text{ d}^{-1}$  respectively. Site 2-C was much lower than sites 2-A and 2-B with respect to  $Q_s$  averaging  $0.61 \pm 0.41 \text{ MJ m}^{-2} \text{ d}^{-1}$ . Similar to hillslope 1, hillslope 2 also experienced a significant decrease in daily  $Q_s$  as a result of a cooling trend on JD 165 as illustrated in Figure 6.14-b.

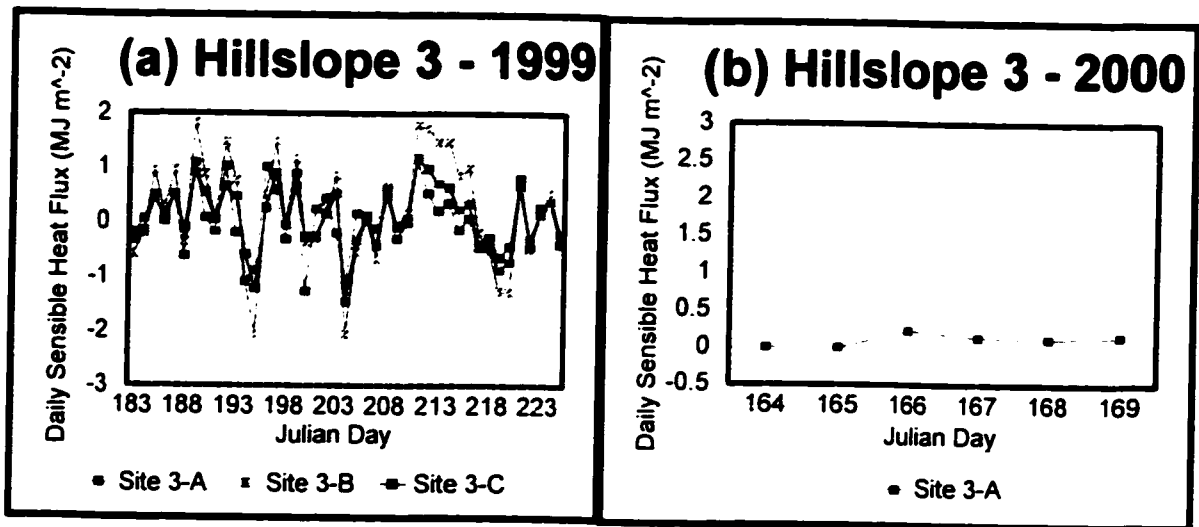


Figure 6.15 -  $Q_s$  on hillslope 3 for (a) 1999 and (b) 2000 study periods.

The most considerable fluctuations in  $Q_s$  occurred on hillslope 3 where peat soils with low bulk density and high heat capacity were more susceptible to changes in air temperature. Although seasonal average values of  $Q_s$  are lower than those of hillslopes 1 and 2 deviations are much more significant with averages and standard deviations of  $0.04 \pm 0.60 \text{ MJ m}^{-2} \text{ d}^{-1}$ ,  $0.23 \pm 0.97 \text{ MJ m}^{-2} \text{ d}^{-1}$  and  $0.09 \pm 0.58 \text{ MJ m}^{-2} \text{ d}^{-1}$  for sites 3-A, 3-B and 3-C, respectively.

Regression analysis comparing average air temperature (independent variable) and average  $Q_s$  (dependent variable) concluded that hillslope 3 had the highest correlation coefficients out of all three hillslopes, with r-squared values of 0.21, 0.55 and 0.61 for sites 3-A, 3-B and 3-C. Measurements of  $Q_s$  during the 2000 study period were limited to site 3-A due to snowcover. Therefore, daily  $Q_s$  is minimal as illustrated in Figure 6.15-b which details the onset of seasonal melt within the soil profile.

Another important consideration to take into account when discussing  $Q_s$  is at what depth the energy is stored within the soil profile. Depending on the soil physical characteristics and soil thermal gradients  $Q_s$  varies with respect to depth and does not necessarily increase or decrease in a linear fashion from the soil surface to the permafrost table. Table 6.8 summarizes the total amount of  $Q_s$  for each soil layer for both the 1999 and 2000 study periods. With the exception of sites 1-B, 1-C and 2-B, the most significant  $Q_s$  is stored in the middle layer of the soil profile during the 1999 field season. During the 2000 field season with sublimation and melt completed and active layer development beginning, the most significant  $Q_s$  is located in the upper 10 cm of the soil profile with a subsequent decrease with depth. During both field seasons sites on hillslope 2 have the largest  $Q_s$  owing to a west-facing aspect and subsequent increased receipt of short-wave radiation.

**Table 6.8** - Sensible heat ( $Q_s$ ) stored in each soil layer for 1999 and 2000 study periods. Midpoints (cm) for each profile layer included above energy values (MJ)

SITE	<u>1999 <math>Q_s</math> FOR EACH SOIL LAYER (MJ)</u>				<u>2000 <math>Q_s</math> FOR EACH SOIL LAYER (MJ)</u>			
	Met	10 cm	30 cm	83 cm		10 cm	30 cm	83 cm
<b>0.8</b>		<b>1.6</b>	<b>0.2</b>		<b>1.9</b>	<b>0.4</b>	<b>0.0</b>	
1-A	14 cm	46 cm	84 cm		14 cm	46 cm	84 cm	
	<b>0.6</b>	<b>0.8</b>	<b>0.0</b>		<b>4.7</b>	<b>0.0</b>	<b>0.0</b>	
1-B	3 cm	13 cm	50 cm		3 cm	13 cm	50 cm	
	<b>0.2</b>	<b>0.9</b>	<b>2.5</b>		<b>0.2</b>	<b>0.3</b>	<b>0.0</b>	
1-C	11 cm	34 cm	64 cm		11 cm	34 cm	64 cm	
	<b>0.9</b>	<b>2.0</b>	<b>2.8</b>		<b>2.2</b>	<b>0.0</b>	<b>0.0</b>	
2-A	17 cm	54 cm	88 cm		17 cm	54 cm	88 cm	
	<b>1.6</b>	<b>2.0</b>	<b>1.8</b>		<b>5.7</b>	<b>2.3</b>	<b>1.0</b>	
2-B	12 cm	40 cm	67 cm		12 cm	40 cm	67 cm	
	<b>2.4</b>	<b>5.0</b>	<b>6.3</b>		<b>4.2</b>	<b>3.3</b>	<b>1.4</b>	
2-C	12 cm	55 cm	95 cm		12 cm	55 cm	95 cm	
	<b>1.5</b>	<b>3.6</b>	<b>2.1</b>		<b>4.2</b>	<b>0.0</b>	<b>0.0</b>	
3-A	3.5 cm	9 cm	32.5 cm	49.5 cm	3.5 cm	9 cm	32.5 cm	49.5 cm
	<b>0.6</b>	<b>1.0</b>	<b>0.0</b>	<b>0.00</b>	<b>0.7</b>	<b>0.0</b>	<b>0.0</b>	<b>0.0</b>
3-B	5 cm	14 cm	40 cm	49.5 cm				
	<b>1.0</b>	<b>5.3</b>	<b>2.9</b>	<b>0.63</b>				
3-C	13 cm	26 cm	41 cm					
	<b>1.6</b>	<b>2.0</b>	<b>0.2</b>					

## 6.8 - GROUND HEAT FLUX ( $Q_G$ )

Soil heat flux is composed of three components including the sensible heat ( $Q_S$ ), latent heat ( $Q_L$ ) and heat flux at the base depth which is directed towards the permafrost table ( $Q_{GRAD}$ ). Table 6.9 summarizes the total  $Q_G$  at each site for the 1999 and 2000 study periods. Despite the fact that the 2000 study period was considerably shorter than that of 1999 (6-20 days and 45 days respectively) total  $Q_G$  was similar

**Table 6.9** - Site  $Q_G$  for 1999 and 2000 study periods. Asterisks represent sites for which  $Q_L$  is unaccounted for.

TRANSECT	SITE	1999	2000
		Total $Q_G$ for Study Period (MJ m <sup>-2</sup> )	Total $Q_G$ for Study Period (MJ m <sup>-2</sup> )
	Met Site	10.1	12.7
<b>Hillslope 1</b>	1-A	11.3	18.7
	1-B	33.1	28.2
	1-C	46.9	26.7
<b>Hillslope 2</b>	2-A	11.9 *	17.0 (n=6)
	2-B	22.8 *	33.3 (n=6)
	2-C	10.9 *	21.6 (n=6)
<b>Hillslope 3</b>	3-A	57.4	24.2 (n=6)
	3-B	92.8	0.0 (n=6)
	3-C	69.6	0.0 (n=6)

for both periods and, in some cases, exceeded 1999 totals. This is due in part to the rapid onset of spring melt and the large latent heat flux associated with active layer

development in the spring of 2000. At this time the thermal conductivity and the temperature of the near surface layers are large as reported by Woo and Xia (1996) due to increased ice content.

During both the 1999 and 2000 field seasons hillslope 1  $Q_G$  values increased downslope. This is similar to findings reported by Carey and Woo (2000). In their study, drier upslope locations had similar values of  $Q_G$  (150 MJ), wetter sites had intermediate values (200 MJ) whereas the permafrost-free sites at the slope base had fluxes approximately twice that of the driest upslope locations (250 MJ). Despite the fact that site 1-C, located at the bottom of hillslope 1, had permafrost, soil moisture contents were higher than at sites 1-A and 1-B resulting in greater thermal conductivity and therefore a deeper active layer causing greater volumes of water to reach the base. Hillslope 1 slope angle increases downslope which, although resulting in a relative decrease in  $Q^*$  at downslope sites, may promote heat transfer by lateral flow of water. This process has been observed in other studies (Rouse, 1984; Halliwell and Rouse, 1987; Hinzman et al., 1993; Carey and Woo, 2000) to increase active layer thickness at footslopes and promote preferential flow strips on slopes and in riparian zones.

Total  $Q_G$  values on hillslope 2 for the 1999 and 2000 study periods were greatest at the midslope location (site 2-B). Soil water contents at all three hillslope 2 sites were found to be very similar throughout the soil profile as well as overall slope gradients (within 4 degrees of each other). Compared to hillslopes 1 and 3, hillslope 2 had the greatest overall slope angle and the greatest seasonal  $Q^*$  due to its west-facing aspect. Although the latent heat term was not accounted for on hillslope 2 during the 1999 field season, 2000  $Q_G$  values indicate a similar trend to that of 1999 in which site 2-A has the

smallest  $Q_G$ , followed by sites 2-C and 2-B respectively.

Compared to hillslopes 1 and 2, hillslope 3 had the greatest  $Q_G$  values due in part to the increased heat capacity and soil water contents related to their peat dominated profiles. Once again,  $Q_G$  at the top of the hillslope was the smallest. However, similar to hillslope 2, the midslope site on hillslope 3 had the largest seasonal  $Q_G$  during the 1999 field season. Water content at site 3-B was notable higher compared to site 3-A resulting in increased hydraulic and thermal conductivity and the deepest active layer of the three hillslope sites. Due to this increased soil moisture and pre-melt ice content, latent heat energy released during the melt season is greater at site 3-B resulting in an increased seasonal value of  $Q_G$ .

In terms of the yearly  $Q_G$  balance Rouse (1984) found that latent heat flux accounts for 82% to 90% of the total ground heat flux depending on the surface and the season. Of the remaining sensible heat term, Rouse stated that 75% goes into heat exchange with the mineral soils and about 25% goes into heat exchange with soil water and ice components although it should be noted that this would depend on the proportion of ice. The present study allows for a more thorough analysis of seasonal trends in each of the  $Q_G$  components, specifically the late-summer (1999) and spring melt (2000) periods.

Illustrated in Figure 6.16 are the individual  $Q_G$  components expressed as a percentage of total  $Q_G$  for the 1999 study period. As discussed previously, hillslope 1  $Q_G$  values increased downslope corresponding with a similar increase in active layer development during the study period. As such,  $Q_G$  at site 1-A which had no change in

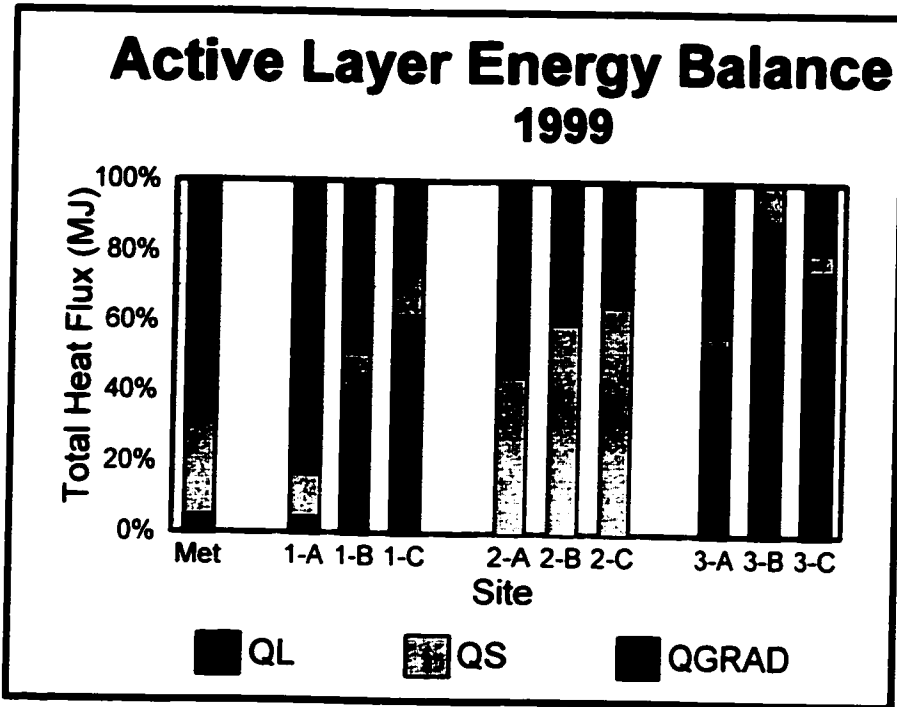


**Figure 6.16** - Active layer heat balance components expressed as percentage of total  $Q_G$  for the 1999 study period.  $Q_L$  for sites on hillslope 2 is not included.

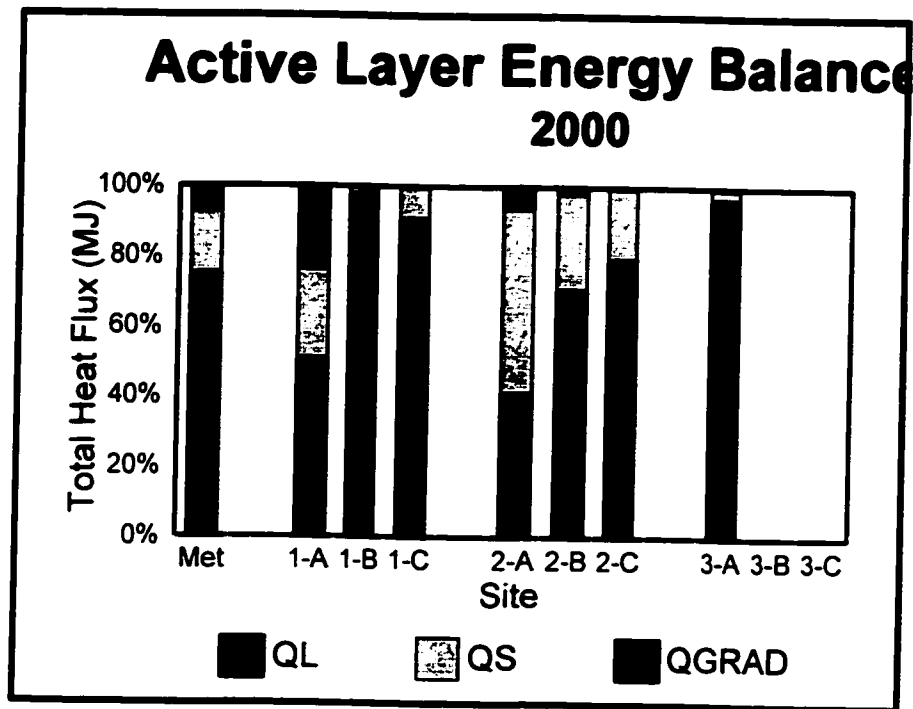


**Figure 6.17** - Active layer heat balance components expressed as percentage of total  $Q_G$  for the 2000 study period

active layer depth was very small, increasing downslope at sites 1-B and 1-C which experienced a 24.2 cm and 30.1 cm increase, respectively. Conversely,  $Q_{GRAD}$ , expressed as a percentage of  $Q_G$  decreased downslope while  $Q_S$  remained relatively similar at all three sites.

Although  $Q_L$  values for hillslope 2 were not recorded for the 1999 study period,  $Q_{GRAD}$  values decreased downslope similar to that of hillslope 1. The remaining component of the ground heat flux,  $Q_S$  increased slightly downslope. The ground heat flux for all sites on hillslope 3 are clearly dominated by the  $Q_L$  component. Specifically at site 3-B where  $Q_L$  accounts for over 89% of  $Q_G$ . The sensible heat component is much smaller on hillslope 3 than on other hillslopes accounting for less than 10% at all sites. At site 3-A,  $Q_{GRAD}$  accounts for 43% of total  $Q_G$ ; whereas it is a much smaller component at sites 3-B and 3-C accounting for 0% and 19%, respectively.

As illustrated in Figure 6.17, the 2000 study period, which coincided with the completion of snow melt and the initial stages of active layer development was dominated by the  $Q_L$  component of  $Q_G$ . Unlike the 1999 field season where the majority of active layer development had occurred prior to the measurement period, latent heat was the dominant component of  $Q_G$  at all sites. On hillslope 1,  $Q_L$  accounted for 51%, 98% and 92% of  $Q_G$  at sites 1-A, 1-B and 1-C, respectively. Of the remaining heat flux balance at site 1-A, 26% was composed of  $Q_S$  and 23% was accounted for by  $Q_{GRAD}$ . On hillslope 2 the relative proportion of  $Q_L$  was slightly smaller than that of hillslope 1 but increased downslope in a similar fashion. The sensible heat component of  $Q_G$  on hillslope 2 was more pronounced than on the other hillslopes accounting for 53%, 27% and 20% of  $Q_G$ .

for sites 2-A, 2-B and 2-C respectively. The remaining component,  $Q_{GRAD}$  was relatively insignificant at these sites. Finally,  $Q_L$  accounted for 97% of  $Q_i$  at site 3-A due in part to the high ice content of the peat at this site.

As illustrated by Figures 6.16 and 6.17 latent heat consumption is a significant component of the active layer heat balance which is a notable feature of permafrost soils (Woo and Xia, 1996). Ground ice content strongly controls active layer thawing depth as noted by Woo and Xia (1996). This is further exemplified through this study in comparing hillslope 3 which has a considerably higher soil water and ice content to hillslopes 1 and 2. Latent heat is large at the beginning of the thaw season during the period of rapid active layer development but is later reduced as ground thaw slows.

Halliwell and Rouse (1987) reported that there is little increase in sensible heat storage in the later part of the summer season and that virtually all energy is stored as latent heat or in the basal flux. Similarly, Woo and Xia (1996) stated that sensible heating of the active layer accounted for only 5% of  $Q_i$  at their polar desert study site on Cornwallis Island, N.W.T. during the snow free period. The present study indicates that  $Q_s$  is a more significant component of  $Q_i$ , specifically at sites where active layer depths are large such as those examined on hillslope 2 during both study periods. This is in agreement with Carey and Woo (2000) who found that sensible heating of the active layer accounted for less than 10% of  $Q_i$  with larger proportions for sites of deeper thaw and wetter conditions, which increased the soil heat capacity.

During the spring melt period basal flux ( $Q_{GRAD}$ ) is not an important component of the total ground heat flux. However, during July and August  $Q_{GRAD}$  represents a

significant proportion of  $Q_G$ . As indicated by Figure 6.16,  $Q_{GRAD}$  during the 1999 study period was found to account for 83% and 55% of  $Q_G$  at the top of hillslopes 1 and 2 but showed a decreasing trend downslope. Similar to findings reported by Woo and Xia (1996) daily fluctuations in  $Q_{GRAD}$  were not large but represented a considerable proportion of outgoing heat flux from the active layer to the permafrost below in both wet and dry study sites.

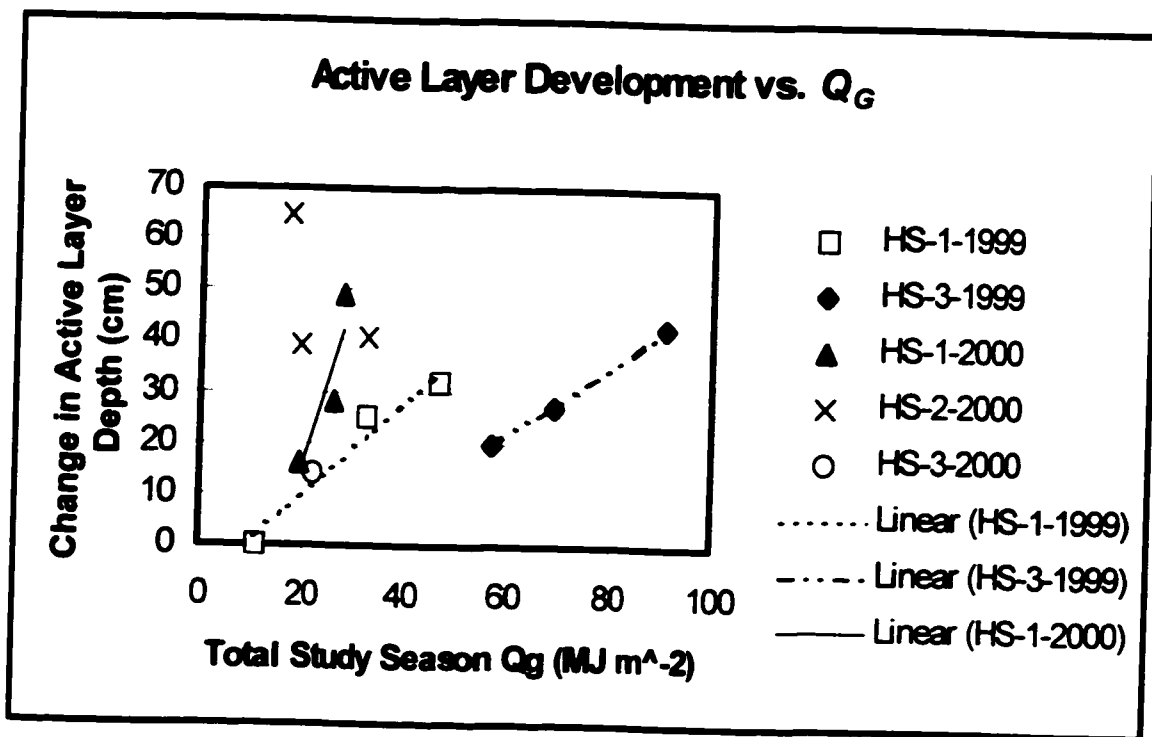


Figure 6.18 - Total active layer development as compared to total study season  $Q_G$ , for 1999 and 2000 study periods.

In comparing the total seasonal  $Q_G$  to the measured change in active layer development at each of the sites some significant relationships are evident with respect to

the amount of energy required to enhance ground thaw. As indicated by Figure 6.18, much more energy is required to thaw the active layer on hillslope 3 as compared to hillslopes 1 and 2 due primarily to the high water content and heat capacity of the overlying peat as discussed previously. Halliwell and Rouse (1987) suggested that such a positive relationship between soil moisture and  $Q_i$ , can be explained partly by elevated values of  $K_s$  that increase conduction in the soil profile. In comparing hillslope 3 to hillslopes 1 and 2 in Figure 6.18 it is evident that much less energy is required to thaw the latter two hillslopes. With the exception of hillslope 2 during the 2000 study period, a linear relationship exists between  $Q_i$  and total increase in active layer development for all hillslopes within the Kakawi Lake basin. Due to the short 2000 measurement period it is difficult to define a clear relationship between  $Q_i$  and active layer development for hillslope 2 aside from the fact that thaw rates were much more progressive on this hillslope with relatively small inputs of  $Q_i$ , as compared to hillslopes 1 and 3.

#### **6.9 - POTENTIAL SOURCES OF ERROR IN DETERMINATION OF $Q_G$**

Rouse (1984) suggested that the standard method of measuring soil heat flux using heat flux plates buried close to the surface can seriously underestimate  $Q_i$ , by as much as 50%. Therefore, in this study the calorimetric method was used to determine  $Q_i$ . As noted by Halliwell and Rouse (1987) this method is sensitive to accuracy of measurement of both soil temperature and water content. Due to the fact that average temperature gradients are much larger in the upper 10 cm of the soil profile as compared to the underlying soil previous studies have placed up to 5 temperature probes within this

portion of the soil. In the present study the thermal properties of the upper 10 cm were treated as a single layer which can lead to underestimation of notable temperature gradients that exist here. However, because the purpose of this study is to compare sites with varying thermal, vegetation, slope and aspect characteristics standardizing this practice between sites subjects each site to the same error thus allowing for reliable comparison of sites.

It was assumed in this study that significant active layer development did not commence prior to complete snow ablation. Due to the insulating properties of the snow pack it is possible that ground thaw did in fact begin prior to measurement in the 2000 study period which may lead to an overestimation of the latent heat component of  $Q_G$ , especially on hillslope 3.

Finally, in regressing sporadic soil temperature data to continuous measurements at the meteorological station some error is introduced in attempting to quantify diurnal fluctuations. Specifically, shallow measurements of soil temperature, when regressed against met data could result in overestimations or underestimations of daily  $Q_S$  at each of the sites. Many papers describe  $Q_G$  in terms of 10 day averages (Carey and Woo, 2000), or as seasonal averages (Rouse, 1984) to minimize uncertainties caused by short-term fluctuations in the sensible heat flux. Although such error may be present in this study an attempt was made to characterize fluctuations in  $Q_S$  on a diurnal basis. Study period totals of both  $Q_S$  and  $Q_G$  are much more accurate as measured soil temperatures at the start and end of each study period coincide very well with regressed data.

## CHAPTER 7 - SURFACE ENERGY BUDGET

Convection is the principal means of transporting daytime energy surplus of the surface away from the ground/air interface (Oke 1987). The availability of water for evaporation governs the relative importance of sensible ( $Q_H$ ) versus latent ( $Q_E$ ) heat. The ratio of these two fluxes is called Bowen's ratio ( $\beta$ ). When  $\beta$  is greater than unity ( $Q_H > Q_E$ ) heat is dissipated from the surface mostly in the form of sensible heat thus resulting in a warmer lower atmosphere. When  $\beta$  is less than unity ( $Q_H < Q_E$ ) heat energy to the atmosphere is mainly in the latent form thus increasing the humidity of the lower atmosphere. Negative  $\beta$  values indicate that  $Q_H$  and  $Q_E$  have different signs which commonly occurs at night when sensible heat fluxes are negative but evaporation continues causing a positive  $Q_E$  value (Oke 1987).

As illustrated in Figure 7.1, daily total sensible and latent heat fluxes varied considerably throughout the 40 day study period. Daily latent heat flux was generally

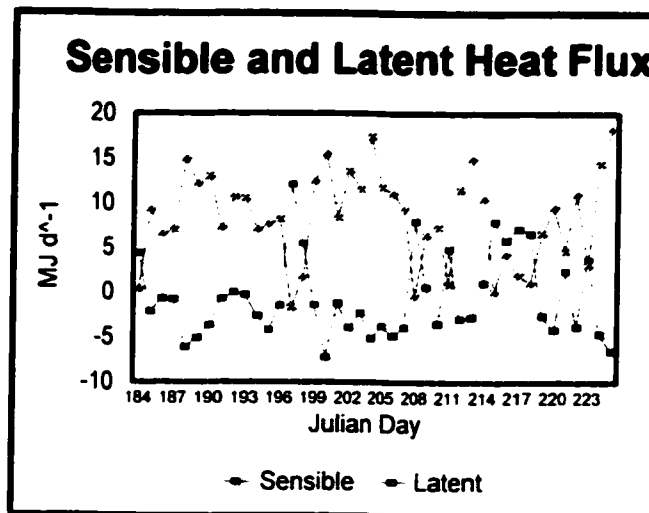


Figure 7.1 - Daily sensible and latent heat fluxes during 1999 study season.

greater than sensible heat flux, a relationship also noted by Lafleur et al. (1992) in a study conducted near Churchill, Manitoba (1992) during the summer months. Lafleur et al. (1992) noted that differences in energy balance were clearly in response to the drying cycle during July and August. During late June and early July, the latent heat term clearly dominates the tundra energy balance attributed to the fact that surface water was freely available at this site. As surface moisture became limiting in late July and into August, the authors noted that the tundra sensible and latent fluxes converged. This relationship is also illustrated in Figure 7.1, however it should be noted that although daily latent heat fluxes correspond with those reported with Lafleur et al. (1992), sensible heat fluxes are underestimated in this study. Daily sensible heat fluxes reported by Petrone et al., (2000), Lafleur et al., (1992), and Lynch et al. (1999) are positive which suggests error in calculation of sensible heat flux using the time-averaged flux-gradient approach used in the present study.

Lafleur et al. (1992) calculated the mean daily Bowen ratio in a tundra environment to be 0.63 and 0.46 for 1989 and 1990 respectively. With respect to summer Bowen ratios, Petrone et al. (2000) reported ranges of 0.2 - 0.3 for a central wetland site near Churchill, Manitoba, and 0.25 - 0.35 and 0.35 - 0.42 for a subarctic wetland and dry site respectively near Inuvik, N.W.T. The average daily Bowen ratio calculated using data presented in Figure 7.1 is 3.74 which is considerably higher than values reported in the literature. Possible sources of error in calculation of the Kakawi Lake energy balance in this study include location of the meteorological station and elevational position of temperature and relative humidity probes. Due to its location on the crest of the esker

surrounding the Kakawi Lake study basin, the meteorological station may have been subjected to wind and temperature trends indicative more of the greater Daring Lake area as opposed to isolated basin effects. As well, dominant north-westerly wind patterns may have been exaggerated upon upward shifts from the surface of Kakawi Lake to the top of the esker due to the steep gradient of the 30 m slope.

Another possible source of error in calculation of the energy balance is in relation to the difference of 1.67 m between temperature and relative humidity probes. This elevational difference may not have been great enough to accurately estimate surface fluxes at the meteorological station. It must also be emphasized that when, as in this study, only two levels are used to calculate the surface energy balance, a straight line profile is calculated which provides, at best, an estimate of the sensible and latent heat fluxes. A meteorological station with multiple sensor levels is required to more accurately quantify vertical fluxes in sensible and latent heat energy from the surface.

## CHAPTER 8 - HYDROLOGY

### 8.1 - HYDROLOGICAL PARAMETERS

Rainfall for the 1999 field season totalled 36.8 mm, most of which fell during the two major precipitation events of the study period. The Kakawi Lake level declined consistently during this time with a slight increase on JD 204 as a result of the second major precipitation event (Figure 8.1). In total, the Kakawi Lake level dropped 0.103 m during the 1999 field season.

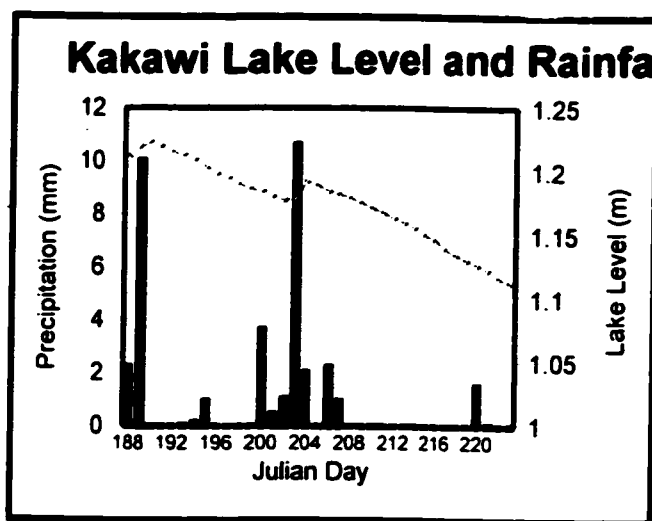


Figure 8.1 - Daily lake level fluctuation and precipitation total for the 1999 study period.

In comparison with sporadic rainfall input to the Kakawi Lake basin during the 1999 field season, outflow remained relatively constant with a slight increase as a result of the second major precipitation event (Figure 8.2). In total, outflow as measured at the discharge weir was 40806 m<sup>3</sup> during the 36 day study period. The Kakawi Lake water mass balance was determined using the relationship:

$$E = P + I - O - \Delta S \quad (19)$$

where  $E$  = volume of lake evaporation

$P$  = total volume of precipitation falling on the lake; 1156 m<sup>3</sup>

$I$  = volume of lateral surface and subsurface inflow

$O$  = volume of surface and subsurface outflow; 40806 m<sup>3</sup>

$\Delta S$  = volumetric change in lake storage; 3142 m<sup>3</sup>

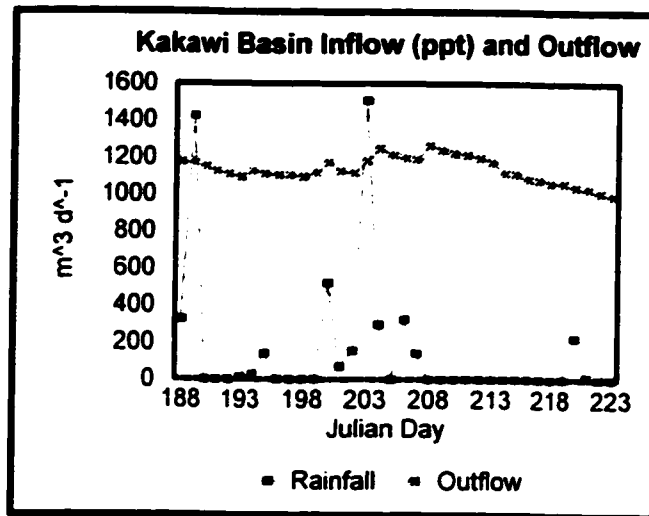


Figure 8.2 - Kakawi Lake basin daily inflow and outflow during the 1999 study period.

Gibson et al. (1996) used three experimental methods to calculate evaporation from a small lake with surface area of 4 ha and a catchment area of 27 ha on the west shore of Contwoyto Lake 100 km north of the Kakawi Lake basin study site. Calculated evaporation for 1992 (54 d) and 1993 (71 d) study periods was 181 mm and 180 mm respectively using the mass balance method. Although lake evaporation was not measured at the Kakawi Lake study basin due to the similar lake size, location and landscape, values from Gibson et al. (1996) may be used to estimate the water mass balance using equation 19. To do this, the average length of the two study periods and the average evaporation (62.5 d and 180.5 mm respectively) were pro-rated to a 36 day

study period corresponding to the present study. This value was calculated to be 104 mm or 3384 m<sup>3</sup> of evaporation for Kakawi Lake.

Substituting known values of  $P$ ,  $O$ , and  $\Delta S$  into equation 19, the remaining components of the water balance are expressed as:

$$E = I - 42792 \text{ m}^3 \quad (20)$$

Furthermore, substituting an estimated evaporation rate of 104 mm (3384 m<sup>3</sup>) from Gibson et al. (1996) results in a residual value of 39892 m<sup>3</sup> for  $I$ . This value is considerably larger than those reported by Gibson et al. (1996) in which the authors found lateral inflow from the catchment area to be negligible. They considered this to result from unsaturated conditions in the hillslope active layer which allowed recharge of incident precipitation and due to high roughness of the frost table which caused active-layer melting to be largely detained in isolated pockets on the hillslope or released by evaporation through the unsaturated zone. Although evaporation rates may have varied slightly for the Kakawi Lake basin compared to estimated values from the literature, this would not significantly alter the magnitude of  $I$  in the water balance equation. In addition, discharge from the Kakawi Lake study basin was most likely underestimated due to subsurface flow which would cause a subsequent increase in  $I$  using methods outlined above.

Water table depths were measured throughout the 1999 field on hillslope 3 as illustrated in Figure 8.3. At each of the three sites, water wells were installed in the middle of the site perpendicular to the hillslope transect where peat depths were the

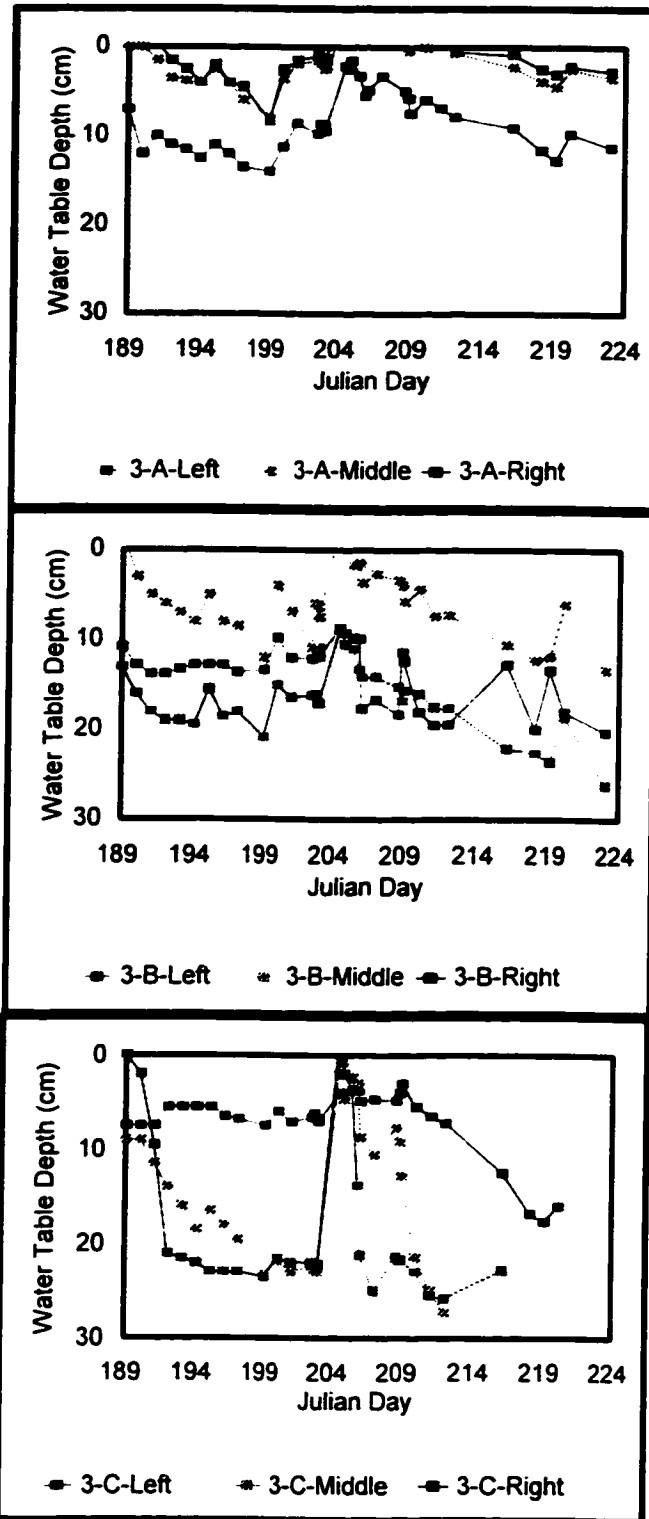


Figure 8.3 - Water level depths at sites 3-A, 3-B and 3-C for 1999 study period.

greatest, as well as on both sides of the perpendicular transect (i.e. left and right sides; facing upslope). In general, water table depths were the highest at site 3-A and were deeper downslope at sites 3-B and 3-C. As well, water table response to rainfall events was least pronounced at sites 3-A whereas sites 3-B and 3-C illustrated greater response respectively to the rainfall event on JD 204 due to their deeper water level antecedent condition. Figure 8.3 indicates that a significant amount of water was stored at site 3-A throughout the 1999 study period.

Upon initiation of a rainfall event, water table depth at site 3-A rises above the surface thus producing surface flow which flows downslope to sites 3-B and 3-C causing a more dramatic increase in water table depth at downslope sites. This is similar to findings reported by Quinton and Marsh (1998) who noted two distinct hydrological phases in patterned wetlands. The first occurs when water losses through seepage and evaporation leads to disconnection of wetland pools into separate microcatchments. The second, as illustrated in Figure 8.3 (JD 204), occurs when water input from rainfall and adjacent nonwetland portions of the basin causes storage capacity to be exceeded. Under such conditions, the wetland drains as a single source area and, as a result, discharge from this area is relatively high.

## **8.2 - HILLSLOPE CONTRIBUTION**

In order to determine the amount of water that hillslopes can conduct within the Kakawi Lake study basin the hydraulic conductivities ( $K$ ) of the subsurface materials must be known. Some commonly cited  $K$  values are listed in Table 8.1. Slug tests

performed on piezometers driven into lake bottom sediment situated at the bottom of hillslopes 1 and 2 and at the berm indicated that *in situ* hydraulic conductivities were very high due to the almost instantaneous recovery of the hydraulic head. A slug test performed on the piezometer located at site 3-B within peat material resulted in a measured *in situ*  $K$  value of  $0.045 \text{ cm s}^{-1}$  ( $4 \times 10^{-2} \text{ cm s}^{-1}$ ) which falls in higher end of the range of  $K$  suggested by Dingman (1993) for peat of  $10^{-4}$  to  $10^{-2} \text{ cm s}^{-1}$ .

Using Darcy's Law the total discharge from a hillslope transect can be defined as:

$$Q = K i a \quad (21)$$

where:  $Q$  = discharge ( $\text{cm}^3 \text{ s}^{-1}$ )

$K$  = hydraulic conductivity ( $\text{cm s}^{-1}$ )

$i$  = gradient

$a$  = area of discharge (saturated thickness \* perimeter length)

Based on hillslope gradient and soil physical characteristics the Kakawi Lake basin was divided into four areas in order to determine theoretical subsurface discharges from each (Figure 8.4). These areas correspond with the north-, south-, west- and east-facing sections of the basin with lake edge perimeters of 200 m, 300 m, 200 m and 300 m respectively. Average gradients determined from survey and GIS analysis are 0.20, 0.08, 0.28 and 0.12 for the corresponding hillslope areas. In order to determine if hillslope discharge could theoretically deliver the amount of water calculated using the mass water balance, a range of hydraulic conductivities and water table depths were used to determine discharge for each hillslope area over the 36 day study period.

**Table 8.1 - Ranges of values of Hydraulic Conductivity**

<b>Sediment</b>	<b>Hydraulic Conductivity (K) (cm s<sup>-1</sup>)</b>	<b>Reference</b>
Clay	10 <sup>-9</sup> - 10 <sup>-6</sup> 10 <sup>-5</sup> - 10 <sup>-4</sup> 10 <sup>-10</sup> - 10 <sup>-7</sup>	Sanders (1998) Dingman (1993) Freeze and Cherry (1979)
Glacial Till	10 <sup>-10</sup> - 10 <sup>-4</sup>	Freeze and Cherry (1979)
Silt. Loam. Loess	10 <sup>-7</sup> - 10 <sup>-3</sup> 10 <sup>-5</sup> - 10 <sup>-3</sup> 10 <sup>-7</sup> - 10 <sup>-3</sup>	Sanders (1998) Dingman (1993) Freeze and Cherry (1979)
Fine Sand	10 <sup>-5</sup> - 10 <sup>-3</sup> 10 <sup>-4</sup> - 10 <sup>-2</sup> 10 <sup>-3</sup> - 1	Sanders (1998) Dingman (1993) Freeze and Cherry (1979)
Coarse Sand	10 <sup>-3</sup> - 10 <sup>-1</sup> 10 <sup>-3</sup> - 10	Sanders (1998) Dingman (1993)
Peat	10 <sup>-4</sup> - 10 <sup>-2</sup>	Dingman (1993)
Gravel	10 <sup>-2</sup> - 10 <sup>2</sup> 10 <sup>-2</sup> - 10 10 <sup>-1</sup> - 10 <sup>2</sup>	Sanders (1998) Dingman (1993) Freeze and Cherry (1979)

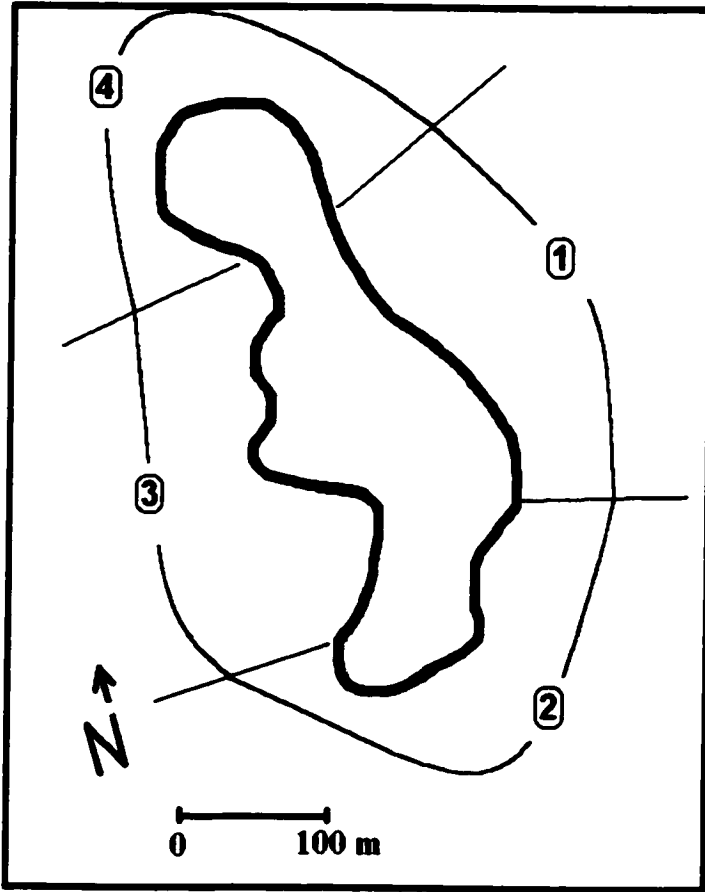


Figure 8.4 - Hillslope areas used in calculation of subsurface discharge

**Table 8.2 - Hillslope discharge calculated using varying groundwater table depths (GWT)**

Area	GWT (m)	Grad	K (ms <sup>-1</sup> )	Q (m <sup>3</sup> )	K (ms <sup>-1</sup> )	Q (m <sup>3</sup> )	K (ms <sup>-1</sup> )	Q (m <sup>3</sup> )	K (ms <sup>-1</sup> )	Q (m <sup>3</sup> )
1	0.35	0.28	10 <sup>-12</sup>	0	10 <sup>-10</sup>	0	10 <sup>-8</sup>	6	10 <sup>-6</sup>	609
2	0.35	0.20	10 <sup>-12</sup>	0	10 <sup>-10</sup>	0	10 <sup>-8</sup>	4	10 <sup>-6</sup>	436
3	0.35	0.12	10 <sup>-7</sup>	39	10 <sup>-6</sup>	392	10 <sup>-5</sup>	3919	10 <sup>-4</sup>	39191
4	0.35	0.08	10 <sup>-6</sup>	261	10 <sup>-5</sup>	2612	10 <sup>-4</sup>	26127	10 <sup>-3</sup>	261273
1	0.20	0.28	10 <sup>-12</sup>	0	10 <sup>-10</sup>	0	10 <sup>-8</sup>	3	10 <sup>-6</sup>	348
2	0.20	0.20	10 <sup>-12</sup>	0	10 <sup>-10</sup>	0	10 <sup>-8</sup>	2	10 <sup>-6</sup>	248
3	0.20	0.12	10 <sup>-7</sup>	22	10 <sup>-6</sup>	223	10 <sup>-5</sup>	2239	10 <sup>-4</sup>	22394
4	0.20	0.08	10 <sup>-6</sup>	149	10 <sup>-5</sup>	1493	10 <sup>-4</sup>	14929	10 <sup>-3</sup>	149299
1	0.05	0.28	10 <sup>-12</sup>	0	10 <sup>-10</sup>	0	10 <sup>-8</sup>	1	10 <sup>-6</sup>	87
2	0.05	0.20	10 <sup>-12</sup>	0	10 <sup>-10</sup>	0	10 <sup>-8</sup>	1	10 <sup>-6</sup>	62
3	0.05	0.12	10 <sup>-7</sup>	5	10 <sup>-6</sup>	56	10 <sup>-5</sup>	559	10 <sup>-4</sup>	5598
4	0.05	0.08	10 <sup>-6</sup>	37	10 <sup>-5</sup>	373	10 <sup>-4</sup>	3732	10 <sup>-3</sup>	37324

**Table 8.3 - Hillslope discharge calculated using varying gradients**

Area	GWT (m)	Grad	K (ms <sup>-1</sup> )	Q (m <sup>3</sup> )	K (ms <sup>-1</sup> )	Q (m <sup>3</sup> )	K (ms <sup>-1</sup> )	Q (m <sup>3</sup> )	K (ms <sup>-1</sup> )	Q (m <sup>3</sup> )
1	0.35	0.33	10 <sup>-12</sup>	0	10 <sup>-10</sup>	0	10 <sup>-8</sup>	7	10 <sup>-6</sup>	718
2	0.35	0.25	10 <sup>-12</sup>	0	10 <sup>-10</sup>	0	10 <sup>-8</sup>	5	10 <sup>-6</sup>	544
3	0.35	0.17	10 <sup>-7</sup>	55	10 <sup>-6</sup>	555	10 <sup>-5</sup>	5552	10 <sup>-4</sup>	55520
4	0.35	0.13	10 <sup>-6</sup>	424	10 <sup>-5</sup>	4245	10 <sup>-4</sup>	42457	10 <sup>-3</sup>	424569
1	0.35	0.28	10 <sup>-12</sup>	0	10 <sup>-10</sup>	0	10 <sup>-8</sup>	6	10 <sup>-6</sup>	609
2	0.35	0.20	10 <sup>-12</sup>	0	10 <sup>-10</sup>	0	10 <sup>-8</sup>	4	10 <sup>-6</sup>	436
3	0.35	0.12	10 <sup>-7</sup>	39	10 <sup>-6</sup>	392	10 <sup>-5</sup>	3919	10 <sup>-4</sup>	39191
4	0.35	0.08	10 <sup>-6</sup>	261	10 <sup>-5</sup>	2612	10 <sup>-4</sup>	26127	10 <sup>-3</sup>	261273
1	0.35	0.23	10 <sup>-12</sup>	0	10 <sup>-10</sup>	0	10 <sup>-8</sup>	5	10 <sup>-6</sup>	500
2	0.35	0.15	10 <sup>-12</sup>	0	10 <sup>-10</sup>	0	10 <sup>-8</sup>	3	10 <sup>-6</sup>	326
3	0.35	0.07	10 <sup>-7</sup>	22	10 <sup>-6</sup>	228	10 <sup>-5</sup>	2286	10 <sup>-4</sup>	22861
4	0.35	0.03	10 <sup>-6</sup>	98	10 <sup>-5</sup>	979	10 <sup>-4</sup>	9797	10 <sup>-3</sup>	97977

As illustrated in Table 8.2 an increase by one order of magnitude in  $K$  results in a similar increase in total subsurface discharge from the hillslope base. Using four  $K$  values representing average and extreme values based on published ranges for each hillslope soil type, total discharge for the 36 day study period was determined for each of the 4 areas as indicated by the bold values. Water table depth was also altered in Table 8.2 as indicated by the italicized values in the second column (GWT). As with  $K$ , a decrease in depth of saturated zone results in a related decrease in total subsurface discharge at the hillslope base. Table 8.3 illustrates the effect of varying hillslope gradient on total subsurface discharge using the same range of  $K$  values as in Table 8.2 to allow for comparison. Similarly, a decrease in gradient results in an overall decrease in subsurface discharge.

As previously discussed, the  $I$  component of the water mass balance accounted for 39892 m<sup>3</sup>, or slightly less than total discharge for the 36 day study period. As indicated by Table 8.2 and Table 8.3 subsurface discharges from the hillslopes into the lake of this magnitude are possible, especially when using  $K$  values at the higher end of published ranges. It should be noted however that area 4, or the berm area, does not contribute a significant amount of hillslope subsurface water to the lake due to the fact that the gradient is greater between the berm and the discharge area at the outflow of the basin than the berm to lake gradient. The saturated soil depth measured at hillslope 3 remained approximately 0.35 m in depth and thus is used as the upper end of the range of GWT depths used in this discussion. Although water table depths were not determined on the other hillslopes depths of 0.20 m and 0.05 m are used to quantify the effect that depth of the saturated area has on total hillslope subsurface discharge. These depths are more

indicative of the drier conditions associated with hillslopes 1 and 2 which have lower water table depths than those recorded on hillslope 3.

Although Table 8.2 and Table 8.3 indicate that it is possible for subsurface inflow to Kakawi Lake to exceed 40000 m<sup>3</sup> it must also be determined if the berm separating the lake and the discharge stream can also conduct subsurface flows of this magnitude.

Figure 8.5 illustrates the difference in elevation between the top of the berm, the lake level and the discharge stream.

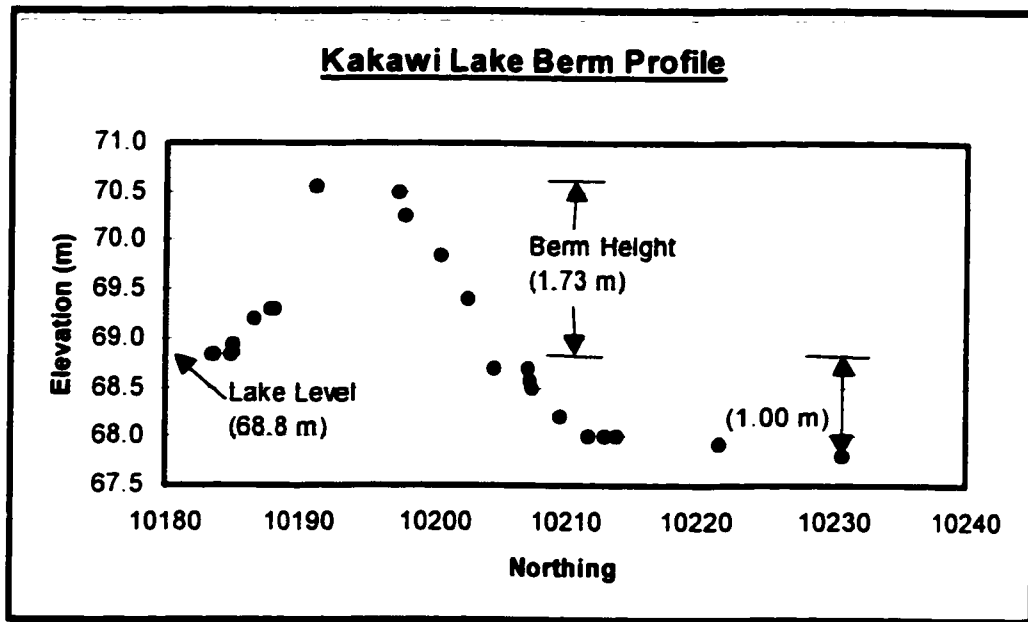


Figure 8.5 - Kakawi Lake discharge berm elevation profile.

Due to the fact that  $Q$  and  $i$  have been measured (40806 m<sup>3</sup> and 0.05 respectively),  $a$  can be altered to represent both a deep and shallow water table thus allowing for the calculation of  $K$  through the berm profile. With a berm length of 90 m, water tables of 0.30 m and 0.05 m were used to calculate  $a$  values of 27.0 m<sup>2</sup> and 4.5 m<sup>2</sup> respectively for subsequent use in equation 20. As such, with water tables of 0.30 m and

0.05 m,  $K$  for the discharge berm was calculated to be  $0.10 \text{ cm s}^{-1}$  and  $0.60 \text{ cm s}^{-1}$ . These values fall into a range of  $10^{-2}$  to  $10^{-1} \text{ cm s}^{-1}$  which corresponds with the range of values reported in Table 8.1 for coarse sand which is the dominant sediment that the berm is composed of.

As previously noted, average yearly precipitation in the Daring Lake area is approximately 300 mm. Therefore, the 14 ha Kakawi Lake basin receives approximately  $42000 \text{ m}^3$  of precipitation per year. This value corresponds closely with the calculated  $I$  value of  $39892 \text{ m}^3$  from the terrestrial basin. Therefore, hillslope subsurface flow along the permafrost table and into the lake in the Kakawi Lake study basin is the most significant component of the hydrological balance during the summer months. Although the lake level dropped only 0.103 m during the 1999 field season, this is not indicative of the total amount of water that moved through this system during this time. Significant snowfall accumulation within the Kakawi Lake basin and subsequent ablation and percolation into the soil matrix accounts for the majority of the input to the water balance. This soil water is transported at depth along the permafrost table over time accounting for a sustained lake level and daily discharge despite minimal inputs into the system in the form of rainfall.

Quinton and Marsh (1999) concluded in their study in the tundra region of the Canadian western arctic that subsurface flow is the dominant mechanism of runoff to the stream channel. They noted that most flow is conveyed through the peat of inter-hummock channels and that subsurface flow through peat and soil pipes can be as rapid as surface flow. Such processes were evident on hillslope 3 in the present study due to

the presence of visible surface flow in inter-hummock areas and in surface pools underlain by peat. Similar to hillslopes 1 and 2 in the Kakawi Lake study basin, Carey and Woo (1999) noted that in summer, the non-transpiring lichens and mosses curtail evapotranspiration rates and that subsurface flow in the organic layer offers an efficient mechanism for water delivery downslope. Carey and Woo (1999) also identified two flow systems which developed: (1) quick-flow along soil pipes and rapid matrix flow in the organic layer, and (2) slow-flow in the mineral soil below, controlled by its very low hydraulic conductivity and a changing thaw depth in the active layer. Furthermore, the authors noted in their study of two slopes in subarctic Yukon that non-permafrost slopes do not contribute baseflow to the receiving stream and that runoff source area is confined to the permafrost slopes.

Similar to findings reported in the present study, Boudreau and Rouse (1995) noted that slow release of water from the groundwater reservoir and thawing soil sustain streamflow during dry conditions. The authors also note that change in groundwater storage is the most difficult term of the water balance to quantify. The calculation of the change in storage for individual terrain types varies considerably due to very different groundwater hydrologies, and radiation and energy balances. However, as is the case for hillslopes 1 and 2, Boudreau and Rouse (1995) found that ridges lose their groundwater most rapidly in discharge to adjacent wetlands causing ridges to have the greatest range of water table depths and the lowest soil moisture. In contrast, the water table fluctuated the least in the sedge wetlands, which displayed the highest soil moisture storage with only a small seasonal range and great spatial uniformity.

---

---

## CHAPTER 9 - CONCLUSIONS

---

---

### 9.1 CONCLUSIONS

This research provides a detailed field study of the radiation, ground energy, and hydrological balances of an arctic esker basin. With respect to the radiation balance, incoming short-wave radiation is the main variable accounting for differences in net radiation amongst the nine study sites in the Kakawi Lake Basin. Although incoming shortwave radiation is primarily responsible for diurnal fluctuations in the net radiation balance on a daily and seasonal basis, as illustrated in this study it represents substantially less than one half (41%) of the radiative supply to the surface. Albedo measurements taken over various surfaces varied little between the different vegetation cover types and did not change diurnally or seasonally.

Throughout the summer season active layer depths on hillslope 1 were the greatest at the mid-slope site and smallest upslope with the bottom of the slope falling in the middle of the two. Overall active layer depths were greatest on hillslope 2 and shallowest on hillslope 3 owing to the increased solar radiation receipt of the west-facing slope and the insulative properties of the overlying peat, respectively. During the 2000 study period, active layer development on hillslopes 1 and 2 began first at the upslope site followed by the bottom site coinciding with beginning of the snow-free period at each. Initiation of active layer development was delayed on both hillslopes at the mid-slope site, but at the end of the study period was the largest compared of both hillslope transects.

Ground heat flux increased downslope on hillslopes 1 and 2 corresponding with a similar increase in active layer development during the summer season. Conversely, basal flux out of the active layer to the underlying permafrost decreased downslope. The sensible heat flux varied the least with depth and between the study sites but accounted for a significant proportion of the ground flux, specifically at sites where active layer depths are large. During the 1999 study period the average active layer depth on hillslope transect 3, dominated by peat and a high water content, was only 59% of the average active layer depth on hillslope 1. This is due to the fact that soils in poorly drained sites such as those on hillslope 3 are often rich in ice which decreases the thermal conductivity of the substrate and consequently retards the development of the active layer.

Latent heat is largest at the beginning of the thaw season when there is rapid active layer development but is later reduced as ground thaw slackens. In the Kakawi Lake Basin total latent heat flux for the 2000 field season was nearly the same as 1999 and in some cases exceeded the 1999 measurements despite the fact that the later period was 25 days longer. During the spring melt period basal flux is not a significant component of the total ground heat flux. However, during July and August it represents a considerable proportion of the total ground heat flux. During the 1999 study period basal flux was found to account for 83% and 55% of the total ground heat flux at the top of hillslopes 1 and 2 but showed a decreasing trend downslope.

With respect to the surface energy balance, daily total sensible and latent heat fluxes varied considerably throughout the 40 day study period as measured at the Laurier meteorological station. Daily latent heat flux was generally greater than sensible heat

flux however the fluxes converged in late July and into early August corresponding with the drying cycle during this time. During late June and early July, the latent heat term clearly dominates the tundra energy balance attributed to the fact that surface water was freely available at this site. As surface moisture became limiting in late July and into August, the sensible and latent fluxes converged. However, underestimations of sensible heat flux using the time-averaged flux-gradient approach lead to subsequent errors in determination of daily and seasonal Bowen ratios for the Kakawi Lake Basin.

In terms of the Kakawi Lake Basin hydrological balance, lateral inflows from hillslopes were estimated to be only 2% less than the total outflow from the basin during the 1999 study season. Hillslope subsurface flow along the permafrost table and into the lake in the Kakawi Lake study basin is the most significant component of the hydrological balance during the summer months. Although the lake level dropped only 0.103 m during the 1999 field season, this is not indicative of the total amount of water that moved through this system during this time. Significant snowfall accumulation within the Kakawi Lake basin and subsequent ablation and percolation into the soil matrix accounts for the majority of the input to the water balance. This soil water is transported at depth along the permafrost table over time accounting for a sustained lake level and daily discharge despite minimal inputs into the system in the form of rainfall.

In general, incoming shortwave radiation receipt at the surface is the most important controlling factor on active layer development in the Kakawi Lake Basin. Although surface cover type has little effect on the ground thermal regime, soil physical properties, especially those associated with peat, affect the rate at which heat energy is

transported through the soil profile to the underlying permafrost table. Soil water and ice content also have notable control on the rate at which the active layer develops during the snow-free season. Results reported in this study expand the current knowledge base of hydrological and energy balance processes in arctic tundra environments to regions in which eskers and related till material are predominant.

Previous studies conducted in permafrost dominated areas including Churchill, Manitoba (Boudreau and Rouse, 1995), Contwoyto Lake, NWT (Gibson et al., 1996, Gibson, 2001), and subarctic Yukon (Carey and Woo, 1999; Carey and Woo, 2001) have reported that hillslope inflows account for a minor portion of the basin hydrological balance. Findings reported in this paper, however, state the importance of hillslope inflows to the basin hydrological balance in areas dominated by eskers and esker related surficial material. Hillslope flow processes induced by snowmelt and heat conducted through the soil profile have subsequent effects on active layer development on hillslope sites. This is highlighted in the present study by the fact that midslope locations have greater active layer depths compared to upper and lower slope sites due to conduction of soil water downslope. Despite minimal precipitation input and evaporation through the summer season, lake water levels and outflows are sustained due to the significant input from basin hillslopes.

Research conducted in the Kakawi Lake basin provides important insight into the possible effects that global climate change could have on arctic environments. West-facing slopes, which receive increased amounts of incoming shortwave radiation as compared to north- and east-facing slopes, experience meteorological conditions

representative of a warmer climate. As well, hillslope processes noted on north-facing slopes, due to their increased receipt of snowfall accumulation, could also be considered representative of some of the effects associated with a warmer climate. As well as forecasting increasing snowfall in the order of 50% to 100%, and increased mean annual temperatures of 3°C to 8°C, global circulation models (GCMs) also predict that evapotranspiration will increase and runoff will decrease (IPCC, 1996). Continued research at the Kakawi Lake Basin scale of study as well at the larger Daring Lake Basin is essential in order to identify spatial and temporal variations in hydrological and energy balance processes and to quantify subsequent changes related to anthropogenic and climate induced disturbance.

## **9.2 - FUTURE RESEARCH**

There are a number of areas in which future research could be directed in building on information gathered at the Kakawi Lake Study Basin. Within the study basin, more thorough field measurement of hillslope flow processes and lake evaporation could help to accurately quantify the basin hydrological balance during the entire ice free period. As well, the addition of instrumentation measuring sensible and latent energy at the Daring Lake meteorological station and the use of portable measuring devices would assist in our understanding of spatial and temporal variations in surface energy balance fluxes.

Results reported in this thesis are also an important foundation necessary for understanding hydrological and energy balance processes at the larger Daring Lake Basin scale of study. Comparison of trends noted here with respect to slope, aspect, vegetation,

and hydrological effects on active layer development with other sub-basins would improve our knowledge of active layer dynamics and the large scale factors that control such processes.

Finally, another important area of research in undisturbed arctic tundra areas such as Daring Lake relates to linking our knowledge of hydrological and energy balance processes with sediment provision and groundwater and surface water chemistry. Such work is essential to quantifying the effects of climate change and anthropogenic induced change associated with mining development to the natural landscape of Canada's Arctic.

## **APPENDIX - A**

Soil temperature regression equations for 1999 and 2000 study periods  
`Therm` - site location and depth (cm)  
`Met` - depth of thermistor at met site (cm) thermistor regressed against

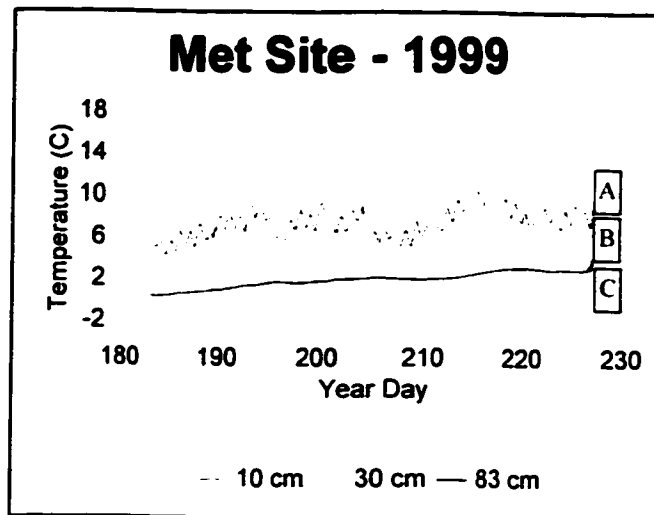
### THERMISTOR REGRESSION EQUATIONS

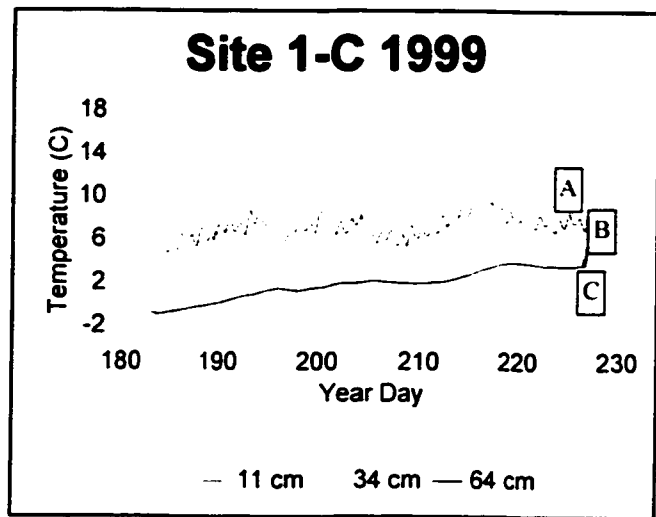
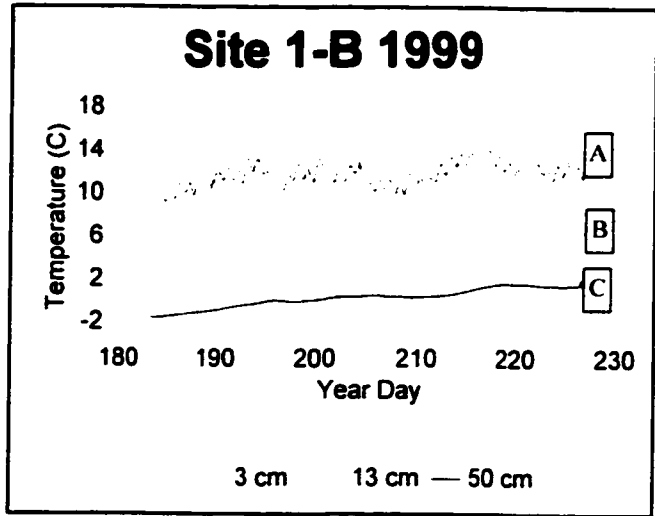
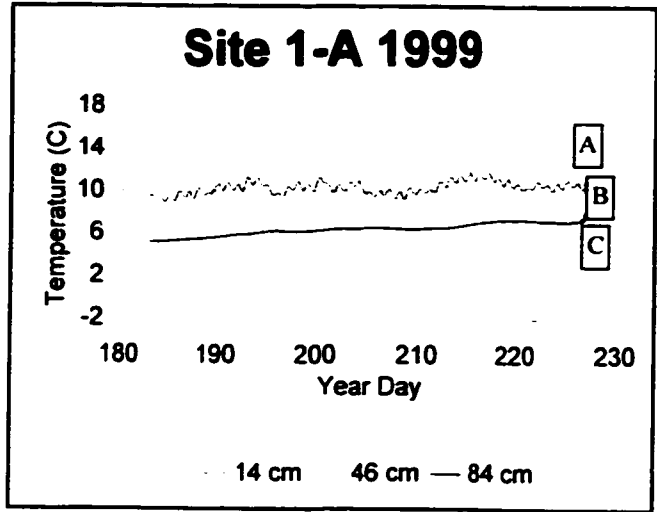
<u>THERM</u>	<u>MET</u>	<u>R2</u>	<u>1999 REGRESSIONS</u>	<u>MET</u>	<u>R2</u>	<u>2000 REGRESSIONS</u>
1-A-14	10	0.48	y= 6.843672+0.473386x	30	0.91	y= -2.06792+2.1384x
1-A-46	30	0.23	y= 6.497714+0.591916x	30	0.94	y= 2.657217+2.88519x
1-A-84	83	0.76	y= 4.846682+0.787858x	30	0.93	y= 2.65195+17.49402x
1-B-3	30	0.66	y= -1.47060+0.26825x	10	0.36	y= -0.82838+-0.01627x
1-B-13	30	0.55	y= 6.957395+0.422564x	10	0.50	y= -1.5029+0.802983x
1-B-50	83	0.93	y= 1.660718+0.755063x	30	0.28	y= -1.57727+0.62396x
1-C-11	10	0.69	y= 1.39612+0.773722x	10	0.61	y= -1.55908+1.202161x
1-C-34	30	0.51	y= -0.63378+1.087382x	30	0.69	y= -0.83497+0.303574x
1-C-64	83	0.97	y= -1.61168+1.720227x	30	0.06	y= -0.0066+0.909419x
2-A-17	10	0.63	y= 6.638206+0.904112x	10	0.87	y= -6.70165+3.638927x
2-A-54	83	0.72	y= 8.713173+1.364941x	30	0.82	y= -1.3054+3.160977x
2-A-88	83	0.70	y= 6.809296+1.307056x	30	0.60	y= 1.391459+16.8875x
2-B-12	30	0.76	y= 0.663499+1.988973x	30	0.85	y= -6.88998+2.326491x
2-B-40	83	0.91	y= 2.335869+3.511242x	83	0.89	y= -5.32192+4.616118x
2-B-67	83	0.89	y= -1.76482+4.432475x	83	0.61	y= -0.08629+70.38902x
2-C-12	10	0.71	y= 5.432942+0.937261x	30	0.74	y= -11.3826+2.86785x
2-C-55	83	0.86	y= 6.188552+1.538518x	30	0.18	y= 0.08043+0.02558x
2-C-95	83	0.24	y=6.094914+0.924578x	83	0.06	y= 1.72367+1.254735x
3-A-3.5	10	0.52	y= -0.64328+1.197159x	10	0.62	y= -6.51135+1.674394x
3-A-9	10	0.44	y= -2.27258+0.807352x	10	0.05	y= -0.2333+-0.05053x
3-A-37.5	10	0.05	y= 1.166525+-0.2655x	30	0.06	y=0.154866+-0.18905x
3-A-49.5	83	0.74	y= -0.99599+0.201397x	30	0.57	y=12.54762+-6.45821x
3-B-5	10	0.48	y= 0.44869+1.2658x			
3-B-14	30	0.73	y= -9.41371+2.476759x			
3-B-40	83	0.91	y= -2.57587+2.418397x			
3-B-48.5	83	0.87	y= -2.5115+2.427513x			
3-C-13	30	0.77	y= -0.79972+1.004116x			
3-C-26	30	0.27	y= -2.00851+1.134749x			
3-C-47	10	0.08	y= 0.07104+0.386751x			

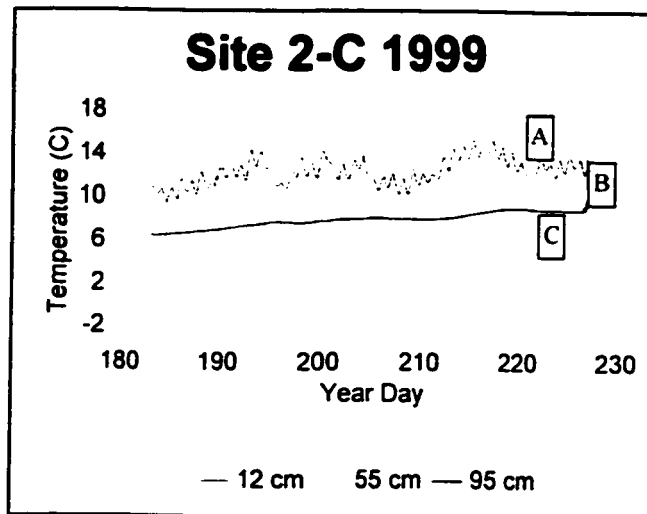
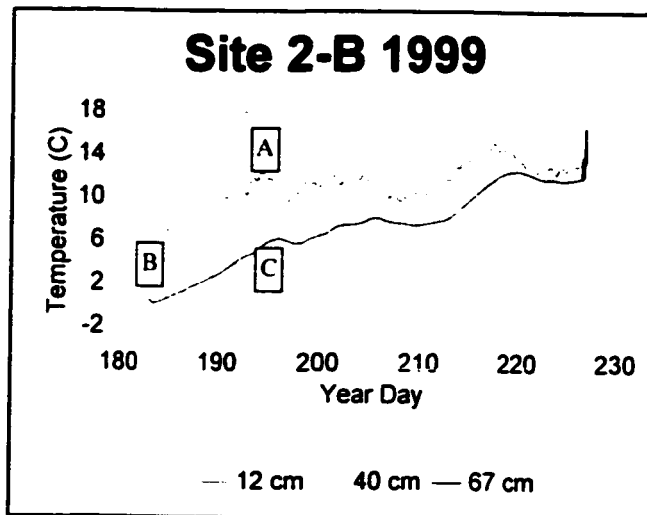
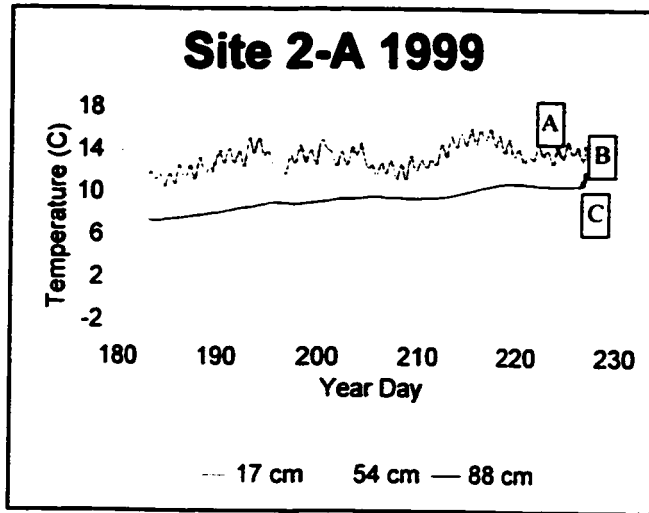
## APPENDIX - B

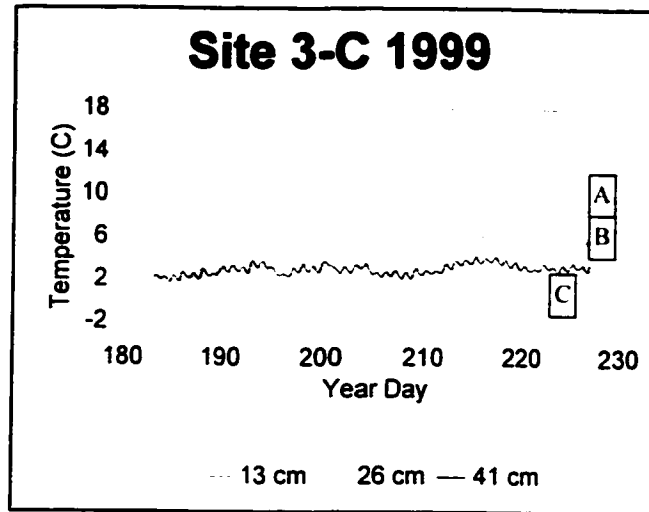
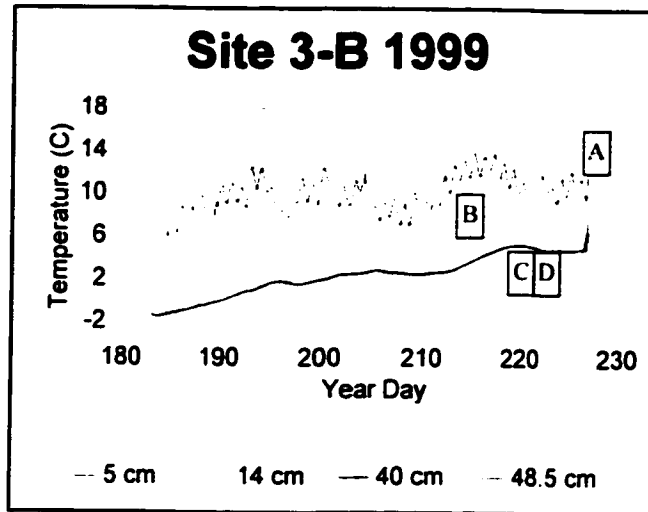
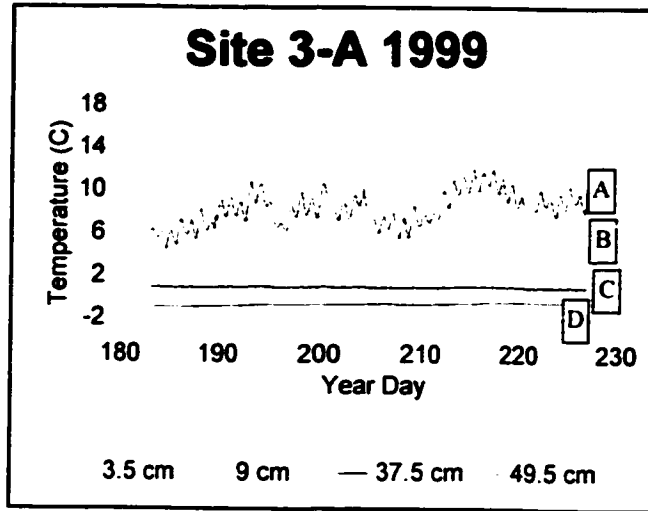
Soil temperature figures for 1999 and 2000 study periods

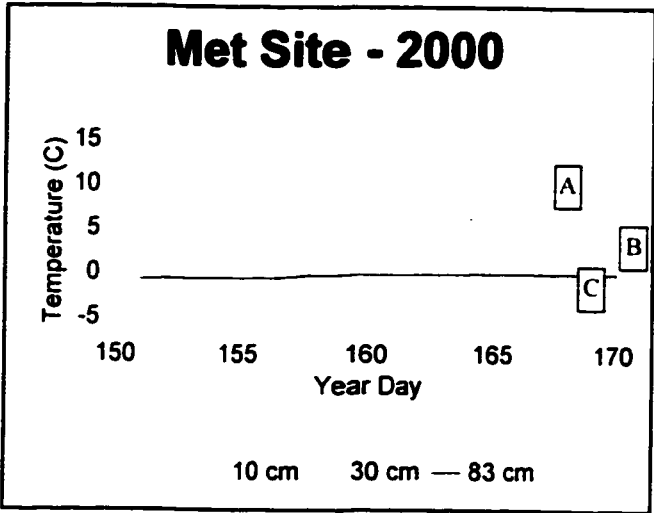
- 'A' - shallowest depth
- 'B' - middle depth
- 'C' & 'D' - deepest depth

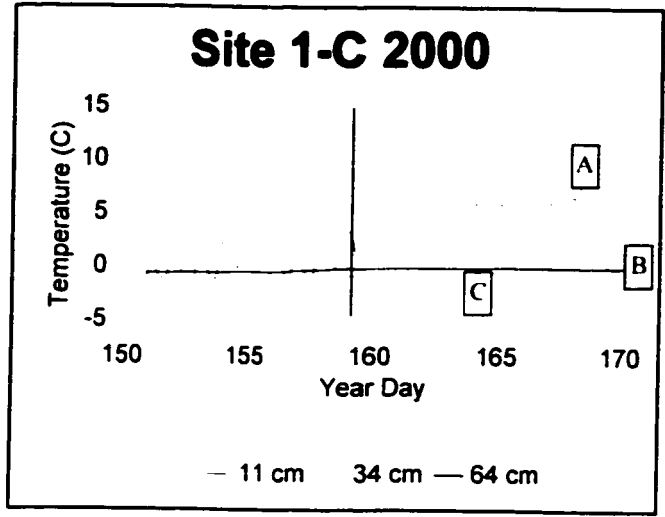
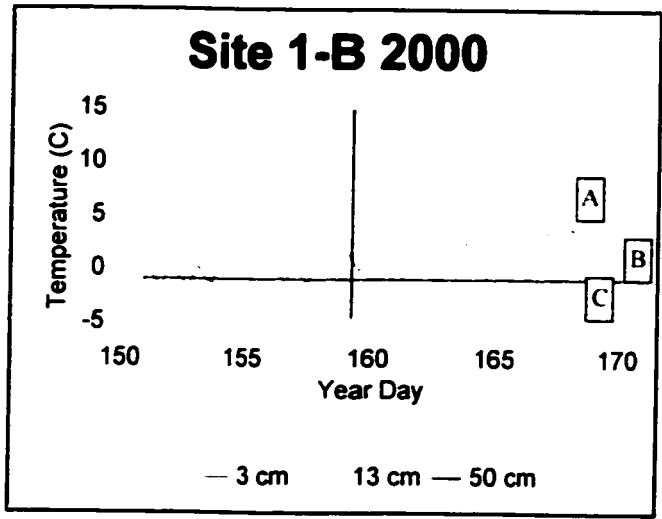
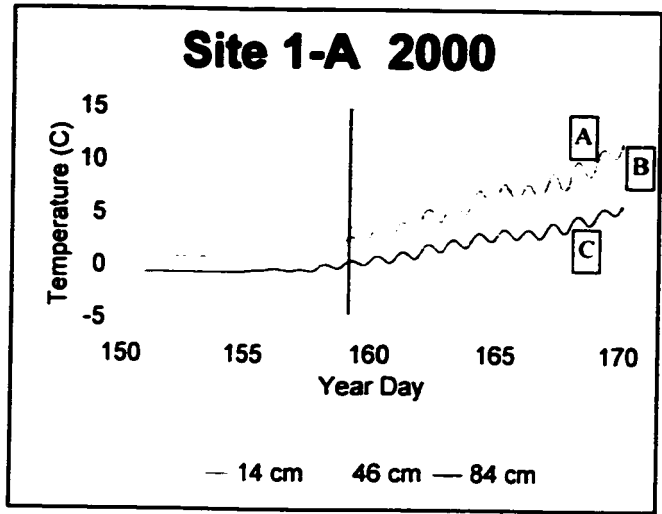


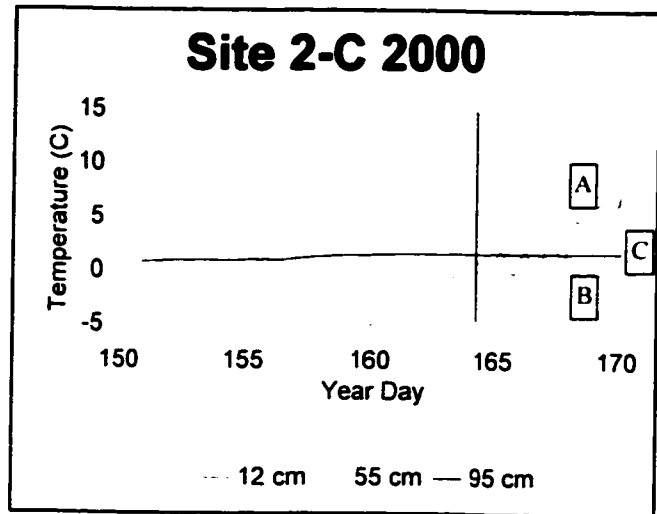
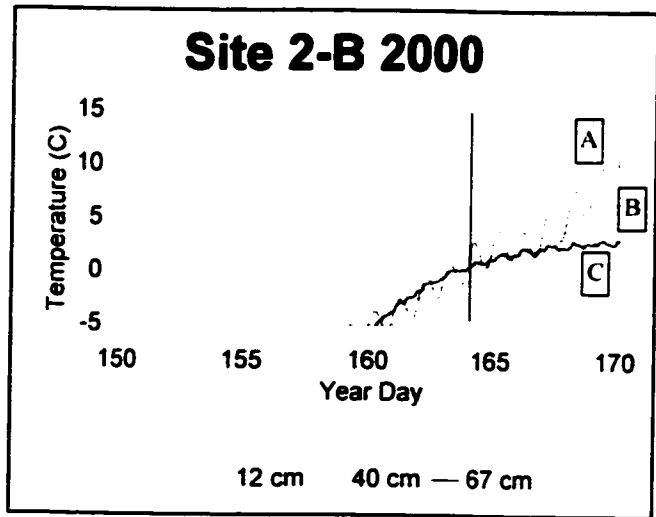
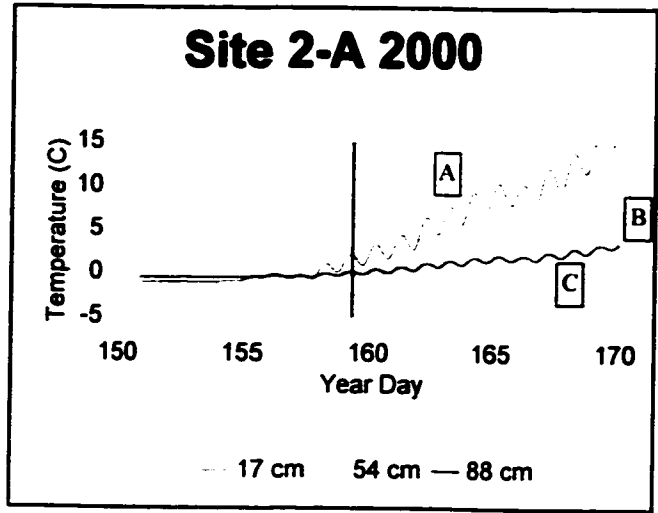












## **APPENDIX - C**

**Active layer development regression equations for 1999 and 2000 study periods**

**ACTIVE LAYER REGRESSIONS - 1999**

<u>SITE</u>	<u>R<sup>2</sup></u>	<u>N</u>	<u>REGRESSION EQUATION</u>
1-A	0.01	32	y= 65.69122+-0.02018x
1-B	0.82	32	y= -10.4202+0.50592x
1-C	0.76	32	y= -50.6378+0.625437x
3-A	0.96	32	y= -50.0956+0.386002x
3-B	0.97	32	y= -134.351+0.862078x
3-C	0.94	32	y= -65.0759+0.545566x

**ACTIVE LAYER REGRESSIONS - 2000**

<u>SITE</u>	<u>R<sup>2</sup></u>	<u>N</u>	<u>REGRESSION EQUATION</u>
1-A	0.71	17	y= -103.20+0.7018x
1-B	0.81	11	y= -809.5+5.0545x
1-C	0.98	17	y= -173.9+1.1913x
2-A	0.82	13	y= -746.451+4.806025x
2-B	0.80	6	y= -1526.21+9.334286x
2-C	0.90	7	y= -793.643+4.900

---

## REFERENCES

---

- Adams, W.P. 1981. Snow and Ice on Lakes. (Ch. 10) Handbook of Snow: Principles/Processes/Management and Use. D.M. Gray and D.H. Male (eds.) Pergamon Press.
- Anderson, D.M. and L.C. Bliss. 1998. Association of plant distribution patterns and microenvironments on patterned ground in a polar desert, Devon Island, N.W.T., Canada. *Arctic and Alpine Research*. 30(2): 97-107.
- Babrauckas, B-R., and T.W. Schmidlin. 1997. Summer radiation balance for alpine tundra on Mount Washington, New Hampshire, U.S.A. *Arctic and Alpine Research*. 29(3): 339-344.
- Baily, Weick and Bowers. 1989. The radiation balance of alpine tundra, Plateau Mountain, Alberta, Canada. *Arctic and Alpine Research*. 21(2): 126-134.
- Blanken, P.D., and W.R. Rouse. 1994. The role of willow-birch forest in surface energy balance at arctic treeline. *Arctic and Alpine Research*. 26(4): 403-411.
- Boike, J. 1997. Thermal, hydrological and geochemical dynamics of the active layer at a continuous permafrost site, Taymyr Peninsula, Siberia.. *Reports on Polar Research* 242, 103 pp.
- Boudreau, L.D. and W.R. Rouse. 1995. The role of individual terrain units in the water balance of wetland tundra. *Climate Research* 5(1): 31-47.
- Brown, R.J.E. 1970. Permafrost in Canada. University of Toronto Press. Toronto.
- Burn, C.R. 1998. The active layer: two contrasting definitions. *Permafrost and Periglacial Processes*. 9: 411-416.
- Burn, C.R. and M.W. Smith. 1993. Issues in Canadian permafrost research. *Progress in Physical Geography* 17(2): 156-172.
- Buttle, J.M., S.W. Lister, and A.R. Hill. 2001. Controls on runoff components on a forested slope and implications for N transport. *Hydrological Processes*. 15: 1065-1070.
- Buttle, J.M., I.F. Creed, and J.W. Pomeroy. 2000. Advances in Canadian forest hydrology, 1995-1998. *Hydrological Processes*: 14: 1551-1578.

- Buttle, J.M. and K.E. Fraser. 1992. Hydrochemical fluxes in a high arctic wetland basin during spring snowmelt. *Arctic and Alpine Research*. 24(2): 153-164.
- Buttle, J.M. and D.M. McDonald. 2000. Soil macroporosity and infiltration characteristics of a forest podzol. *Hydrological Processes*. 14: 831-848.
- Carey, S.K., and M-K Woo. 2000. Within-slope variability of ground heat flux . Subarctic Yukon. *Physical Geography* 21(5): 407-417.
- Carey, S. and M.K. Woo. 1997. Snowmelt hydrology of two subarctic slopes, southern Yukon, Canada. *Northern Research Basins - Proceedings. Eleventh International Symposium and Workshop*.
- Carey, S.K., and M.K. Woo. 1999. Hydrology of two slopes in subarctic Yukon, Canada. *Hydrological Processes*. 13(16): 2549-2562.
- Carey, S.K. and M.K. Woo. 2001. Slope runoff processes and flow generation in a subarctic, subalpine catchment. *Journal of Hydrology* 253: 110-129.
- Carey, S.K. and M.K. Woo. 2001. Spatial variability of hillslope water balance. Wolf Creek Basin, subarctic Yukon. *Hydrological Processes* 15: 3113-3132.
- Deangelis, M.L. and E.F. Wood. 1998. A detailed model to simulate heat and moisture transport in a frozen soil. *IAHS Publication no. 248*: 141-148.
- Dingman, S.L. 1994. Physical Hydrology. Prentice-Hall Inc., New Jersey.
- Duguay, C.R., W.R. Rouse, P.M. Lafleur and L.D. Boudreau. 1999. Radiation balance of wetland tundra at northern treeline estimated from remotely sensed data. *Climate Research*. 13(1): 77-90.
- Edlund, S.A., M.K. Woo, and K.L. Young. Climate, hydrology and vegetation patterns Hot Weather Creek, Ellesmere Island, Arctic Canada. *Nordic Hydrology*. 21: 273-286.
- Environment Canada, 1986. Climatic Atlas, Map series 2 - Precipitation. Atmospheric Environment Service, Environment Canada, Downsview, Ontario, 2pp. + 48 plates
- Ford, J. and B.L. Bedford. 1987. The hydrology of Alaskan wetlands, U.S.A.: a review. *Arctic and Alpine Research*. 19(3): 209-229.
- Freeze, R.A. and J.A. Cherry. 1979. Groundwater. Prentice-Hall Inc. New Jersey.

- French, H.M. 1996. The Periglacial Environment. 2<sup>nd</sup> ed. Longman Group. Singapore**
- Garnier, B.J. and A. Ohmura. 1970. The evaluation of surface variations in solar radiation income. *Solar Energy* 13: 21-34.**
- Geological Survey of Canada. 1997. Lac de Gras; District of Mackenzie, Northwest Territories. 1:125 000. Map 1870A.**
- Giblin, A.E., K.J. Nadelhoffer, G.R. Shaver, J.A. Laundre, and A.J. McKerrow. 1991. Biogeochemical diversity along a riverside toposequence in arctic Alaska. *Ecological Monographs*. 61(4): 415-435.**
- Gibson, J.J., T.W.D. Edwards, and T.E. Prowse. 1993. Runoff generation in a high boreal wetland in Northern Canada. *Nordic Hydrology*. 24:213-224.**
- Gibson, J.J., T.W.D. Edwards, G.G. Bursey and T.D. Prowse. 1993. Estimating evaporation using stable isotopes: quantitative results and sensitivity analysis for two catchments in Northern Canada. *Nordic Hydrology*. 24: 79-94.**
- Gibson, J.J., T.D. Prowse, and T.W.D. Edwards. 1996. Evaporation from a small lake in the continental arctic using multiple methods. *Nordic Hydrology*. 27: 1-24.**
- Gibson, J.J. R. Reid, and C. Spence. 1998. A six-year isotopic record of lake evaporation at a mine site in the Canadian subarctic: results and validation. *Hydrological Processes* 12: 1779-1792.**
- Gibson, J.J. 2001. Forest-tundra water balance signals traced by isotopic enrichment in lakes. *Journal of Hydrology* 251: 1-13.**
- Glenn, M.S. and M.K. Woo. 1997. Spring and summer hydrology of a valley-bottom wetland, Ellesmere Island, Northwest Territories, Canada. *Wetlands* 17(2): 321-329.**
- Gomersall, C.E., and K.M. Hinkel. 2001. Estimating the variability of active-layer thaw depth in two physiographical regions of Northern Alaska. *Geographical Analysis* 33(2): 141-155.**
- Goryachkin, S.V., N.A. Karavaeva, V.O. Targulian, and M.V. Glazov. 1999. Arctic soils: spatial distribution, zonality and transformation due to global change. *Permafrost and periglacial processes*. 10: 235-250.**
- Gould, W.A., D.A. Walker, and M.K. Reynolds. Canadian Transect and Mapping for the Circumpolar Arctic Vegetation Map. Poster presented at National Science**

Foundation ARCSS LAII Science Workshop, Seattle, Washington. Feb 23-26. 2000.

- Gude, M. and D. Scherer. 1997. Snowmelt and water movement in saturated snow layers of high latitude areas. Northern Research Basins - Proceedings. Eleventh International Symposium and Workshop.
- Guymon, G.L. and J.N. Luthin. 1974. A coupled heat and moisture transport model for arctic soils. *Water Resources Research*. 10(5): 995-1001.
- Hagen, J.O. and B. Lefauconnier. 1995. Reconstructed runoff from the High Arctic Basin Bayelva based on mass-balance measurements. *Nordic Hydrology*. 26: 285-296.
- Halliwell and W. Rouse. 1987. Soil heat flux in permafrost: characteristics and accuracy of measurement. *International journal of climatology*. 7(6): 571-584.
- Harazono Y., M. Yoshimoto, M. Mano, G.L. Vourlitis and W. Oechel. 1998. Characteristics of energy and water budgets over wet sedge and tussock tundra ecosystems at North Slope in Alaska. *Hydrological Processes* 12: 2163-2183.
- Harris, S. 1998. Effects of vegetation cover on soil heat flux in the southern Yukon Territory. *Erdkunde*. 52(4): 265-283.
- Hillel, D. 1980. Fundamentals of Soil Physics. Academic Press. New York.
- Hinkel, K.M. 1997. Estimating seasonal values of thermal diffusivity in thawed and frozen soils using temperature time series. *Cold Regions Science and Technology*. 26(1): 1-15.
- Hinkel, K.M. and S.I. Outcalt. 1994. Identification of heat-transfer processes during soil cooling, freezing and thaw in central Alaska. *Permafrost and Periglacial Processes*. 5:217-235.
- Hinzman, L.D., D.L. Goering and D.L. Kane. 1998. A distributed thermal model for calculating soil temperature profiles and depth of thaw in permafrost regions. *Journal of Geophysical Research* 103(D22) 28,975-28991.
- Hinzman, L.D., D.L. Kane, R.E. Gieck, and K.R. Everett. 1991. Hydrologic and thermal properties of the active layer in the Alaskan Arctic. *Cold Regions Science and Technology*. 19: 95-110.
- Hoelzle, M., C. Mittaz, B. Etzemuller, and W. Haeberli. 2001. Surface energy fluxes and distribution models of permafrost in European mountain areas: an overview of

- current developments. *Permafrost and Periglacial Processes*. 12: 53-69.
- Huddart, Bennett and Glasser. Morphology and sedimentology of a high-arctic esker system: Vebreen, Svalbard. *Boreas* 28(2): 253-273.
- Humlum, O. 1998. Active layer thermal regime 1991-1996 at Qeqertarsuaq, Diski Island, Central West Greenland. *Arctic and Alpine Research*. 30(3) 295-305.
- Isard, S.A. 1986. Factors influencing soil moisture and plant community distribution on Niwot Ridge, Front Range, Colorado, U.S.A. *Arctic and Alpine Research*. 18(1): 83-96.
- Jacobsen, A. and B.U. Hansen. 1999. Estimation of the soil heat flux/net radiation ratio based on spectral vegetation indexes in high-latitude Arctic areas. *International Journal of Remote Sensing*. 20(2): 445-461.
- Jahn, A., and H. J. Walker. 1983. The active layer and climate. *Geomorphology*. 47: 97-108.
- Janowicz, J.R. 1997. Wolf Creek research basin: a move towards integration. *Northern Research Basins - Proceedings. Eleventh International Symposium and Workshop*.
- Kane, D.L., L.D. Hinzman, J.P. McNamara, Z. Zhang, M. Sturm and C.S. Benson. 1997. An overview of a nested watershed study in the Alaskan Arctic, the Kuparuk River Basin. *Northern Research Basins - Proceedings. Eleventh International Symposium and Workshop*.
- Kane, D.L., L.E. Hinzman, C.S. Benson, and G.E. Liston. 1991. Snow hydrology of a headwater Arctic Basin. 1: physical measurements and process studies. *Water Resources Research*. 27(6) 1099-1109.
- Kane, D.L., Hinzman, L.D., and J.P. Zarling. 1991. Thermal response of the active layer in a permafrost environment to climate warming. *Cold Regions Science and Technology*. 19: 111-122.
- Kane, D.L., R.E. Gieck and L.D. Hinzman. 1990. Evapotranspiration from a small Alaskan Arctic watershed. *Nordic Hydrology*. 21:253-272.
- Klene, A.E., F.E. Nelson, and N.I. Shiklomanov. 2001. The N-factor in natural landscapes: variability of air and soil-surface temperatures, Kuparuk River Basin, Alaska, U.S.A. *Arctic, Antarctic and Alpine Research*, 33(2): 140-148.
- Lafleur, P.M. and W.R. Rouse. 1995. Energy partitioning at treeline forest and tundra

- sites and its sensitivity to climate change. *Atmosphere-Oceans* 33: 121-133.
- Lafleur, P.M. and W. Rouse. 1988. The influence of surface cover and climate on energy partitioning and evaporation in a subarctic wetland. *Boundary Layer Meteorology*. 44(4): 327-347.
- Lafleur, P.M., Rouse, and Carlson. 1992. Energy balance differences and hydrologic impacts across the northern treeline. *International Journal of Climatology*. 12(2): 193-203.
- Lafleur, P.M., Renzetti and Bello. 1993. Seasonal changes in the radiation balance of subarctic forest and tundra. *Arctic and Alpine Research*. 25(1): 32-36.
- Leverington, D. 1995. A field survey of late-summer depths to frozen ground at two study areas near Mayo, Yukon Territory, Canada. *Permafrost and Periglacial Processes*. 6:373-379.
- Linell, K.A. and J.C.F. Tedrow. 1981. Soil and permafrost surveys in the arctic. Clarendon Press. Oxford.
- Lynch, A.H., G.B. Bonan, F.S. Chapin and W. Wu. 1999. Impact of tundra ecosystems on the surface energy budget and climate of Alaska. *Journal of Geophysical Research*. 104(D6): 6647-6660.
- Lynch, A.H., F.S. Chapin, L.D. Hinzman, W. Wu, E. Lilly, G. Vourlitis, and E. Kim. 1999. Surface energy balance on the arctic tundra: measurements and models. *Journal of Climate*. 12(8-2): 2585-2606.
- Matthews, S. and K. Clark. 1996. Tundra Ecosystem Research Station: Daring Lake, Northwest Territories. Operation Guide and Monitoring Protocols. Department of Resources, Wildlife and Economic Development. Wildlife and Fisheries Division, 600, 5102 50<sup>th</sup> Ave. Yellowknife NT.
- Maxwell, B. 1992. Arctic climate: potential for change under global warming. Arctic Ecosystems in a Changing Climate: An Ecophysiological Perspective. Academic Press. Toronto.
- McGaw, R.W., S.I. Outcalt and E. Ng. 1978. Thermal properties and regime of wet tundra soils at Barrow, Alaska. In: *Proceedings of the Third International Conference on Permafrost*. July 10-13, 1978. Edmonton, Alberta, Canada.
- McNamara, J.P., D.L. Kane, and L.D. Hinzman. 1997. Hydrograph separations in an Arctic watershed using mixing model and graphical techniques. *Water Resources*

Research. 33(7): 1707-1719.

- McNamara, J.P., D.L. Kane, and L.D. Hinzman. 1998. An analysis of streamflow hydrology in the Kuparuk River Basin, Arctic Alaska: a nested watershed approach. *Journal of Hydrology* 206: 39-57.
- Munro, D.S. and G.J. Young. 1982. An operational net shortwave radiation model for glacier basins. *Water Resources Research* 18(2): 220-230.
- Munro, D.S. 1990. Comparison of melt energy computations and alblatometer measurements on ice and snow. *Arctic and Alpine Research*. 22(2): 153-162.
- Munro, D.S. 1991. A surface energy exchange model of glacier melt and net mas balance. *International Journal of Climatology* 11(6): 689-700.
- Nakano, Y. and J. Brown. 1972. Mathematical modeling and validation of the thermal regimes in tundra soils, Barrow, Alaska. *Arctic and Alpine Research* 4: 19-38
- Nelson, F.E, K.M. Hinkel, N.I. Shiklomanov, G.R. Mueller, L.L. Miller and D.A. Walker. 1998. Active-layer thickness in north central Alaska: systematic sampling, scale, and spatial autocorrelation. *Journal of Geophysical Research*. 103(22) 28,963-28,973.
- Nicholson, F.H. 1978. Permafrost modification by changing the natural energy budget. In *Proceedings of the Third International Conference on Permafrost*. July 10-13, 1978. Edmonton, Alberta, Canada.
- Nixon, J.F. 1975. The rold of convective heat transport in the thawing of frozen soil, *Canadian geotechnic Journal*. 12: 425-429.
- Ohmura, A. 1982. A historical review of studies of the energy balance of arctic tundra. *Journal of Climatology*. 2(2): 185-195.
- Ohmura, A. 1982. Climate and energy balance on the arctic tundra. *Journal of Climatology*. 2: 65-84.
- Ohmura, A. The derivation of a formula to calculate direct short-wave radiation on slopes.
- Onishchenko, V.G., I.S. Lisker, and A.G. Georgiadi. 1999. A generalized description of soil thermal conductivity. *Eurasian Soil Science*. 32(2): 185-188.
- Osterkamp, T.E. 1987. Freezing and thawing of soils ad permafrost containing unfrozen

- water or brine. *Water Resources Research*. 23(12): 2279-2285.
- Outcalt, S.I. and K.M. Hinkel. 1996. The response of near-surface permafrost to seasonal regime transitions in tundra terrain. *Arctic and Alpine Research* 28(3): 274-283.
- Owens, E.H. and J.R. Harper. 1977. Frost table and thaw depths in the littoral zone near Peard Bay, Alaska. *Arctic* (30): 155-168.
- Passerat de Selans. A. B.A. Monteny, and J.P. Lhomme. 1997. The correction of soil heat flux measurements to derive an accurate surface energy balance by the Bowen ration method. *Journal of Hydrology*. 188-189: 453-465.
- Petrone, R.M., W.R. Rouse, and P. Marsh. 2000. Comparative surface energy budgets in western and central subarctic regions of Canada. *International Journal of Climatology* 20(10): 1131-1148.
- Pauwels and Wood. 1999. A soil-vegetation-atmosphere transfer scheme for the modeling of water and energy balance processes in high latitudes. *Journal of Geophysical Research*. 104(D22): 27811-27839.
- Petrone, R.M., T.J. Griffis and W.R. Rouse. 2000. Synoptic and surface climatology interactions in the central Canadian subarctic: normal and El Nino seasons. *Physical Geography* 21(4): 368-383.
- Pienitz, R., J.P. Smol, and D.R.S. Lean. 1997. Physical and chemical limnology of 24 lakes located between Yellowknife and Contwoyto Lake, Northwest Territories (Canada). *Canadian Journal of Fisheries and Aquatic Science*. 54:347-358.
- Podniesinski, G.S. and D.J. Leopold. Plant community development and peat stratigraphy in forested fens in response to ground-water flow systems. *Wetlands* 18(3): 409-430.
- Price, J.S. 1987. The influence of wetland and mineral terrain types on snowmelt runoff in the Subarctic. *Canadian Water Resources Journal*. 12(2): 43-52.
- Prowse, T.D. 1990. Northern Hydrology: An overview. In: *Northern Hydrology, Canadian Perspectives*. T.D. Prowse, C.S.L. Ommanney, Editors. NHRI Science Report No. 1
- Putkonen, J. 1998. Soil thermal properties and heat transfer processes near Ny-Alesund, northwestern Spitsbergen, Svalbard. *Polar Research* 17(2): 165-179.
- Quinton, W.L. and N.T. Roulet. 1998. Spring and summer runoff hydrology of a subarctic

- patterned wetland. *Arctic and Alpine Research*. 30(3): 285-294.
- Quinton, W.L. and P. Marsh. 1998. The influence of mineral earth hummocks on subsurface drainage in the continuous permafrost zone. *Permafrost and Periglacial Processes*. 9: 213-228.
- Quinton, W.L. and Marsh. 1999. A conceptual framework for runoff generation in a permafrost environment. *Hydrological Processes*. 13: 2563-2581.
- Quinton, W.L., Gray, and Marsh. 2000. Subsurface drainage from hummock-covered hillslopes in the arctic tundra. *Journal of Hydrology*. 237(1-2): 113-125.
- Riseborough, D.W. and C.R. Burn. 1988. Influence of an organic mat on the active layer. In: 5<sup>th</sup> International Conference on Permafrost in Trodenham, Norway. Tapir Publishers.
- Romanovsky, V.E., T.E. Osterkamp and N.S. Duxbury. 1997. An evaluation of three numerical models used in simulations of the active layer and permafrost temperature regimes. *Cold Regions Science and Technology*. 26: 195-203.
- Romanovsky, V.E. and T.E. Osterkamp. 2000. Effects of unfrozen water on heat and mass transport processes in the active layer and permafrost. *Permafrost and Periglacial Processes*. 11: 219-239.
- Romanovsky, V.E. and T.E. Osterkamp. 1995. Interannual variations of the thermal regime of the active layer and near-surface permafrost in Northern Alaska. *Permafrost and Periglacial Processes*. 6:313-335.
- Rott, H. and F. Obleitner. 1992. The energy balance of dry tundra in West Greenland. *Arctic and Alpine Research*. 24(4): 352-362.
- Roulet, N.T. and M.K. Woo. 1986. Hydrology of a wetland in the continuous permafrost region. *Journal of Hydrology*. 89: 73-91.
- Rouse, W.R., P.M. Lafleur, and T.J. Griffis. 2000. Controls on energy and carbon fluxes from select high-latitude terrestrial surfaces. *Physical Geography* 21(4): 345-367.
- Rouse, W.R. 2000. Progress in hydrological research in the Mackenzie GEWEX study. *Hydrological Processes*. 14(9): 1667-1685.
- Rouse, W.R. 1998. A water balance model for a subarctic sedge fen and its application to climatic change. *Climatic Change*. 38(2): 207-234.

- Rouse, W.R. 1984. Microclimate at arctic tree line (Parts 1, 2 and 3). *Water Resources Research*. 20(1): 57-66.
- Rouse, W.R. and R.L. Bello. 1983. The radiation balance of typical terrain units in the Low Arctic. *Annals of the Association of American Geographers*. 73(4): 538-549.
- Rouse, W.R., M.S.V. Douglas, R.E. Hecky, A.E. Hershey, G.W. Kling, L. Lesack, P. Marsh, M. McDonald, B.J. Nicholson, NT. Roulet and J.P. Smol. 1997. Effects of climate change on the freshwaters of arctic and subarctic North America. 11: 873-902.
- Ruhland, K. and J.P. Smol. 1998. Limnological characteristics of 70 lakes spanning Arctic treeline from Coronation Gulf to Great Slave Lake in the Central Northwest Territories, Canada. *International Review of Hydrobiology*. 83(3): 183-203.
- Sanders, L.L. 1998. A manual of field hydrogeology. Prentice-Hall Inc. New Jersey.
- Santeford, H.S. 1978. Snow soil interactions in interior Alaska. Proceedings: Modeling of Snow Cover Runoff. S.C. Colbeck and M.R. Ray (eds.) U.S. Army Cold Regions Research and Engineering Laboratory. Hanover, New Hampshire.
- Saunders, I.R., J.D. Bowers, Z. Huo, W.G. Bailey, and D. Verseghy. 1999. Simulation of alpine tundra surface microclimates using the Canadian Land Surface Scheme: I. albedo and net radiation modeling. *International Journal of Climatology*. 19: 913-926.
- Shikomanov, N. 1999. Analytic representation of the active layer thickness field, Kuparuk River Basin, Alaska. *Ecological Modeling*. 123(2-3): 105-125.
- Smith, M.W. 1977. Computer simulations of microclimate and ground thermal regimes: test results and program description, ALUR Report 75-76-72, Department of Indian and Northern Affairs, Ottawa, 74 pp.
- Szidler, K., G.H.R. Henry, E.P. Lozowski, and C. Labine. 1996. Diagnosing the diurnal surface energy balance over the summer tundra at Princess Marie Bay from simple short-period measurements. *Theoretical and Applied Climatology*. 54: 201-211.
- Tarnawski, W. 1993. Modeling the thermal conductivity of frozen soils. *Cold Regions Science and Technology*. 22(1): 19-31.
- Tatenhove, F.G.M. 1994. Ground temperature and related permafrost characteristics in West Greenland. *Permafrost and Periglacial Processes*. 5:199-215.

- Topp, G.C., J.L. Davis and P. Annan, 1980. Electromagnetic determination of soil water content: measurement in coaxial transmission lines. *Water Resources Research*. 16(3): 574-582
- Tuomenvirta, H., H.Alexandersson, A. Drebs, P. Frich, and P.O. Nordli. 2000. Trends in nordic and arctic temperature extreme ranges. *Journal of Climate*. 13: 977-990.
- U, K.T.P. and W. Gao. 1988. Applications of solutions to non-linear energy budget equations. *Agricultural and Forest Meteorology*. 43: 121-145.
- Vourlitis, G.L. and W.C. Oechel. 1997. Landscape CO<sub>2</sub>, H<sub>2</sub>O vapour and energy flux of moist-wet coastal tundra ecosystems over two growing seasons. *Journal of Ecology*. 85: 575-590.
- Washburn, A.L. 1980. Geocryology: a survey of periglacial processes and environments. John Wiley and Sons. New York.
- Wedel, J.H., B.J. Olding, M. Palmer. 1988. An overview study of the Coppermine River Basin. NWT Programs, Inland Waters Directorate, Environment Canada, Yellowknife, N.W.T.
- Weller, G. and G. Wendler. 1990. Energy budgets over various types of terrain in polar regions. *Annals of Glaciology*. 14: 311-314.
- Woo, M.K. and Z. Xia. 1996. Effects of Hydrology on the thermal conditions of the active layer. *Nordic Hydrology*. 27: 129-142.
- Woo, M.K., P. Marsh and J.W. Pomeroy. 2000. Snow, frozen soils and permafrost hydrology in Canada, 1995-1998. *Hydrological Processes*. 14: 1591-1611.
- Woo, M.K. and T.C. Winter. 1993. The role of permafrost and seasonal frost in the hydrology of northern wetlands in North America. *Journal of Hydrology*. 141: 5-31.
- Woo, M.K. 1993. Northern Hydrology (Ch. 5). Canada's Cold Environments. H.M. French and O. Slaymaker (eds) McGill-Queen's University Press. Montreal.
- Woo, M.K. 1983. Hydrology of a drainage basin in the Canadian High Arctic. *Annals of the Association of American Geographers*. 73(4):577-596.
- Young, G.J. The mass balance of Peyto Glacier, Alberta, Canada 1965-1978. *Arctic and Alpine Research*. 13: 307-318.

- Young, K.L., M.K. Woo, and S.A. Edlund. 1997. Influence of local topography, soils, and vegetation on microclimate and hydrology at a high arctic site, Ellesmere Island, Canada. *Arctic and Alpine Research*. 29(3): 270-284.
- Zhang, T. and K. Stamnes. 1998. Impact of climatic factors on the active layer and permafrost at Barrow, Alaska. *Permafrost and Periglacial Processes*. 9: 229-246.
- Zhang, Z., D.L. Kane and L.D.. Hinzman. 1997. Spatially distributed simulations of Arctic hydrological processes. *Northern Research Basins - Proceedings. Eleventh International Symposium and Workshop*.